Antithrombotic Peptide Delivery from Glow-Discharge Plasma-Coated Controlled Release Matrices

Marc Masayuki Takeno

A dissertation
submitted in partial fulfillment of the
requirements for the degree of

Doctor of Philosophy

University of Washington

2005

Program Authorized to Offer Degree:
Department of Bioengineering

University of Washington
Graduate School

This is to certify that I have examined this copy of a doctoral dissertation by

Marc Masayuki Takeno

and have found that it is complete and satisfactory in all respects,
and that any and all revisions required by the final
examining committee have been made.

Chair of Supervisory Committee:

_____
Buddy D. Ratner

Reading Committee:

_____
Buddy D. Ratner

_____
Thomas A. Horbett

_____
Patrick S. Stayton

Date:_____

Signature_____

Date_____

University of Washington

Abstract

Antithrombotic Peptide Delivery from
Glow-Discharge Plasma-Coated Controlled Release Matrices

Marc Masayuki Takeno

Chair of the Supervisory Committee:
Professor Buddy D. Ratner
Department of Bioengineering

A novel polymeric matrix system has been developed to deliver agents to block platelet adhesion or inhibit thrombin activation on implanted biomaterials. The base material of the system used was BioSpan®, a medical-grade polyether-urethane urea (PEUU) elastomer, which contained a dispersion of an active agent: either an anti-platelet-adhesion peptide (echistatin), small peptide (RGDSGY), or direct antithrombin peptide (hirudin), along with bovine serum albumin (BSA) or poly(ethylene glycol) (PEG) as an excipient and pore-former. The PEUU-peptide matrix was subsequently processed using radio-frequency glow-discharge (RFGD) plasma polymerization of acrylate monomers, either 2-hydroxyethyl methacrylate (HEMA), n-butyl methacrylate (BMA), or N-isopropyl acrylamide (NIPAAm) to create a barrier membrane.

Control of plasma parameters changed the cross linking of this thin, conformal barrier, and produced different release rates of the active agents from the matrix. Biologically active echistatin and hirudin were delivered successfully, but some matrices exhibited a limited reduction in release rate due to osmotic rupturing of the matrix and coating. For RGDSGY-containing matrices, the reduction in release rate with RFGD plasma coating was greatest for matrices with PEG excipients of 10,000 and 20,000 molecular weight.

TABLE OF CONTENTS

LIST OF FIGURES

Figure Number Page

LIST OF TABLES

Table Number Page

ACKNOWLEDGEMENTS

In lengthy graduate studies, many professional and personal relationships are formed. I hope to highlight a few of these for special acknowledgement and thanks.

I wish to thank my advisors, Professors Buddy Ratner and Thomas Horbett, for their guidance, mentoring, friendship, and support throughout my doctoral research. Their willingness to co-advise me was invaluable and this advising arrangement worked well was very well suited to my project. I would also like to thank the other members of my committee, Professors Pat Stayton and Albert Fuchs, for their valuable feedback and advice. Professor Paul Yager provided much appreciated desk space, encouragement, and help at a critical time. Professor Sandy Spelman was very helpful in encouraging me toward completion of my degree, as were many other faculty members in the Department of Bioengineering.

I thank Dae-Duk Kim for his cheerful attitude and helpful discussions on pharmaceutics, as well as our collaboration on the hirudin experiments. Winston Ciridon was invaluable in teaching me the finer points of plasma deposition and sample preparation. Deborah Leach-Scampavia was of great help in obtaining and analyzing ESCA data. Stephanie Lara was very helpful in teaching me electron microscopy.

Housemates, friends, and colleagues, James Bain, Ann Schmierer, Bob Schreiner, Todd Edwards, John Grunkemeier, Stephen Porter, and Jane Grande, made late nights at the lab and home not only bearable, but enjoyable. A special word of thanks goes to Kip Hauch, for professional advice, personal encouragement, and highly valued friendship.

My parents and brother were constant sources of love and encouragement through the tough times.

Finally, my deepest appreciation goes to my wife, Mimi, for her unwavering love, support, and understanding of a graduate research career.

DEDICATION

For Mimi and Yoshi

1 INTRODUCTION

1.1 Device-related Thrombosis

Most long-term blood-contacting artificial biomaterials have associated thrombus formation at their surfaces due to reactions of blood proteins and activation of platelets at the material surface. These reactions are a result of serum proteins denaturing at a material surface and subsequent interactions of the adsorbed protein layer with other non-adsorbed blood proteins and platelets [1]. For an implanted biomaterial, it would be desirable to inhibit these coagulation reactions at the material surface by altering some intrinsic property of the material itself. The goal of total elimination of coagulation in the long-term has been elusive, despite more than 30 years of research; much remains to be studied for long-term blood biocompatibility, either passive or active [2, 3]. A recent NHLBI/FDA conference on thrombosis singled out anticoagulation therapy as a research opportunity and noted that "Site-specific (intra-device) antithrombotic drug delivery could be particularly effective while minimizing systemic side effects" [4].

Current therapies for patients with implanted biomaterials can employ systemic anticoagulants, which require careful regulation and monitoring. With some anticoagulants in certain patients, dosing can be difficult and bleeding complications occur. In operative procedures which use systemic anticoagulation to prevent device-related thrombosis, such as percutaneous transluminal coronary angioplasty (PTCA, or simply "angioplasty"), bleeding at the femoral insertion site is a common complication of the procedure [5].

It may be possible to reduce or eliminate systemic anticoagulation by restricting antithrombotic treatment to the implant material itself. One of the first, and most studied, examples of anticoagulation at a material surface is the use of ionically- or covalently-bound heparin to the surface of the material [6]. However, this approach has disadvantages: coating chemistries may not work for a particular material; the concentration of surface conjugation may not be high enough for effective anticoagulation;

plasma proteins can adsorb and shield the antithrombotic activity of the surface; and the surface-bound material may be subject to degradation over the long-term.

Researchers have turned to polyurethanes in many blood-contacting applications, for they exhibit good manufacturability and desirable physical compliance characteristics. Polyurethanes have therefore been studied extensively, and there have been many attempts to improve the blood compatibility (a fairly good review is found in the following reference: [7]).

Another possible route to localized antithrombotic delivery is the incorporation of antithrombotic pharmacologic agents within the material itself. This could in theory be achieved with small-molecule nonspecific antiplatelet agents such as aspirin and dipyridamole, but the amounts required for effective anticoagulation are prohibitive for surface-restricted delivery.

Recently discovered and characterized highly potent antithrombotics appear to solve the problem of insufficient loading amounts of other small-molecule agents. Antithrombotic potency is an important design parameter for an implantable device, since it helps dictate not only the required flux of drug/peptide to be delivered, but also the effective lifetime of the device. Theoretically effective surface anticoagulation is now achievable with these materials (see section 2.2). This work extends the current body of research to explore a peptide-based antithrombotic therapy rather than small molecule (traditional “drugs”) or carbohydrate-based therapies such as heparin.

1.2 Specific Aims and Hypotheses

- To deliver biologically active anticoagulant peptides from a plasma-coated polymeric matrix.
- To use a plasma-coating process to reduce peptide release rates, ideally to zero-order kinetics, from coated matrices as compared to control matrices.
- To use various surface analysis techniques as aids in analyzing and optimizing the plasma-coating process in order to achieve the desired film cross link density, and a desired release rate.

1.3 Applications

By combining plasma deposition technology with a polymeric matrix delivery system, we have developed a method to fabricate a rate-controlled, antithrombotic-releasing material. In addition, the technology could be extended beyond antithrombotics and blood-contacting materials, and may be applied generally to other monolithic polymer-based peptide and protein delivery systems. Controlled delivery technology can provide commercial benefits such as product differentiation, market expansion, and patent extension. Further applications for this type of system are discussed in Chapter 9, Future Directions.

2 BACKGROUND AND LITERATURE REVIEW

Developments in the biomaterials, drug delivery, and platelet biology fields have enabled a synthesis of techniques and materials to produce a material that can address device-related platelet thrombosis.

2.1 Potent Antithrombotics

The discovery and intensive study of naturally occurring peptide antithrombotics such as echistatin, an RGD-containing "disintegrin," [8] have spurred pharmaceutical companies to develop structure-based small-molecule analogues. Many compounds have emerged as a result of structural studies of naturally occurring disintegrin peptides: synthesized small peptides; peptide derivatives; peptidomimetics; and non-peptide small molecules, discovered and refined through traditional synthetic organic chemistry methods and structure-based drug design. Recent reviews describe many of these recently-developed small-molecule antithrombotics [9, 10].

These potent antithrombotics have been pursued for systemic therapy, but preliminary calculations (section 2.2) show that the potency of these new antithrombotics is sufficient for local anticoagulant therapy, for example, from the wall of a vascular graft or catheter. Therefore, incorporating such antithrombotics in a polymeric matrix coated with a rate-limiting barrier, to enable a very low release rate, is an attractive strategy for surface anticoagulation.

A key feature of inhibiting fibrinogen-mediated adhesion via GP IIb/IIIa blockers is the blockade of the "final common pathway" for thrombosis. Therefore, rather than inhibiting the multiple metabolic pathways responsible for platelet activation and aggregation, one antiaggregatory agent can be administered for increased efficiency. Combining peptides and drugs in a solid delivery form such as that described in this dissertation is relatively simple if the agents do not have adverse interactions with each other. Multiple thrombotic pathways can be targeted in the same device; for example, a GP IIb/IIIa inhibitor, direct antithrombin, and smooth muscle cell antiproliferative agent could be an effective

combination of therapeutics for use after angioplasty in the prevention of restenosis. Moreover, the synergistic effects of some combinations of antithrombotics could be exploited.

Biochemical data for the echistatin and heparin, the antithrombotics used in preliminary studies, are presented in Section 3.5.

2.2 *Surface-Directed Anticoagulation Strategy*

This dissertation describes the development of a drug delivery system that delivers a potent peptide antithrombotic at the surface of a biomaterial. This surface-localized, or "local," delivery strategy offers several advantages over conventional systemic antithrombotic delivery [11]. First, local delivery would allow very high local concentrations of drug to be delivered at the needed site of action, even for agents prone to rapid degradation in the systemic circulation. Secondly, by concentrating the drug at the target site only, without systemic delivery, adverse side effects can be minimized. Third, with certain forms of local delivery, prolonged administration or residence time of drug delivery may be achievable.

The following mass transfer calculations provide an estimate of the feasibility of the approach of controlled release of an antithrombotic agent from a solid matrix into the bloodstream. The necessity of a rate-limiting barrier can be justified partly on the basis of such calculations.

Accurate models of cardiovascular hemodynamics are extremely complex, and full modeling of the dynamic circulation is nowhere near completion. In order to make models more tractable, many assumptions are made. In most cases, these assumptions are sufficient to describe circulatory hemodynamics to a first approximation [12].

The following assumptions are made of the model: Vessels: 1) have rigid walls; 2) are long, therefore have fully developed flow; 3) are straight, unbranched; 4) have a constant, circular cross-section. Blood: 1) is Newtonian; 2) is under steady flow; 3) is under laminar flow; 4) flows straight (no helical or spiral flow); 5) is incompressible; 6) has a constant fluid viscosity. These assumptions and their implications have been discussed by other authors ([12], [13]).

A model with these assumptions describes the simplest case of flow in a straight tube (or annulus). Further assumptions will simplify the mass transfer equations. For example, Basmadjian and Sefton [14] state that for release of heparin from a tube wall at a constant rate into a fluid in steady laminar flow, the equation of interest, translated from the analogous heat transfer case [15] is:

$$\frac{C_s - C_o}{Nr_0 / D} = \frac{4(x / r_0)}{Re\,Sc} + \frac{11}{24} + \sum_{n=1}^{\infty} A_n \exp\left[-\frac{B_n x / r_0}{Re\,Sc}\right] \tag{2.1}$$

For small values of $(x/r_0)/ReSc$, the series term converges slowly. The more convenient Leveque solution (which holds for $(x/r_0)/ReSc$ that are no larger than 10^{-3}) can be used:

$$\frac{C_s}{Nr_0 / D} = A\left[\frac{x / r_0}{Re\,Sc}\right]^{1/3} \tag{2.2}$$

Variables:

Cs = wall surface concentration (μg/cm^3)
r_0 = tube radius (cm)
A = constant for tube geometry, 1.22
Re = Reynolds number = $2r_0v\rho/\mu$
$(x/r_0)/ReSc$ is a dimensionless distance

N = release rate (μg/cm^2 s)
D = diffusivity in fluid (cm^2/s)
x = axial distance from the entrance (cm)
Sc = Schmidt number = $\mu/\rho D$

Nearly identical equations are obtained for flow in annular tubes (which is a model of a catheterized blood vessel), with release of agent from the inner wall of the annulus (i.e., the catheter). For annular flow, r_0 in equation (2) is replaced with r_0 - r_i where r_i is the inner radius of the annulus. The constant A varies depending on the size of the annulus (e.g. for $r_i / r_0 = 0.25$, $A = 0.945$) and a modified relationship between wall shear rate ($\dot{\gamma}$) and velocity (v) [14].

As an example, the following values represent the model case of elution of echistatin from a straight tube wall:

Cs = IC_{50} : concentration required for 50% inhibition of ADP-stimulated platelet aggregation by echistatin; $IC_{50} = 3 \times 10^{-8}$ M; for 90% inhibition, $IC_{90} = 10^{-7}$ M [8])

r_0 = 0.3 cm (tube diameter of 6 mm)

D = 1.9 x10^{-7} cm^2/s, an estimate based on permeability studies conducted in our laboratory

Sc = ν/D = kinematic viscosity / diffusivity ≈ 5.8 x 10^4 (dimensionless)

A = 1.22, which is a constant for tube geometry

The diffusion coefficient used for echistatin has the same magnitude we observed for the permeability obtained from echistatin permeation experiments.

Solutions to Equation 2.2 are shown for x/ r_0 from 0.1 to 100 and for Reynolds numbers from 10 to 2000:

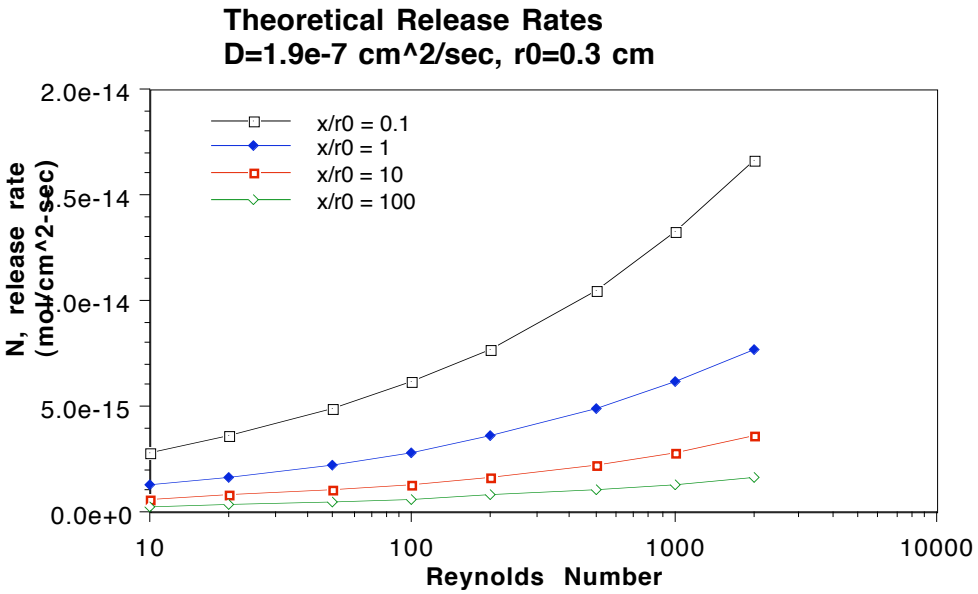

Figure 2-1. Theoretical model release rates.

If we take a dimensionless length of x/r_0 = 0.1 (at the entry of the tube) and a typical Reynolds number of 200, the required release rate is then $N_{required}$ = 7.73 x10^{-15} mol/cm^2 s. This is equivalent to a daily release rate of N = 3.6 µg/cm^2 day. As a "worst case" scenario, with the parameters of x/ r_0 = 0.1 and Re = 2000, the required release rate is N = 1.67 x 10^{-14} mol/cm^2 s, equivalent to 7.8 µg/cm^2 day.

These calculated release rates are useful in the estimation of a boundary or skimming layer. Using Fick's first law of diffusion to describe the boundary layer as a first approximation: J = D (dC/dx) ≈ D(C_s - C_0)/δ. We also make the assumption that J = N (the calculated mass flux from the previous

equations) and use a value of $N = 10^{-15}$ mol/cm^2 s. Also, $C_s = IC_{50} = 3 \times 10^{-8}$ M ; and the bulk concentration $C_0 = 0$. The calculated boundary layer thickness is then $\delta = 6 \times 10^{-3}$ cm, or 60 µm.

At the scale of a platelet, this boundary layer is quite large (Figure 2-2). For example, consider the concentration at 10 µm from the tube wall surface. If the average size of a platelet is roughly 2 µm in diameter, this distance represents a skimming layer thickness of 5 monolayers of platelets. The corresponding distance along the boundary layer is 10 µm / 60 µm, or only 1/6 the full boundary layer thickness. Therefore, at 10 µm away from the wall, the concentration of echistatin is still 5/6 of the wall concentration Cs, or 83% of its initial value. Platelets nearer than 10 µm to the wall will experience concentrations of echistatin higher than 83% of the wall surface value. This approximate calculation using Fick's law helps to justify the restriction of antithrombotic delivery to the wall surface within a certain diffusion boundary layer. Although this layer is "thin" (~ 60 µm), it is actually quite large on the scale of platelets. Note that in a 6 mm diameter tube (3 mm radius), the diffusion boundary layer is only 1/50 the tube radius.

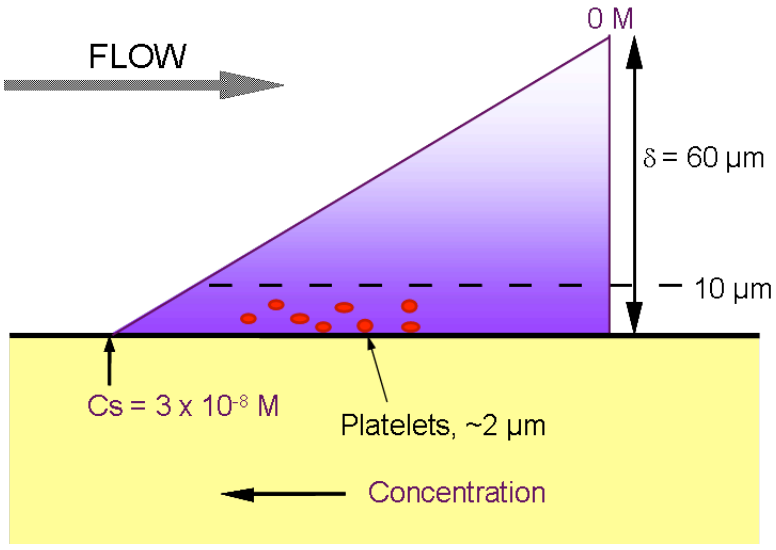

Figure 2-2. Boundary layer relative to platelet size.

A "time of effective delivery" can be calculated based on the theoretical calculations performed in the previous section. Estimating that protein can occupy 30% of a 1 mm x 1 cm x 1 cm

matrix, this allows 0.03 cm^3 "protein volume". At an estimated 1 g/cm^3 density, this is equivalent to 30 mg of protein. Suppose 50% of this is carrier protein (albumin), and 50% is active agent (echistatin). Then the total mass of available echistatin is 15 mg.

At a release of echistatin at its IC_{50} concentration, into a tube at Re = 200 and at $x/r_0 = 0.1$ (at the entry of the tube), the required release rate is $N_{required} = 7.73 \times 10^{-15}$ $mol/cm^2 s$. Since flux = amount / (area x time), the time delivering a steady flux = amount / (flux x area). A total loading of 15 mg into a 1 mm x 1 cm x 1 cm matrix will release at a constant flux for 100,000 hours, or 11.4 years.

2.3 Protein Drug Delivery

Langer and Folkman were among the first researchers to demonstrate effective delivery of large, biologically active polypeptides from a polymeric matrix [16]. Since then, this group and many others have shown that the concept can be extended to other materials and proteins. Most notably, Edelman continued Langer's work, showing release of various macromolecules from poly (ethylene-co-vinyl acetate) (EVAc) systems: insulin [17], periadventitial heparin delivery to rat carotid arteries [18] and antisense oligonucleotide delivery to rat carotid arteries [19].

Bioactive basic fibroblast growth factor (bFGF) was released from tubes formed from a mixture of poly(ether urethane-urea) and bFGF. bFGF released from these tubes stimulated growth and proliferation of human endothelial cells in culture [20]. This type of geometry and delivery system demonstrated feasibility for delivery in a vascular graft system.

Levy and coworkers [21] have delivered dexamethasone from silicone polymers, which were implanted in the periadventitial space around stented porcine carotid arteries. Results for this delivery system showed that this mode of delivery had potent anti-inflammatory and anti-fibrotic effect. Levy *et al.* also have prevented calcification in bioprosthetic cardiac valves [22] by delivery of diphosphate from silicone matrices, and have demonstrated antiarrythmic agent delivery from similar systems [23].

Greisler demonstrated acidic fibroblast growth factor (aFGF) and heparin release from fibrin glue-impregnated expanded poly(tetrafluoroethylene) (ePTFE) grafts, in a canine model [24]. Released

aFGF stimulated ingrowth of capillary-rich mesenchymal tissue and led to near-total endothelialization at 1 month.

Larger-molecule release has also been successfully demonstrated in polymeric matrix systems. Parkhurst and Saltzman demonstrated controlled delivery of monoclonal antibodies against leukocyte adhesion receptors from an EVAc matrix system, in order to inhibit leukocyte-epithelial adhesions [25]. Similarly, Aggarwal et al. have demonstrated monoclonal anti-rabbit glycoprotein IIb/IIIa antibody release from polymer-coated intracoronary stents [26].

In all of these applications, researchers who seek to control the release rate from most of these matrices depend on formulation parameters such as drug solubility, drug-excipient compatibility, and matrix polymer-drug (or peptide/protein) compatibility. Although in general it is possible to achieve a wide range of delivery rates, most systems have limitations, particularly in the low delivery rate (low mass flux) regime. By using a rate-limiting barrier coating on these matrices, it may be possible to shift the design emphasis away from the limitations of the base matrix and allow for tailored delivery rates controlled by the membrane alone.

2.4 Plasma Polymerization in Diffusion Applications

It would also be desirable to control the antithrombotic release rate from this finite matrix reservoir, independent of the formulation variables used to make the matrix. By uncoupling the control of release rate from the formulation and incorporation process, it may be possible to:

- Create a material which can preserve the biological activity of the incorporated antithrombotic;
- Have the desired bulk physical properties (mechanical, structural, and chemical);
- Still allow a controlled diffusion barrier with the right characteristics to provide an efficient and effective release rate at the material surface.

In addition, a membrane diffusional barrier may allow the rate of release of the antithrombotic to be designed to be independent of variables such as blood flow velocity and surrounding tissue pH

that might have affected more environment-sensitive matrices that did not have a rate-controlling membrane.

RFGD plasma deposition is used in this research in a new application: forming a rate-limiting barrier film in order to create a reservoir-type, constant-source controlled-release system from a matrix- or monolithic-type delivery system. Ideally, a membrane would eliminate the burst effect associated with monolithic systems; in addition, applying a rate-limiting membrane should change the release kinetics from the commonly observed Fickian "$t^{1/2}$ kinetics" of monolithic systems, originally described by Higuchi [27], to "zero-order kinetics," characterized by a constant rate of release.

RFGD plasma processing technology has several advantages over traditional processing methods. One is the possibility of creating a non-fouling or biocompatible coating in the same processing step, in addition to the rate-limiting barrier. This non-fouling coating may be useful in blood-contacting or gastrointestinal tract applications. Conversely, a bioadhesive coating could conceivably be deposited as the final outer coating of an implant, if the implant site is a mucosal-tissue lined location in the body. A number of research groups are promoting mucosal surfaces for protein and peptide drug delivery; plasma coating may be an attractive method of providing a rate-limiting and protective barrier, as well as a bioadhesive layer, in one processing step, using, for example, a plasma treatment yielding a poly(2-(dimethylamino-ethyl) methacrylate) (pDMAEMA) type [28], poly(acrylic acid-co-vinyl alcohol) [29] or poly(acrylic acid)-cysteine [30] type structure. Finally, RFGD processing can be a sterilizing process, which may be important in the manufacture of materials and devices intended for implantation [31].

There have been reports in the literature of the use of plasma films for separation membranes in many industrially important processes; gas separation membranes, and plasma-deposited membranes on porous support materials for reverse-osmosis applications are some examples [32, 33]. Control of release rate in these studies is achieved via radio frequency glow-discharge (RFGD) plasma polymerization, a new coating technology as applied to controlled release systems [34, 35].

Lee and Shim used plasma polymerization to graft acrylic acid and N-isopropylacrylamide to polyamide membranes [36] [37], and acrylic acid to poly(vinylidene fluoride) membranes [38]. These methods created pH- and temperature-sensitive membranes that affected the permeation of riboflavin (which served as a model drug). Though this was not a membrane-coated matrix system, the study did demonstrate plasma polymerization as applied to diffusion control.

In our own research group, we have used RFGD plasma to initiate polymerization of methacrylic acid-co-butyl methacrylate on poly(vinylidene difluoride) porous membranes [39]. Glucose oxidase immobilized on these grafted membranes exhibited glucose concentration sensitive (and pH-sensitive) behavior in hydraulic permeability measurements.

Also in our research group, RFGD was used to deposit n-butyl methacrylate (BMA) as a rate-limiting barrier on a ciprofloxacin-loaded polyurethane matrix [40]. This antibiotic-releasing system was based on studies and techniques described in this dissertation. It was shown that plasma-deposited BMA could reduce the ciprofloxacin release rate from samples and extend the effective time of delivery above the minimum killing flux to at least 128 hours.

The use of plasma polymerization in the application described in this dissertation, that is, to control diffusion of an antithrombotic peptide from a polymeric matrix, has not been published before as far as is known.

3 MATERIALS AND METHODS

3.1 BioSpan ®

Polyurethane was chosen as the base matrix material due to its traditional use in blood-contacting medical devices. Polyurethanes have the desired properties of toughness and high cycle lifetimes in cardiovascular applications. The particular polyurethane used in this study is a formulation of the commercially available polyether urethane urea (PEUU), BioSpan®, obtained from the Polymer Technology Group, Inc. (Emeryville, CA).

In all of these studies, the so-called "additive free" base polymer formulation of BioSpan was used; that is, the polyurethane consisting of a polytetramethylene oxide (PTMO) soft segment, ethylene diamine (ED) and 1,3-cyclohexane diamine (1,3-CHD) chain extenders, and methylene diisocyanate (MDI) hard segments (Figure 3-1).

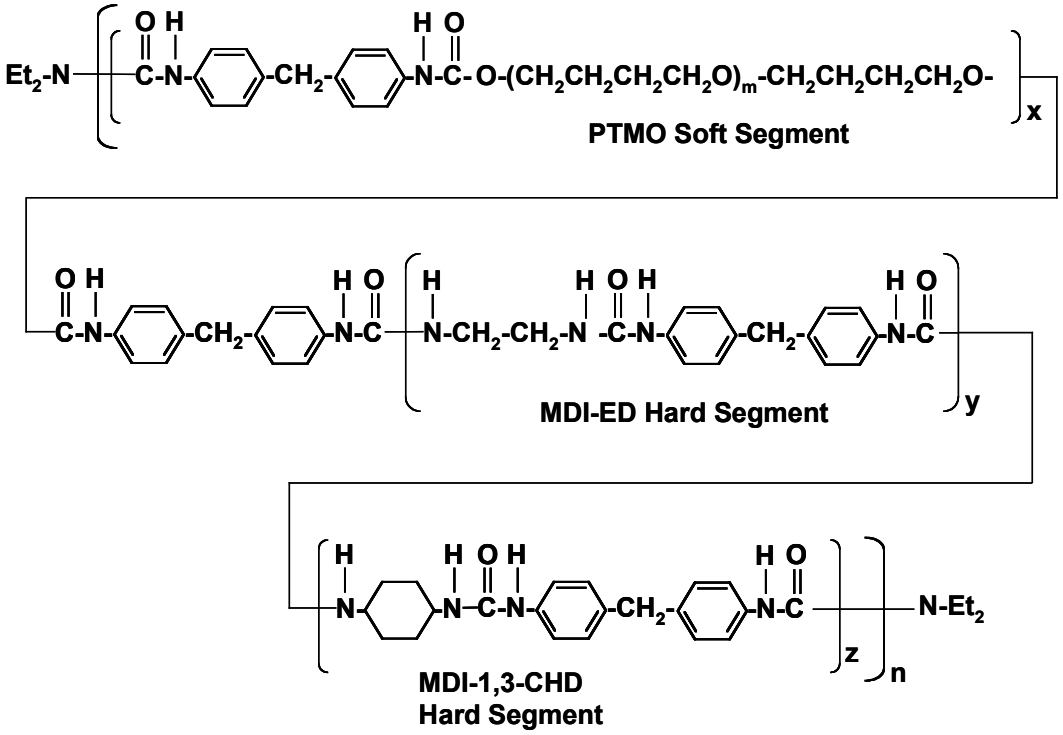

Figure 3-1. Generalized structure of BioSpan®.
Redrawn from Polymer Technology Group literature [41]

This polymer was supplied as a viscous solution of approximately 24% solids in dimethyl acetamide (DMAc). There were no other ingredients such as antioxidants and surface-modifying additives, commonly found in the commercially available preparation of BioSpan. The additive-free base polymer was used in order to avoid unnecessary complications with the surface analysis of the polyurethane matrix material. This particular preparation of BioSpan was obtained *via* special order from the Polymer Technology Group (lot numbers 071392, 110293, 071795, 102797).

3.2 Polyethylene Glycol

Polyethylene glycol (PEG) was used in most matrix formulations in order to achieve several intended goals. First, a basic premise of the matrix delivery system is that the material to be released must be at a high enough loading level to form pores and continuous or semi-continuous channels throughout the matrix (see Section 1.2). This is necessary for the diffusive release of the active agent to take place. The channel-forming function of the excipient could be fulfilled by several polymers, but PEG was chosen based on several criteria.

PEG has long been studied and used in the drug delivery field, and has been accepted and "generally recognized as safe" as used in biomaterials and medical devices. PEG has also been shown to exhibit some "protective effects" [42] when formulated with proteins, acting to preserve enzymatic activity and binding capabilities of certain proteins. In addition, PEG is water soluble (or swellable) and in certain formulations can assist in the delivery of proteins in a matrix system via osmotic mechanisms.

Several sources of PEG were used in these formulations (Polysciences, Warrington, PA; Sigma / Fluka, St. Louis, MO); in general, the grade of PEG used was of high purity, either pharmaceutical or reagent grade. A range of molecular weight preparations of PEG (3.4k, 4k, 10k, 20k, 100k, 1M, 2M) was used in order to determine the effect of the excipient molecular weight on the characteristics of active agent release.

3.3 Bovine Serum Albumin

Bovine serum albumin (BSA) was used as an excipient in some formulations due to its previous use by other researchers in solid formulations [43].

The BSA used was generally prepared using the Cohn Fraction V method (cold ethanol precipitation). The BSA used in these studies was purchased from two suppliers: Miles (Pentex BSA, Fraction V, Catalog No. 81-066-2); and ICN (BSA Fraction V, Catalog No. 810033). BSA was used without further purification. BSA preparations from the two suppliers did not show appreciable differences in handling or formulation characteristics.

3.4 Mannitol

In some experiments, the sugar alcohol mannitol was used as an excipient. Previous use in traditional pharmaceutical dosage forms (such as oral formulations) and reports of additional protein stability with mixtures of mannitol and protein led to the selection and use of mannitol in our experiments with hirudin (Chapter 7). D-Mannitol (Catalog No. M8429, Sigma) was used as received.

3.5 Antithrombotic Agents

3.5.1 Echistatin

Echistatin, a 49-amino acid residue peptide (MW approx. 5420) originally isolated from the venom of the viper *Echis carinatus* [8], is commercially available as a recombinant DNA product. Echistatin is a potent disintegrin, with an IC_{50} (concentration inhibiting 50% cells) of about 3×10^{-8} M (~ 30 nM) in platelet-rich plasma. Echistatin contains four disulfide bonds, and NMR structural studies confirm that the structure of the peptide is relatively compact and has indications of being very stable in solution. Stability issues are important to the matrix formulation process, since the peptide undergoes several processing steps *en route* to the form assayed (formulation steps are described in Section 3.8).

Echistatin used in these studies was purchased from Sigma Chemical Co. (echistatin, synthetic, Catalog No. E-2138, ~ 97% purity). Echistatin was used as received, without further purification.

3.5.2 Hirudin

Hirudin, a 65-residue peptide (MW approx. 7000), was originally isolated from the venom of *Hirudo medicinalis*, the medicinal leech, and can currently be obtained as a recombinant DNA-produced product. Hirudin is the most potent natural anti-thrombin known. It is often termed a "direct" antithrombin, because it binds directly to the active site of thrombin, and does not require other cofactors such as heparin cofactor II and antithrombin III for activity. Hirudin binds to thrombin with an inhibitory constant of $K_i = 2.7 \times 10^{-13}$ M (0.27 pM) and an $IC_{50} = 5.7 \times 10^{-9}$ M (5.7 nM) against thrombin-stimulated platelets in platelet-rich plasma (PRP) [44]. Hirudin has been evaluated in several clinical trials, and it has shown to be particularly effective in cases of unstable angina and coronary artery disease [45] in preventing recurrent thrombosis.

The hirudin used in these studies was purchased from Sigma (Catalog No. H9022, lyophilized from leeches) and used as received.

3.5.3 RGDS-6 (RGDSGY)

In order to provide a test peptide for delivery that was smaller (of lower molecular weight) than previously used RGD-containing proteins, a short peptide was designed with certain criteria. The first design criteria was that the sequence of the peptide contained an RGD (Arg-Gly-Asp) motif to impart physical and biochemical characteristics to the peptide that are similar to natural peptides and commercially available peptide-derived antithrombotics. Additionally, it was desired that the peptide be small enough to show differences in its delivery characteristics based on its molecular weight, as compared to larger peptides such as echistatin and hirudin. The peptide would also have a tyrosine residue to allow it to be radiolabeled. Finally, if the peptide had a significant antiplatelet activity, it could be assayed using a similar method as echistatin. It has been shown in the literature [8] that even short peptides containing the sequence –RGDS– have some measurable anti-platelet activity.

Based on these criteria, a peptide of the sequence RGDSGY was synthesized at the University of Washington Peptide Core Synthesis Facility, purified by HPLC, and the molecular weight was

confirmed by mass spectrometry (MW = 654.7). The peptide was provided to our group as a lyophilized, white powder, and was stored at –20 °C until used in formulation.

3.6 RFGD Plasma-Deposition Precursors (monomers)

Several criteria influenced the selection of precursor molecules (also referred to as "monomers") for plasma deposition in this system:

- Suitability of final deposited ("polymerized") film product
- Minimizing the possibility of the deposited film leaching cytotoxic compounds
- Ability of precursor to be processed in plasma state with available equipment
- Ease of handling, including toxicity considerations and physical state (liquid vs. solid at room temperature; vaporization / boiling point; viscosity; thermal stability, etc.)
- Previous experience with similar precursors in our research group.

Based on these criteria, the following precursors were chosen for deposition on these controlled-release matrices: 2-hydroxyethyl methacrylate, n-butyl methacrylate, and N-isopropyl methacrylate. Specific information about these precursors are presented in the following sections.

3.6.1 2-Hydroxyethyl Methacrylate (HEMA)

2-hydroxyethyl methacrylate (HEMA) is a monomer which has a long history of use in the medical device industry as a "building block" for conventionally polymerized water-swellable hydrogels. Soft contact lenses manufactured with poly(hydroxyethyl methacrylate), or pHEMA, have been used successfully for many years, and aspects of protein adsorption and performance of these hydrogels have been researched extensively.

pHEMA has also been studied for its water-swellable properties and because of its potential blood compatibility, and for its applications in the drug delivery field. Previous work in our research group has shown that changing plasma polymerization conditions (such as deposition power, power pulsing time, reaction pressure, deposition time, co-reactants, substrate temperature, post-deposition annealing) can cause changes in the resultant polymerized film structure. Moreover, the nature of this

dependence of film characteristics, such as hydrophobicity, crosslink density, thickness, and reactivity, on plasma deposition conditions is understood at a basic level and this relationship between plasma deposition parameters and resultant film chemistry and structure is continually being expanded by our research group.

The HEMA used in these experiments was purchased from Polysciences, Inc. as a liquid monomer (2-hydroxyethyl methacrylate, 99.5 % ophthalmic grade, Catalog No. 04675). As supplied, the HEMA contained 10 ppm MEHQ (hydroquinone monomethyl ether, or 4-methoxyphenol) as a polymerization inhibitor. It was assumed that, due to the high boiling point of MEHQ (~243 °C at 760 mm Hg [46]), it would not readily vaporize and inhibit gas-phase plasma polymerization of HEMA; therefore, it was not removed prior to use, as is usually done in conventional polymerization reactions.

3.6.2 n-Butyl Methacrylate (n-BMA)

The straight-alkane chain analogue to HEMA, n-butylmethacrylate (n-BMA or BMA), was also selected for plasma deposition for comparison to HEMA. Previous studies indicated that plasma polymer films prepared from n-BMA were more hydrophobic, at least in surface character, than HEMA films [40, 47]. The underlying physical structure of plasma polymerized n-BMA films were expected to be analogous to that of plasma polymerized HEMA, and this was thought to be useful in analysis, comparison, and interpretation of data.

n-butylmethacrylate was purchased from Polysciences, Inc. (Catalog No. 02059). Like HEMA, n-BMA (as supplied) contained a small amount (~10 ppm) of MEHQ as a polymerization inhibitor, but it was not removed prior to the use of n-BMA in the plasma deposition reactor.

3.6.3 N-Isopropyl Acrylamide (NIPAAm)

Another monomer used in plasma polymerization was N-isopropylacrylamide (NIPAAm). Polymers of NIPAAm exhibit unusual properties. Among the most-studied properties of poly(NIPAAm) is the temperature and pH-dependence of its equilibrium hydration state. It was

hypothesized that plasma-deposited films of NIPAAm may exhibit similar environmental sensitivity as conventionally polymerized poly(NIPAAm). Therefore, the performance of plasma-deposited films might be assessed by observing any changes in the behavior of the plasma-deposited films during release experiments, if the films were exposed to a suitable environmental change.

NIPAAm, Aldrich (Catalog No. 41,532-4, Aldrich, St. Louis, MO), was used as received. At room temperature and atmospheric pressure, NIPAAm is a solid, white, crystalline powder. A "heated-monomer" reagent chamber was constructed (Section 3.9.3) and used to introduce the NIPAAm into the reaction chamber.

3.7 Peptide Iodination

3.7.1 Iodine Monochloride (ICl)

In order to quantify the amount of peptide incorporated in the matrices and released into buffer, echistatin was labeled with radioactive iodine using the iodine monochloride (ICl) technique.

Generally, the ICl technique uses a borate and salt buffer system to generate a hypoiodide ion which attacks the aromatic ring of tyrosine and substitutes in a para- position. The method used is based on the protocol by McFarlane [48]. The reaction taking place in solution can be thought of as follows [49, 50]:

$$ICl + NaOH \rightarrow HOI + NaCl$$

$$HOI + \text{tyrosine residue} \rightarrow \text{iodinated tyrosine residue} + H_2O$$

The preparation of radiolabeled echistatin proceeded similarly to published protocols, except that the reagent amounts and reaction volumes were scaled down considerably. 50 µg of echistatin is equivalent to 9.23 nmole of peptide, on the molecular weight basis of 5417 g/mole. 50 µg of lyophilized echistatin was reconstituted in 25 µl of citrate-phosphate buffered saline, with sodium azide added ("CPBSz": 0.12 M sodium chloride, 0.01 M citric acid, 0.01 M sodium phosphate, 0.02 % (by wt.) sodium azide). A 1:1 molar ratio of ICl to protein was used in the reaction. This amount of ICl

was measured into 2 M NaCl, and a volume of ICl/NaCl mixture equal to that of the peptide (25 µl) was used. The third component for pH buffering was a borate solution at 2x reaction concentration ("2x borate buffer": 0.32 M NaCl, 0.40 M H_3BO_3, pH 7.8).

The reaction proceeded as follows: 1 mCi of ^{125}I (as NaI) was mixed with 25 µl of the 2x borate buffer, on ice. The ICl/NaCl solution (25 µl) was added to this and mixed. Finally the echistatin solution was added to the reaction and mixed. The reaction proceeded on ice for 15 min. At the end of the reaction time, the total reaction volume was loaded onto a 0.6 cm diameter x 18 cm (~ 5 mL) prepared polyacrylamide gel column (Bio-Gel P4, Bio-Rad, Hercules, CA). The column flow rate was adjusted to be approximately 35 µl/min. Approximate 280 µl volume fractions from the column were collected with an automatic fraction collector. 2 µl aliquots were taken from each fraction, placed in a 12 x 75 mm glass test tube, then a polystyrene tube (Falcon 2025, Becton-Dickinson), capped, and assayed in a gamma counter (Model 1185, TM Analytic). The earlier-eluting peak from the chromatogram indicated which fractions were retained for use/analysis or further column purification. A specific activity of 140 µCi/mg and efficiency of 67% incorporation was calculated from the chromatogram.

If it was judged that the free iodide peak was not sufficiently separated from the labeled peptide peak, then a second separation was performed on another column. A drawback to repeated column purifications is dilution of the labeled peptide with column buffer. However, for formulations which called for subsequent lyophilization of the peptide, dilution was not an issue.

Labeled ^{125}I-echistatin was generally used immediately in the next processing step (mixing with excipient and lyophilization), or if not used immediately, ^{125}I-echistatin was stored cold (4 °C) in solution under lead shielding and used within one day of synthesis.

3.7.2 Iodo-Beads™

The small peptide RGDSGY (also referred to as RGDS-6; see Section 3.5.3) was iodinated using a form of Chloramine-T immobilized on polystyrene beads, sold under the trade name "Iodo-Beads™" (Cat. No. 28665, Pierce Chemical Co.). This method was chosen for RGDSGY iodination

because the reaction is amenable to small volumes, and the level of radiolabeled iodine incorporation that is theoretically achievable with the Iodo-Beads system is higher than that of ICl. The protocol used to iodinate RGDSGY was essentially the same as that supplied by Pierce Chemical Company, referenced in Tsomides, *et al.* [51].

Lyophilized RGDSGY was used as received from the University of Washington Peptide Core Synthesis Facility. RGDSGY was resuspended in deionized water to a concentration of 10 mg/ml. 0.5 mg in a volume of 50 μl was incubated with an Iodo-Bead in 150 μl of 0.1 M phosphate buffer, pH 6.5, for 5 minutes at room temperature in a 1.5 ml microcentrifuge tube. 0.5 mCi of ^{125}I were added, then incubated for 30 minutes.

The iodination reaction solution was loaded onto a pre-conditioned reverse-phase chromatography column (~ 0.8 cm diameter x 1 cm length, Sep-Pak Plus C18, Catalog No. 20515, Waters, Milford, MA). Increasing proportions of methanol (20%, 40%, 60%, 80%) in 0.1% trifluoroacetic acid elution buffer was used to dissociate the labeled peptide from the column. Fractions were collected with an automated fraction collector, then small aliquots were taken and counted in a gamma counter as in the previous section (3.7.1). As in the previous protocol, if it was judged that the free iodide peak was not sufficiently separated from the labled peptide peak, a second column purification was performed, with an intermediate lyophilization step to concentrate the starting solution.

The labeled peptide was incorporated with 84% efficiency, and had a final specific activity of 283mCi/mmol, or 432 μCi/mg.

3.8 Matrix Fabrication

3.8.1 Lyophilization

Radiolabeled peptide was combined with a solution of unlabeled peptide and excipient then lyophilized to dryness. This was done with a lyophilizer (Labconco), generally by freezing the sample with liquid nitrogen, in a thin shell inside a lyophilization flask. Lyophilization to dryness generally required subjecting the sample to vacuum overnight, depending on the sample volume and

concentration. An in-line activated carbon trap, and post-main condenser liquid nitrogen cold trap was used to trap any possible radioactive species before the vacuum pump. Also, the pump was vented to a laminar flow hood dedicated to radioactive material use.

3.8.2 Sizing and Mixing

After lyophilization, the peptide-excipient mixture was carefully crushed to a fine powder in a laminar flow hood (dedicated to radioactive material use), using a mortar and pestle. Precautions to guard against excessive dust formation and release were taken; a shield and box were used to minimize swirling airflow in the hood, and protective masks and clothing was worn to minimize contact with stray fine particulate. Powders were sieved to size in some preparations, using standard gauge brass wire mesh sieves. In some preparations, a mechanized sifter was used to fractionate particle sizes (Model L3P, ATM Corporation, New Berlin, WI).

The prepared powder was then mixed with a BioSpan solution in dimethyl acetamide (DMAc). The concentration of supplied BioSpan varied, depending on the manufacturing lot, but ranged from 18% to 24% solids in DMAc. DMAc was added to some preparations in order to adjust the viscosity of the polymer solution for ease of mixing and casting.

3.8.3 Casting

Mixtures of BioSpan, excipient, and peptide were mixed thoroughly and cast into either custom-made 5/8 diameter (16 mm) x 3/16 inch (4.8 mm) deep circularly machined polytetrafluoroethylene (PTFE) molds (Figure 3-2), or a 37 x 82 x 19 mm perfluroalkoxy (PFA) flat rectangular mold (Figure 3-3; Catalog No. D1069670, Saint-Gobain Performance Plastics).

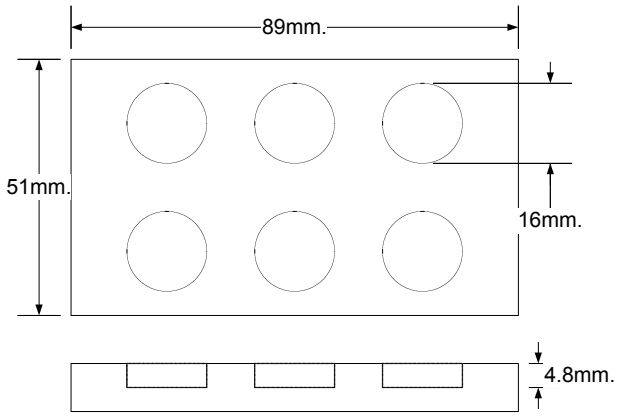

Figure 3-2. PTFE casting mold.

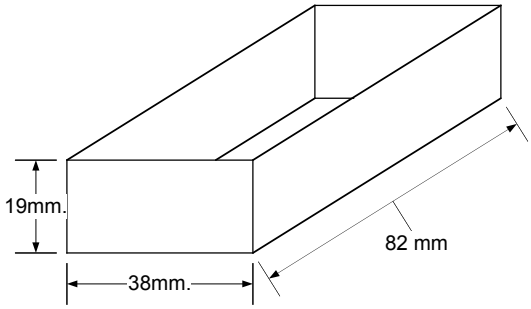

Figure 3-3. PFA casting tray.

3.8.4 Drying

The formulation was dried in a small oven under mild house vacuum (1.5 mmHg) and moderate temperature (~60 °C) to constant weight. Slightly different drying protocols were used for the different matrices. Sample disks were punched or squares cut from the dried films; disks were generally one of the following diameters: 11.3 mm (1/2 inch); 9.5 mm (3/8 inch), or .7.9 mm (5/16 inch). Final thickness of the matrices was approximately 1 mm.

3.8.5 Formulation Summary Flowchart

A flowchart of the formulation procedure (and assay, described in 3.11) is shown below.

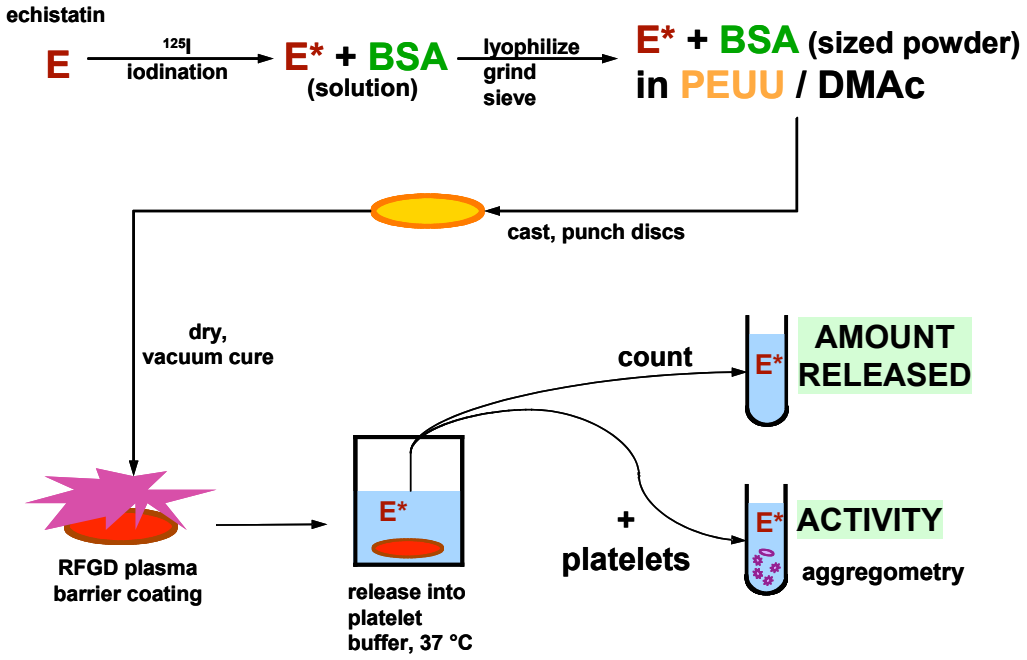

Figure 3-4. Flowchart of experimental procedure.
(Echistatin specifically shown)
E, echistatin; E*, 125I-labeled echistatin; BSA, bovine serum albumin; PEUU/DMAc, polyether urethane in dimethyl acetamide; RFGD, radio frequency glow discharge

3.9 RFGD Plasma Deposition

3.9.1 Deposition on a Substrate at Ambient Temperature

A capacitively coupled, tubular glass reactor was used for RFGD plasma deposition; details of the apparatus have been published previously [52]. Samples were exposed to argon plasma (40 Watts, 175 mtorr (23.3 Pa, 2.33 x 10^{-4} bar), 5 minutes) immediately before deposition. Ophthalmic-grade HEMA, n-BMA, or NIPAAm was used as a monomeric precursor. The monomer was heated to increase its vapor pressure and vapor flow into the reactor was regulated by a PTFE stopcock. In a typical deposition protocol, monomer vapor pressure was maintained at 250 mtorr (33.3 Pa, 3.33 x 10^{-4} bar), and energized with 40 W of RF power; however, several deposition variables were investigated. Surface analysis by ESCA (Section 3.10.1) was used to monitor the chemical structure of the plasma-deposited films.

The designation “pp” is used to refer to plasma-polymerized films of a particular monomer. Thus, “ppHEMA” is the film or coating that results from plasma polymerization of HEMA.

3.9.2 Deposition on a Substrate at Cooled Temperature

Previous work by our group [52] indicates that a low-temperature deposition scheme provides an additional means to control the deposited polymer structure. In addition, a low temperature substrate stage in the plasma reactor prevents excessive heating of the substrate, which may be a concern with certain proteins and peptides.

In low temperature deposition experiments, a stage temperature of 0 °C is maintained by a circulating a coolant mixture (either a mixture of glycerol / water, or water, cooled by water ice or dry ice) in a sample platform. The platform was custom-fabricated, either of borosilicate glass (Figure 3-5), or an aluminum platform with a circulating loop of stainless steel and brass (Figure 3-6).

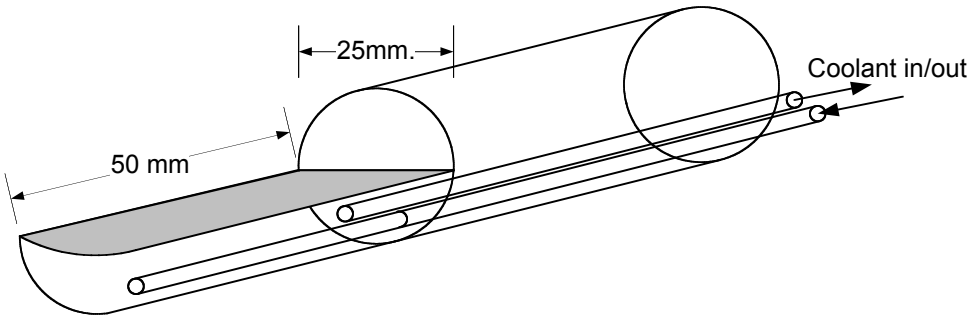

Figure 3-5. Sample cooling platform (glass).
Gray area indicates where sample was placed.

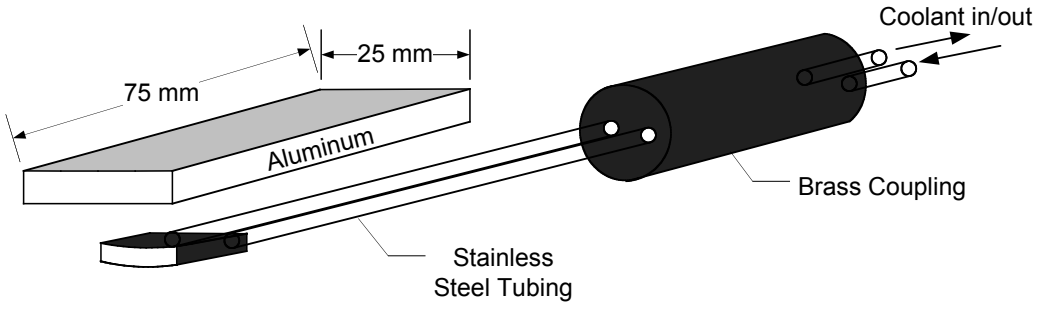

Figure 3-6. Sample cooling platform (aluminum/stainless steel).
Gray area indicates where sample was placed.

3.9.3 Continuous Wave Plasma Deposition

A schematic of the system used to deposit RFGD polymer films is shown in Figure 3-7.

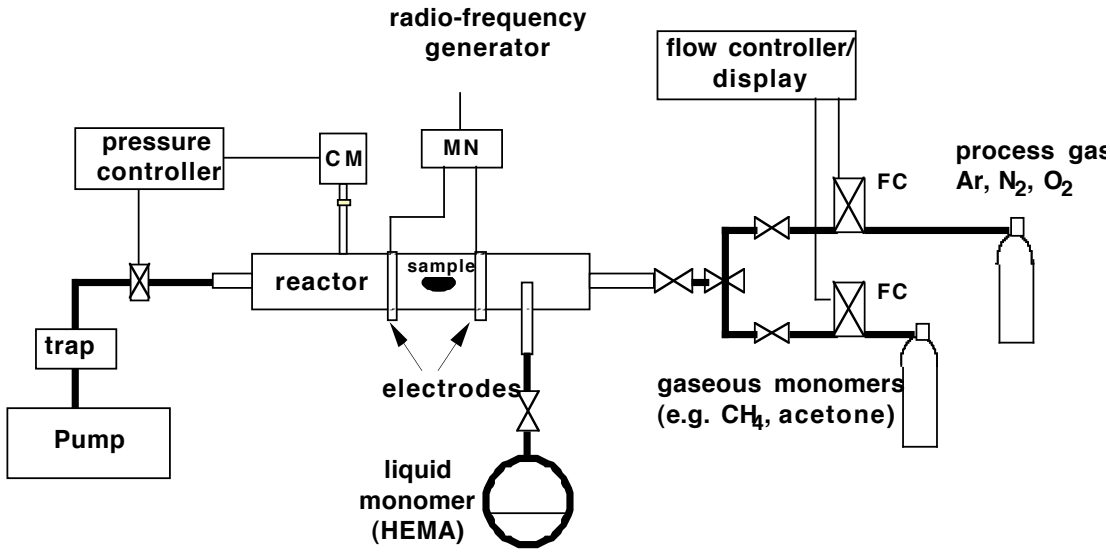

Figure 3-7. RFGD reactor schematic.
CM, capacitance manometer; MN, matching network (manual); FC, mass flow controllers

The general method for continuous wave (CW) plasma polymerization involved the following steps: 1) an oxygen plasma etch to clean the reactor; 2) freezing and thawing the monomer under vacuum, which degassed the monomer of atmospheric gaseous contaminants; 3) loading samples; 4) cleaning the samples with a short argon plasma etch; 5) introducing monomer vapor through a small stopcock or needle valve, and controlling the vapor pressure in the reactor; 6) igniting the radio frequency generator and tuning the RF field with the manual matching network; 7) stopping the RF plasma, but continuing to quench unreacted species by flowing monomer vapor through the reactor; and 8) evacuating the reactor, backfilling with inert gas (usually argon), before opening the reactor to atmospheric pressure and saving samples for the next step in analysis .

Various times, pressures, and temperatures were used to vary the reaction conditions in this general reaction framework. Pressure control in this system was achieved by balancing the inlet flow rate with a varying exhaust pumping rate *via* an automatically controlled butterfly outlet valve. In some cases, heating tape was used to externally heat the reactor walls in order to prevent monomer condensation in undesired areas.

3.9.4 Pulsed Plasma

Other researchers have shown that pulsing the RF field power during plasma-aided film deposition can offer another measure of control over film characteristics [53].

A digitally controlled pulsing radio frequency generator (RF5S, RF Power Products) was coupled to a manual matching network, and then to brass capacitor coupling plates around the reactor. Several different reaction conditions were used and are described in detail in following chapters.

3.10 Surface and Microscopic Analysis

3.10.1 ESCA

Electron Spectroscopy for Chemical Analysis (ESCA), also known as X-ray Photoelectron Spectroscopy (XPS), was used to study the chemistry of the surface of the matrix. ESCA was used to verify that the surfaces obtained by plasma polymer deposition exhibited the expected chemistry.

A Surface Science Instruments (SSI) Model S-Probe or X-Probe was used. Analysis parameters were: Mg Kα energy, 150 eV slit pass energy, approximately 1000 x 400 μm spot size, take-off angle of 55°; a low-energy electron flood gun of 5 eV was used to minimize charging of these insulating samples. These conditions resulted in an analysis depth of about the top ~100 Å of the surface. Detailed scans of the C1s region of the spectra were used to monitor changes in the oxidation state and chemical environment of carbon atoms at a material surface.

3.10.2 Scanning Electron Microscopy

Matrix samples were mounted on aluminum stubs with "carbon cement", a colloidal graphite suspension in xylene/toluene. Stubs were then placed in a bell-jar type sputter coater (Denton Vacuum Systems), evacuated to ~ 75 mtorr, and then sputtered for 90 seconds at 40 mA with an Au/Pd target.

A JEOL JSM 35C microscope (University of Washington Pathology; 15 kV accelerating voltage) was used to image the samples.

3.10.3 Light Microscopy

A microscope with epifluroescent capability (Diaphot, 10x/0.3 NA or 20x/0.4 NA objectives, Nikon) was used in phase contrast mode to image real-time swelling of fabricated matrices. A cooled-CCD camera (CH250/AT200, Photometrics / Roper) and software (MetaMorph™ version 2.5, Universal Imaging, Brandywine, PA) were used for digital image acquisition. Matrix samples were sectioned by razor blade, mounted under glass cover slips, and visualized on edge. At the beginning of the image acquisition, distilled H_2O was introduced to the matrix by capillary wicking at the edge of the cover slip, and image acquisition was timed and recorded. A combination of bright field, dark field, and phase contrast illumination was used.

3.10.4 Fluorescence Microscopy

Fluorescently labeled protein was used as a visualization aid in microscopy of prepared matrices. This aided conceptualization of the matrix structure. Fluorescein isothiocyanate-labeled albumin (FITC-Albumin, Sigma #A-9771, approx. 11.2 moles FITC/mole albumin) and bovine serum albumin (BSA, Miles Pentex Fraction V, #81-066-2) were combined in 1:50 labeled:unlabeled weight ratio. This mix of albumin was then added to an equal weight amount of poly(ethylene glycol), (PEG, Polysciences #16861, 4000 MW). 1 g of this mixture was diluted in 20 mL distilled H_2O, then lyophilized overnight to dryness.

The lyophilized mixture was kept cold and dark. When ready to be incorporated into a polymer mixture, it was brought to room temperature, ground with a mortar and pestle, and sifted with a sonic

sifter (ATM Corporation, Model L3P). Particles that were smaller than 75 μm were retained and used in the film casting step.

A 40% weight fraction of albumin/PEG to matrix total weight was calculated and mixed into a slurry with a 24% solution of BioSpan™. This was then cast into a PFA mold, degassed under vacuum, then dried at atmospheric pressure at 55-60 °C. Samples were cut from the film and embedded in Paraplast® paraffin (Thermo Electron Corp.) for cross-sectioning. Thin (ca. 300 – 500 μm) sections were mounted in low-background fluorescence immersion oil and illuminated under epifluorescence mode (Nikon Diaphot, as in previous section, 3.10.3), with a fluorescence filter set: 485 nm excitation, 535 nm emission, 505 nm dichroic (Omega Optical, Inc. set #XF23).

3.11 Release Experiment Protocol

Prepared matrix samples, usually as circularly punched disks of 7.9 mm (5/16 inch) or 9.5 mm (3/8 inch) diameter, are counted in a gamma counter (TM Analytic, Model 1185). Sample disks are dip-rinsed in release buffer, then placed in glass scintillation vials filled with either 3 or 5 mL of release buffer, usually citrated phosphate buffered saline containing sodium azide and 0.01% gentamicin sulfate (CPBSz – GM sulfate, see Section 3.7.1). In some cases, platelet suspension buffer (PSB, Section 3.12) was used as a release buffer, especially if the released peptide was subsequently assayed using platelet aggregometry. Vials were placed in a shaking water bath maintained at 37 °C. Aliquots of buffer with released peptide (sometimes referred to as “releasate” in the text) were taken at various timepoints, with more frequency at the beginning of a release experiment. The buffer with peptide was stored at 4 °C, and then replaced with fresh buffer immediately. This maintained a “zero-order sink” condition for the release. Aliquots of the buffer with released peptide were then counted in a gamma counter (TM Analytic, model 1185), and the amount of released radioactive peptide was calculated, subtracting background radiation with a control buffer sample, and taking decay of the radioisotope into account.

A sample calculation for a time point of released radioactive echistatin is given using the following equations:

Correction for decay and background

$$n_1' = \frac{(n_1 - \mathrm{b})}{e^{-\lambda t_1}} \tag{3.1}$$

Correction for count time, volume fraction and sensitivity

$$n_{corr(1)} = \frac{(T)(V)(n_1')}{\mathrm{f}} \tag{3.2}$$

Where, at timepoint 1,

n_1 = counts at timepoint 1, per count time and sample volume (for echistatin, for example, 5000 counts per 0.2 minutes, 50 μL aliquot sample volume
b = background counts for blank control (constant; e.g. 40 counts/min)
λ = decay constant (-4.8 x 10^{-4} $hour^{-1}$ for ^{125}I)
t_1 = elapsed time from start of release
n_1' = counts corrected for decay and background
T = time correction factor for counting time (e.g. $T = 5$, to convert counts per 0.2 minutes to counts per minute)
V = volume correction factor for sampling volume (e.g. $V = 60$, if sampling volume was 50 μL and total volume was 3 mL)
f = gamma counter sensitivity; e.g. for the TM Analytic 1185, f = 0.726
$n_{corr(1)}$ = final corrected counts at timepoint 1

To calculate fractional release, the total available material is estimated, using either the counts measured at the beginning of the release experiment, or calculated from counting the exhausted matrix at the end of the release experiment and assuming that represents the unreleased fraction of material in the matrix.

3.12 Platelet Isolation

The potency of echistatin to inhibit platelets was assayed using light-transmissive platelet aggregometry. This assay is sensitive and specific to platelet activity; however, it should be noted that preparation of live human platelets can be time-consuming and error prone in the hands of the novice researcher. Careful preparation, understanding of the characteristics of platelets and the need for particular buffer conditions, and practice are keys to a useful assay.

Whole human blood from volunteers (who were medication- and aspirin-free for two weeks) was collected by venipuncture of the median cubital or other suitable peripheral vein into 1/10 volume ACD (acid-citrate-dextrose solution, NIH Formula A, 1 part ACD: 9 parts blood; 136 millimolar dextrose, 85 mM sodium citrate, 38 mM citric acid, pH 6.5). Usually a large-diameter needle such as a 19 gauge "butterfly" infusion set was used to minimize puncture- and shear stress-related activation of the platelets. Lowering of blood plasma pH and the chelation of most of the plasma free calcium prevents coagulation, and wholesale adventitious platelet activation. Anticoagulated blood is centrifuged for 20 minutes at 220 x *g*. The platelet rich layer is then carefully harvested by pipetting. The platelet suspension was passed through a gel filtration column. A 10 mL plastic syringe barrel was prepared with approximately 5 mL of Sepharose 2B (Sigma Chemical Co.), pre-equilibrated with platelet suspension buffer (PSB calcium free, 140 mM NaCl, 2.5 mM KCl, 1 mM $MgCl_2$, 2 mM NaH_2PO_4, 4.72 mM HEPES, 0.1% (w/v) dextrose, pH 7.4). PRP is layered on the column, and fractions are collected by hand at the outlet. The appearance of platelets is readily apparent in the fractions due to the milky or turbid appearance of the eluate. Fractions appearing in the middle of the platelet peak are pooled and the concentration determined using a Coulter particle counter (model ZBI, Coulter Electronics).

Platelet poor blood plasma (PPP) was prepared from previously separated red cells by centrifugation at 1600 x g for 10 minutes. PPP was used to adjust the final concentration of platelets in the gel-filtered PRP to 2 x 10^8 platelets/mL.

3.13 Echistatin Assay - Platelet Aggregometry

The inhibitory activity of echistatin in buffer was evaluated in a platelet aggregation assay similar to one which has been previously published [8].

Platelets were incubated in a 500 μL cuvette in an aggregometer (Model 530, Chrono-Log) with fibrinogen (F4883, Sigma) at a final concentration of 100 μg/mL, and Ca^{2+} at a final concentration of 1 mM. ADP initiated aggregation at a final concentration of 20 μM. The light transmission was recorded on an X-Y plotter and later digitized using computer software.

Varying amounts of echistatin were then added to PRP / fibrinogen / Ca^{2+} in a siliconized cuvette and incubated for a minimum of 3 minutes in the aggregometer. Platelets were stimulated with ADP to a final concentration of 10 µM. The aggregation of the platelets is measured by light transmittance through the cuvette. Increased light transmittance indicates the formation of platelet aggregates.

Buffer containing released echistatin from the two sets of plasma-treated membranes (B and C) was also tested for inhibitory activity, and the results of these aggregations were compared to a echistatin standard dilution series. In this manner, the relative amount and potency of the released echistatin was evaluated.

3.14 Hirudin Assay - Thrombin Inhibition

Aliquots of released hirudin were assayed with a thrombin inhibition protocol [54]. An aliquot of hirudin in buffer, released from a matrix, is mixed with a known amount of thrombin (final concentration in assay = 1.25 Units/mL; T-6634, Sigma Chemical Co.), and urea (final concentration = 42 mM). This mixture is then allowed to incubate for a short time (1 minute), then is mixed with a chromogenic substrate (final concentration = 0.4 mM, Chromozym® , T-1637, Sigma). The substrate is cleaved by the excess residual thrombin that is not bound to hirudin. By measuring the rate of change of optical density at 405 nm (the maximal absorbance of the cleaved chromophore, 4-nitroaniline), the concentration of thrombin, and therefore hirudin, can be determined, assuming complete binding of hirudin to thrombin. This was done using an automated microplate reader (Vmax Kinetic Microplate Reader, Molecular Devices). Note that this assay is not only a quantitative assay, but also an assay for biological activity. Therefore a separate step to determine activity is not needed, as it is with echistatin.

3.15 Formulation Summary Chart

The following table summarizes the preparation of controlled release matrices. Generally speaking, for each “sample code”, there were at least three individual replicate samples prepared for that set of formulation conditions.

Table 3-1. Comprehensive chart of formulations
(legend at end of table, Page 38)

Sample Code	Base Matrix	Excipient			Active Agent			Plasma Treatment				Comments
	BioSpan (Lot No.)	PEG (MW)	BSA (wt.%)	Man-nitol	Echistatin	Hirudin	RGDS-6	Ar	HEMA	n-BMA	NIPAAm	
A145	071392		30%		A131							release A162
A263	071392		50%		A229 9.63µg/disk							release "A1-A4"
A275	071392		50%		A229 9.63µg/disk			30 sec. 40 W 250 mtorr	5 min. CW 40 W 250 mtorr			release "B1-B3" cooled substrate
A279	071392		50%		A229 9.63µg/disk			4 min. 40 W 250 mtorr	5 min. CW 40 W 250 mtorr			release "C1-C3" cooled substrate
B162(A-M)	071392		50%									
C32	071392		50%					5 min. 40 W 175 mtorr	10 min CW 80 W 260 mtorr			
C45	071392		50%					5 min. 40 W 175 mtorr				80%:20% HEMA/MMA 10 min CW 80 W 200 mtorr
C55	071392		50%					5 min. 40 W 175 mtorr				ppMMA 10 min CW 80 W 275 mtorr
C139	110293		50%					5 min. 40 W 175 mtorr		5 min CW 80 W 150 mtorr		
C142	110293		50%					5 min. 40 W		5 min CW 120 W		

Table 3-1 continued

Sample Code	Base Matrix	Excipient			Active Agent			Plasma Treatment				Comments
	BioSpan (Lot No.)	PEG (MW)	BSA (wt.%)	Man-nitol	Echistatin	Hirudin	RGDS-6	Ar	HEMA	n-BMA	NIPAAm	
								175 mtorr		150 mtorr		
C145	110293		50%					5 min. 40 W 175 mtorr		10 min CW 120 W 100 mtorr		
C164	110293		50%									
C206	110293		50%									
E122A,B	071795		20%									
E122C,D,E	071795		30%									
E138A,B,C	071795		20%					10 min. 20 W 200 mtorr	(liq. poly)			Ar-initiated liquid polymerization
E144A,B,C	071795		20%					10 min. 20 W 200 mtorr		(liq. poly)		Ar-initiated liquid polymerization
E145A,B	071795		20%						immersion			immersion control
E145C,D	071795		20%							immersion		immersion control
F90	071795		40%			DDK†		5 min. 40 W 175 mtorr	10 min CW 40 W 150 mtorr			BAH-40
F91	071795			40%		DDK†		5 min. 40 W 175 mtorr	10 min CW 40 W 150 mtorr			BMH-40
F190A	071795	4k					LS*					
F190B	071795	4k					LS*	5 min	10 min CW			

Table 3-1 continued

Sample Code	Base Matrix	Excipient			Active Agent			Plasma Treatment				Comments
	BioSpan (Lot No.)	PEG (MW)	BSA (wt.%)	Man-nitol	Echistatin	Hirudin	RGDS-6	Ar	HEMA	n-BMA	NIPAAm	
								40 W 125 mtorr	40 W 150 mtorr			
F190C	071795	4k					LS*	5 min. 40 W 175 mtorr		10 min CW 40 W 150 mtorr		
G32A	102797	3.4k					G31					G31: RGDS-6 specific activity 283 mCi/mmol
G32B	102797	10k					G31					
G32C	102797	20k					G31					
G44A	102797	100k					G31					
G44B	102797	200k					G31					
G54A	102797	400k					G31					
G54B	102797	1M					G31					
G61A	102797	3.4k					G31	5 min 40 W 175 mtorr	20 min CW 40 W 250 mtorr			
G65A	102797	10k					G31	5 min 40 W 175 mtorr	20 min CW 40 W 250 mtorr			
G65B	102797	20k					G31	5 min 40 W 175 mtorr	20 min CW 40 W 250 mtorr			
G65C	102797	100k					G31	5 min 40 W 175 mtorr	20 min CW 40 W 250 mtorr			

Table 3-1 continued

Sample Code	Base Matrix	Excipient			Active Agent			Plasma Treatment				Comments
	BioSpan (Lot No.)	PEG (MW)	BSA (wt.%)	Man-nitol	Echistatin	Hirudin	RGDS-6	Ar	HEMA	n-BMA	NIPAAm	
G65D	102797	200k					G31	5 min 40 W 175 mtorr	20 min CW 40 W 250 mtorr			
G68D	102797	3.4k					G31	5 min 40 W 175 mtorr		20 min CW 40 W 250 mtorr		
G68E	102797	10k					G31	5 min 40 W 175 mtorr		20 min CW 40 W 250 mtorr		
G68F	102797	20k					G31	5 min 40 W 175 mtorr		20 min CW 40 W 250 mtorr		
G68G	102797	100k					G31	5 min 40 W 175 mtorr		20 min CW 40 W 250 mtorr		
G68H	102797	200k					G31	5 min 40 W 175 mtorr		20 min CW 40 W 250 mtorr		
G72A	102797	3.4k					G31	20 min CW 40 W 250 mtorr				
G72B	102797	10k					G31	20 min CW 40 W 250 mtorr				
G72C	102797	20k					G31	20 min CW 40 W				

Table 3-1 continued

Sample Code	Base Matrix	Excipient			Active Agent			Plasma Treatment				Comments
	BioSpan (Lot No.)	PEG (MW)	BSA (wt.%)	Man-nitol	Echistatin	Hirudin	RGDS-6	Ar	HEMA	n-BMA	NIPAAm	
								250 mtorr				
G159	102797	400k					G31	1 min 40 W 290 mtorr			1 min / 80 W 10 min CW 40 W 250 mtorr	
G161	102797	400k					G31	1 min 40 W 250 mtorr			1 min / 80 W 20 min CW 40 W 250 mtorr	
G163	102797	400k					G31	1 min 40 W 290 mtorr			1 min / 80 W 20 min pulsed 40 / 0 W (100 msec at 50%) 290 mtorr	
G165	102797	1M					G31	1 min 40 W 250 mtorr			1 min / 80 W 10 min CW 40 W 250 mtorr	
G167	102797	1M					G31	1 min 40 W 250 mtorr			2 min / 80 W 20 min CW 40 W 250 mtorr	

Table 3-1 continued

Sample Code	Base Matrix	Excipient			Active Agent			Plasma Treatment				Comments
	BioSpan (Lot No.)	PEG (MW)	BSA (wt.%)	Man-nitol	Echistatin	Hirudin	RGDS-6	Ar	HEMA	n-BMA	NIPAAm	
G169	102797	1M					G31	1 min 40 W 250 mtorr			1 min / 80 W 20 min pulsed 40 / 0 W (100 msec at 50%) 290 mtorr	
G172A	102797	400k					G31					
G172B	102797	1M					G31					

Legend:
† = Dae-Duk Kim's preparation
* = Lei Shen's preparation
CW = "continuous wave" plasma treatment

4 SURFACE ANALYSIS OF PLASMA-DEPOSITED FILMS

BioSpan films ("additive free BioSpan, Lot 071795", Polymer Technology Group; see Section 3.1) were cast to provide a control sample for analysis. The resultant survey spectrum (0 - 1000 eV) is shown in Figure 4-1.

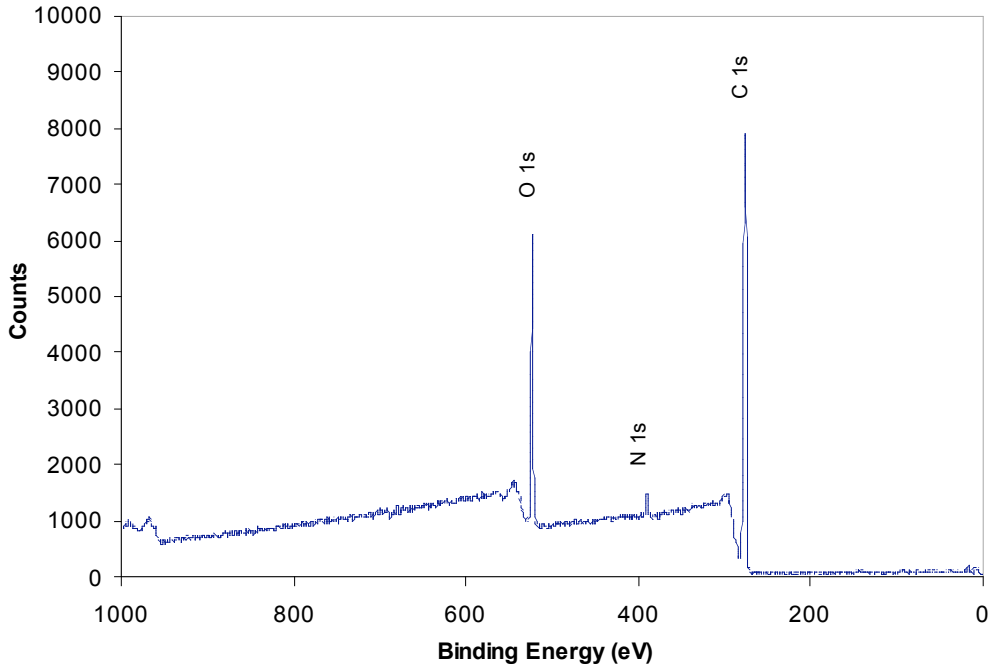

Figure 4-1. ESCA survey spectrum of BioSpan polyurethane, control sample.

The peaks identified in the spectrum as C 1s, O 1s and N 1s were used to quantify the relative surface elemental composition (except for hydrogen and helium). The surface was determined to contain 79.5% carbon, 17.9% oxygen, and 2.6% nitrogen. Trace amounts of silicon were also detected but were assumed the result of adventitious contamination and were ignored for this particular quantitative analysis. These atomic percentage ratios are consistent with the results from a separate lot of BioSpan (Lot 110293), of composition 77.8% C, 17.4% O, 4.7% N (amounts may not add to 100.0% due to rounding). Small differences in carbon and nitrogen concentrations between lots could be due to

small differences in surface concentrations of hard segment vs. soft segment in the analysis spots, as well as normal variability in synthesis, manufacturing, and processing.

The high-resolution C 1s spectrum (Figure 4-2) shows a peak structure indicative of various chemical functionalities reflecting oxidation states of carbon in the polyurethane backbone. The binding energy of the hydrocarbon peak was referenced to 285.0 eV. A four-peak fit, corresponding to four functional groups and carbon atom binding environments, is shown. Although other chemical states are most likely present, given the known synthesis of BioSpan [55], it may be difficult to accurately determine these states with this type of curve-fitting analysis without further chemical derivatization or other techniques.

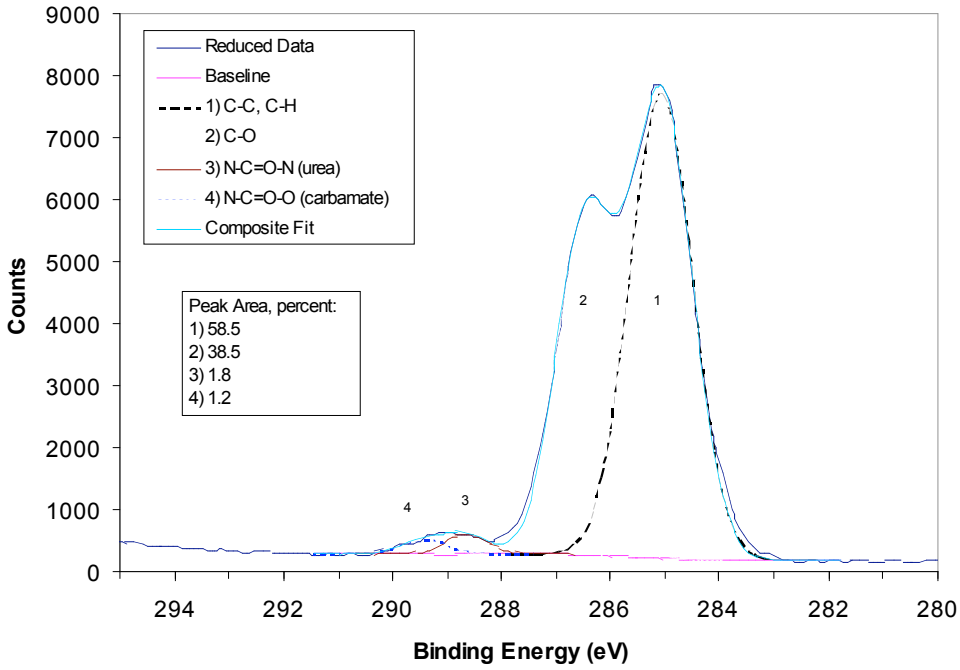

Figure 4-2. High-resolution C 1s spectrum of BioSpan polyurethane control.
Numbered peaks indicate carbon atoms bound in different putative chemical environments as shown in the legend.

Similar spectra were acquired for matrices including excipient (for example, PEG or BSA) as controls. Survey (Figure 4-3) and high-resolution C 1s spectra (Figure 4-4) for BioSpan polyurethane mixed with PEG-4k excipient (28 wt.%) reveals a surface composition slightly higher (in relative

concentration) in carbon, and lower in oxygen and nitrogen (86.3% C, 11.9% O, 1.8% N), than that of unblended BioSpan.

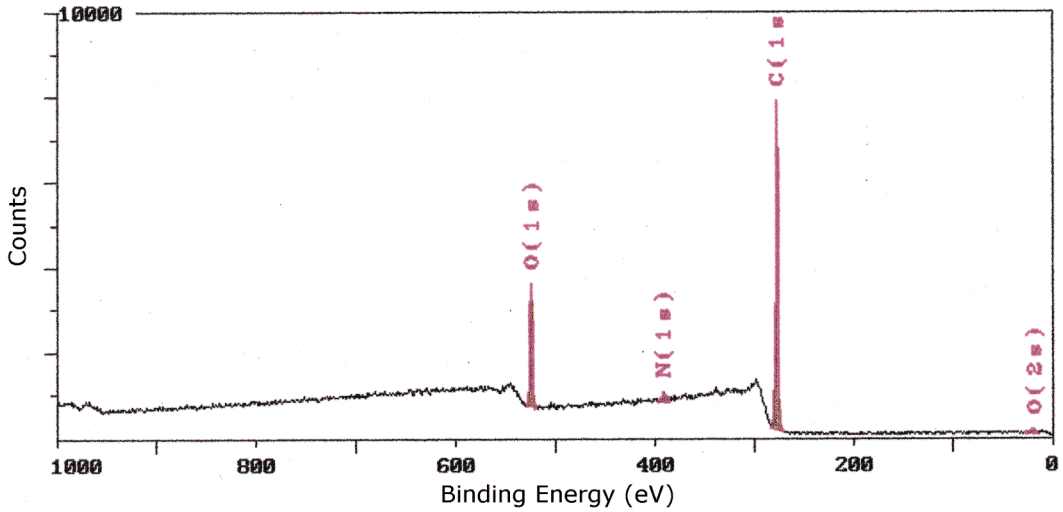

Figure 4-3. Survey spectrum of BioSpan with PEG-4k excipient.

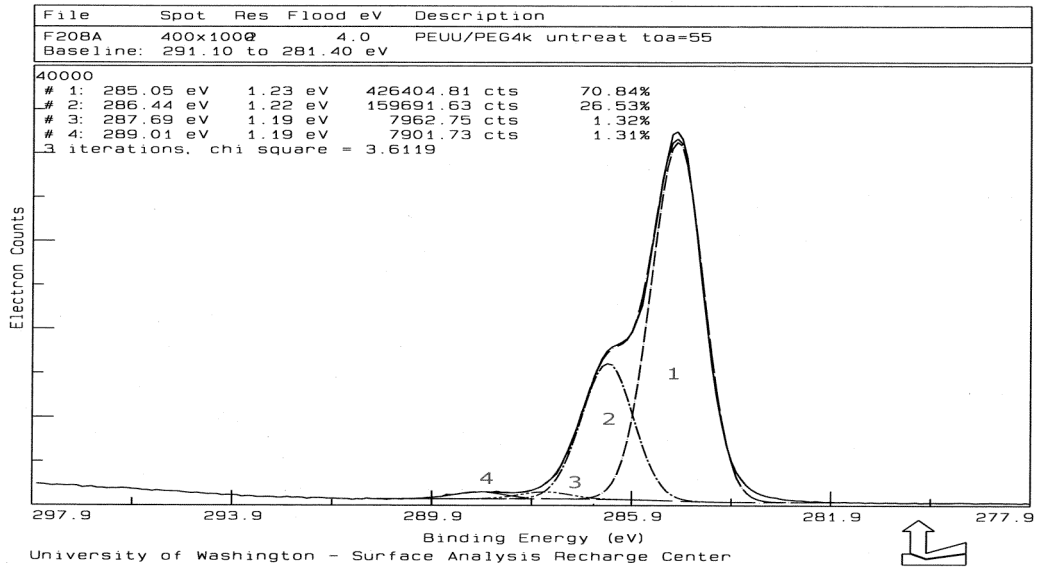

Figure 4-4. High-resolution C 1s spectrum of BioSpan with PEG-4k excipient.

Higher carbon content could be due to surface enrichment with higher C/O and C/N containing segments of the polyurethane, or surface contamination from adsorbed hydrocarbon contamination from processing steps. Some evidence for adventitious contamination is the increased C-Hx / C-C component of the C 1s spectrum (70.8% peak 1, 285.0 eV) relative to unblended control BioSpan (Figure 4-2, 58.5% peak 1, 285.0 eV). For comparison, a surface composed primarily of high-molecular weight PEO, neglecting end group effects, would present a stoichiometry of 66.6% C, 33.3%O, and show 100% peak area of the C 1s spectrum as C-O ether / alcohol moieties (286.5 eV).

Analysis of BioSpan blended with PEG-100k yielded compositional percentages similar to that of BioSpan / PEG-4k, but with contaminants identified as silicon and calcium:

Table 4-1. Surface composition of BioSpan and excipient mixtures.

	C (at. percent)	O (at. percent)	N (at. percent)	Other
BioSpan (Lot 071795)	79.5	17.9	2.6	Si trace
BioSpan / PEG-4k	86.3	11.9	1.8	
BioSpan / PEG-100k	86.0	10.2	--	Si 1.7, Ca 2.1
BioSpan / PEG-4k Argon plasma treated 40 W / 250 mtorr / 20 min	71.0	21.2	2.2	Si 5.5
BioSpan / PEG-100k Argon plasma treated 40 W / 250 mtorr / 20 min	74.7	18.7	2.1	Si 4.5

The silicon and calcium detected on the untreated BioSpan / PEG-100k blend may have been contaminants in the as-supplied PEG-100k used in formulation, rather than contamination post-formation, because Si or Ca were not detected on other matrices prepared for surface analysis in a parallel fashion and analyzed in the same experimental session. Furthermore, plasma treatment of this BioSpan / PEG-100k blend produced a surface that consisted of plasma polymer only (results following) with no other trace elements detected. Also, extended argon plasma treatment of the

BioSpan / PEG-100k blend failed to remove the Si or Ca trace amounts. This suggests that these elements were incorporated throughout the matrix rather than simply adhering to the surface layer.

4.1 HEMA Films

HEMA was deposited *via* plasma deposition on glass cover slip substrates, with the following conditions: 40 W power, 250 mtorr pressure, for 20 minutes. Deposition proceeded alongside BioSpan / PEG / RGDS-6 matrices. The survey scan (Figure 4-5) shows a surface composed primarily of plasma-deposited polymer. This was expected since visual inspection of the cover slip prior to ESCA analysis indicated a thick plasma deposition, and previous experience in our laboratory indicated that the deposition conditions should yield a fairly thick film.

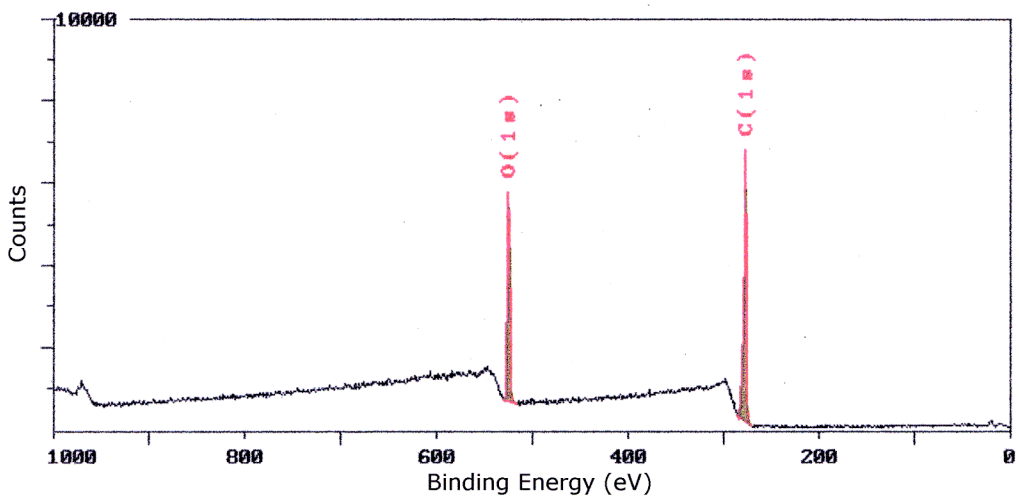

Figure 4-5. Survey spectrum of ppHEMA deposited on a glass cover slip.

Elemental composition of this ppHEMA sample was 77.0% C, 23.0% O. The increased carbon in elemental composition (conventional polymerization stoichiometry: C:O atomic ratio = 2:1, or 66% C, 33% O), indicates oxygen "abstraction" or removal from the surface, consistent with presumed cross-linking and other chemical changes tending toward a more glassy, hydrocarbon-like polymer rather than the oxygen-rich polymer known as a hydrogel material [52]. The C 1s spectrum (Figure 4-6)

shows typical plasma-deposition-induced changes in the HEMA molecular structure. Though the actual chemical structure of the plasma deposited polymer may not be exactly known, it can be inferred through judicious curve-fitting and comparison to other reference polymers.

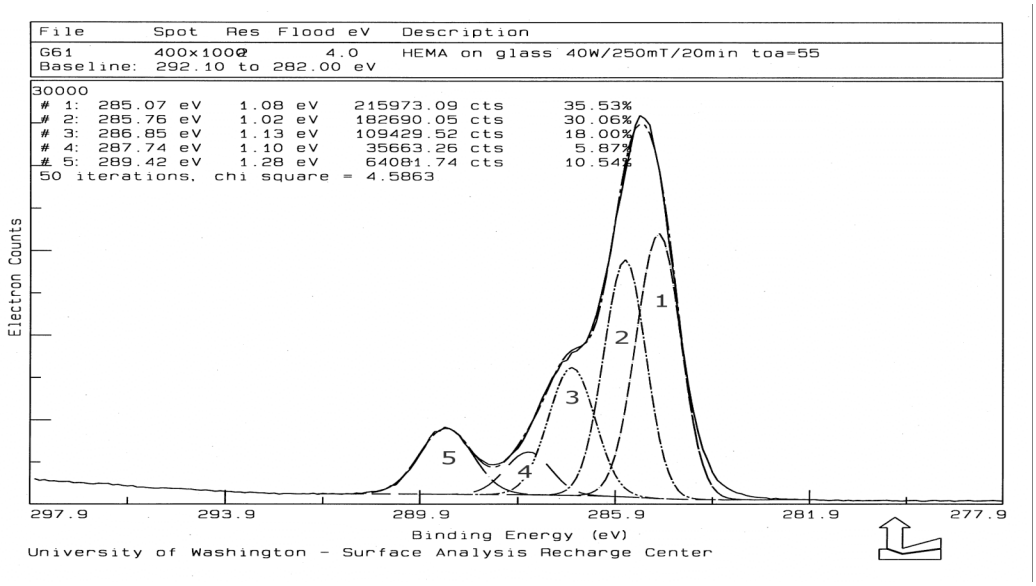

Figure 4-6. High resolution C 1s spectrum of ppHEMA on a glass cover slip.

A theoretical 4-peak spectrum from conventional poly(HEMA) would have peaks at the following eV, with relative peak area in parentheses: 285.0 (2); 285.7 (1); 286.6 (2); 288.9 (1). These peaks would represent the six different environments of the carbon atoms in poly(HEMA). As can be seen in Figure 4-6, the ppHEMA spectrum differs markedly from the conventional poly(HEMA) reference spectrum.

ESCA analysis of plasma-deposited HEMA films on BioSpan / Mannitol / Hirudin matrices revealed that the RFGD plasma films showed evidence of considerable oxygen loss (as evidenced by elemental survey spectra), and the C 1s spectra (Figure 4-7, 3-peak fit for the 40 W spectrum) of plasma films also suggested ester and hydroxyl loss. This chemical change in the structure of HEMA films is indicative of oxygen abstraction and increased film cross linking, which was anticipated to be a desired

trait in this type of diffusion control application. It was this type of chemical analysis that guided further development of plasma treatment protocols for coating and release experiments.

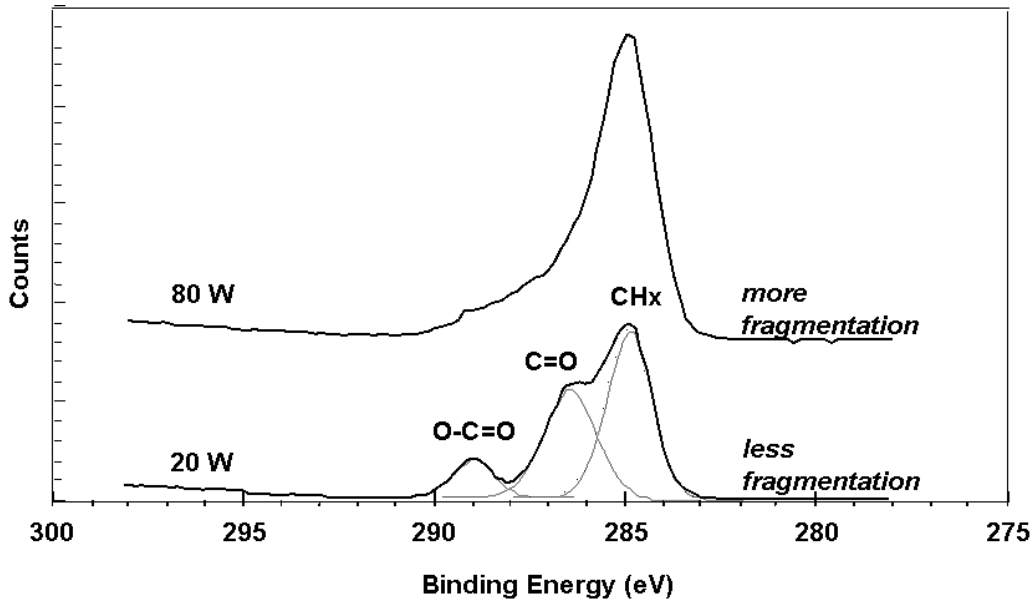

Figure 4-7. High resolution C 1s spectra of ppHEMA deposited on hirudin matrices.
Plasma conditions as noted above count trace; both at 200 mtorr, 20 min.

4.2 n-BMA Films

Plasma polymerized n-butyl methacrylate was deposited on glass cover slips under the same conditions as those for ppHEMA, described in Section 4.1 (40 W, 250 mtorr, 20 minutes). The survey spectrum is shown in Figure 4-8, and the high-resolution C 1s spectrum is shown in Figure 4-9.

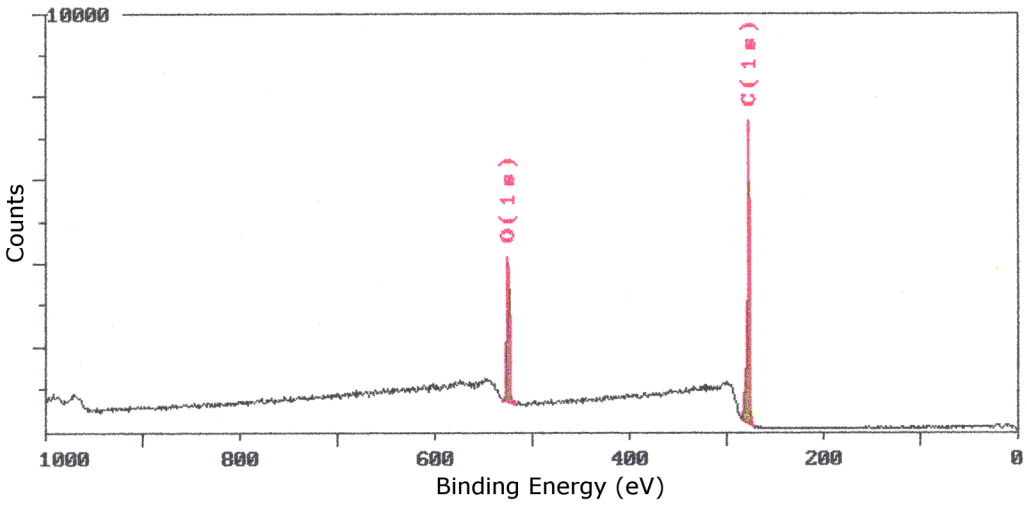

Figure 4-8. Survey spectrum of ppBMA deposited on a glass coverslip.

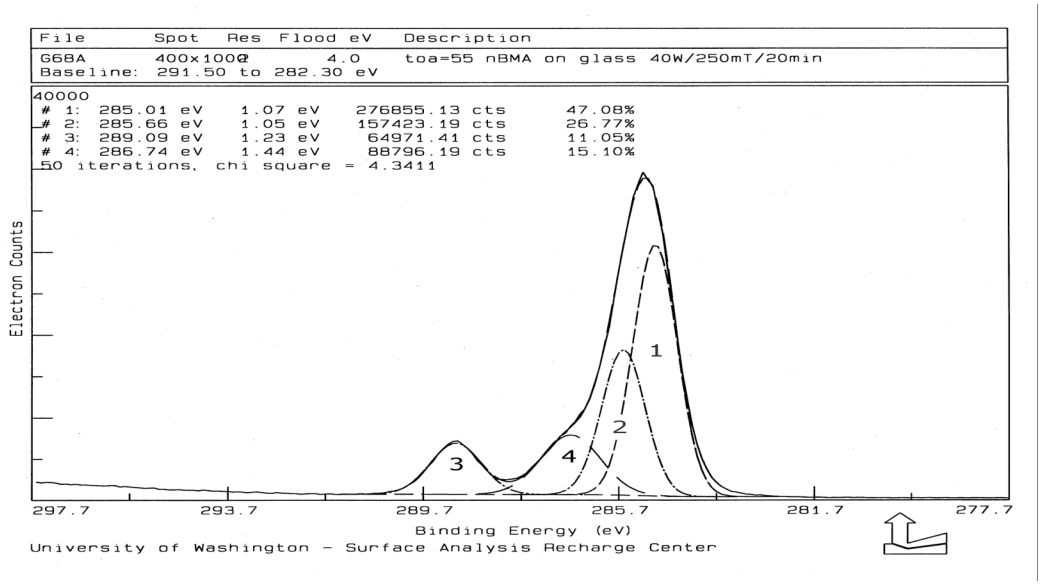

Figure 4-9. High resolution C 1s spectrum of ppBMA deposited on a glass coverslip.

The surface composition of ppBMA films on glass under these deposition conditions was 81.6% C, 18.4% O (stoichiometry for conventionally polymerized poly(BMA) is 80% C, 20% O). The high resolution spectrum shows a 4-peak fit, which reflects the four chemical binding environments of carbon in conventionally polymerized poly(BMA); these are C-Hx / C-C (peak 1, 285.0 eV); C_{β} ester (peak 2, 285.7 eV); C-O ether / alcohol (peak 4, 286.5 eV); C-C=O ester (peak 3, 289.0 eV). The

relative areas of these four peaks in conventionally polymerized nBMA are: 5:1:1:1, or in percentages, 62.5:12.5:12.5:12.5. The plasma-deposited nBMA shows some broadening of peaks 1, 2, and 4, which is typical for methacrylate plasma polymers.

5 CONTROLLED RELEASE OF ECHISTATIN

Release of an incorporated antithrombotic agent or drug from a blood-contacting material could inhibit device-related platelet aggregation, particularly at the material surface, where it is most needed. Qualities for such a released agent might include potency and specificity; as described in the Introduction (Chapter 1). Echistatin was selected as a candidate to demonstrate this type of controlled release due to these properties and the experience of our research group on conducting platelet-based assays.

5.1 Echistatin-containing Matrix Fabrication

Echistatin (recombinant, from Sigma Chemical Co., St. Louis, MO) was received as a lyophilized powder. 50 µg of echistatin was reconstituted in 25 µl of citrate-phosphate buffer (concentration 2 mg/ml). The echistatin was then iodinated using the iodine monochloride (ICl) technique, as described in Section 3.7.1 to a specific activity of 16 µCi/µg; excess iodine was removed by gel filtration chromatography. Matrix fabrication proceeded as described in Section 3.8, using BSA as an excipient and pore former at an overall loading of 50% (w/w). The formulation was dried under vacuum to constant weight, and then at least three (3) 11 mm sample disks were cut from the dried films for each treatment protocol. The final amount of echistatin in each disk averaged 9.6 µg total; the total weight of each disk averaged 122 mg, yielding a mass ratio of active agent, echistatin, to (BSA carrier protein + matrix) of 1:12,700. This protocol yielded matrices of reasonable uniformity and suitability for plasma coating treatment. Fabricated echistatin disks were generally kept refrigerated at 4 °C to maintain peptide activity.

5.2 HEMA RFGD Plasma Treatment

Echistatin matrices were treated at a reduced temperature in order to preserve the biological activity of echistatin as much as possible. The procedure described in Section 3.9.2 was used. The

cooling fluid in the circulating loop was a mixture of glycerol and water , 50% vol./vol. cooled to approx. 15 °C with solid CO_2 (dry ice).

Table 5-1. HEMA plasma treatment conditions for echistatin matrices.

Sample code	Ar plasma			HEMA plasma		
	Time (seconds)	Power (W)	Pressure (mtorr)	Time (seconds)	Power (W)	Pressure (mtorr)
A275 (B1-B3)	30	40	250	300	40	250
A279 (C1-C3)	240	40	250	300	40	250
A265 (A1-A4)	(Control - No plasma treatment)					

Plasma treatments were conducted under continuous wave conditions. The two sets of matrices differed only in the time of argon plasma pretreatment. Three replicate samples were prepared for each plasma treatment.

5.3 Microscopy of Echistatin-Containing Matrices

5.3.1 Light Microscopy

Micrographs of a thin section of BioSpan matrix with incorporated echistatin and FITC-BSA are shown in Figure 5-1. Fluorescence microscopy clearly reveals the dispersed structure of the particulate protein mixture. The cloudy appearance toward the center of the matrix might be due to some suspended fines that were generated during the mixing procedure. These fines most likely will not be released from the matrix since they might not interconnect with the larger pore-forming particles, but rather remain fully suspended and enclosed in the matrix material.

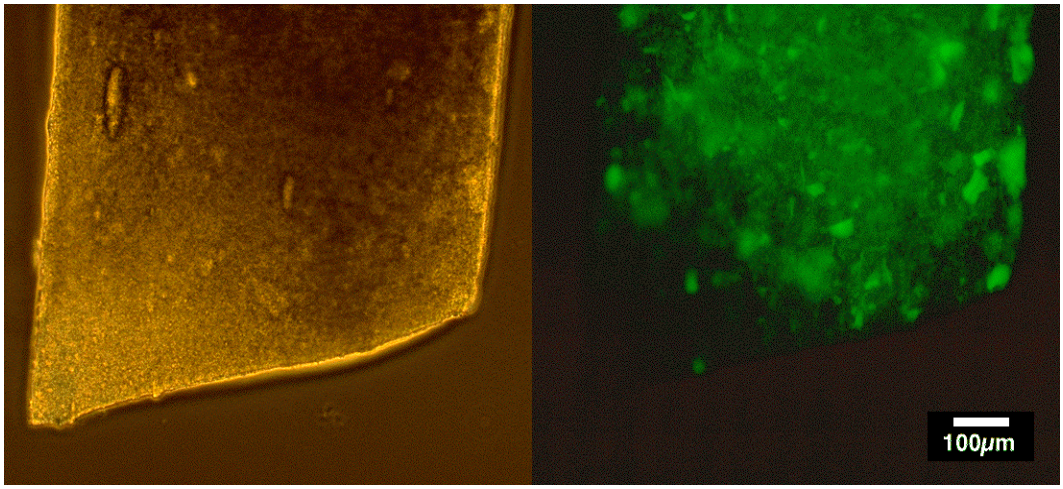

Figure 5-1. Light microscopy of BioSpan – FITC-BSA - echistatin matrix.
Left, phase illumination; right, epifluroescent illumination.
Bar = 100 µm (both panels are at the same scale and magnification)

Comparison of the phase micrograph with the fluorescent reveals that entrapped echistatin / FITC-BSA domains are not always clearly visible by phase microscopy. Conversely, entrapped bubbles and other granular structures in the phase micrograph do not cause appreciable fluorescence. This study showed that it is useful to have complimentary optical analysis techniques to elucidate the structure of the material.

5.3.2 Scanning Electron Microscopy

A cross-section of a BioSpan matrix with incorporated echistatin / BSA mixture is shown in Figure 5-2.

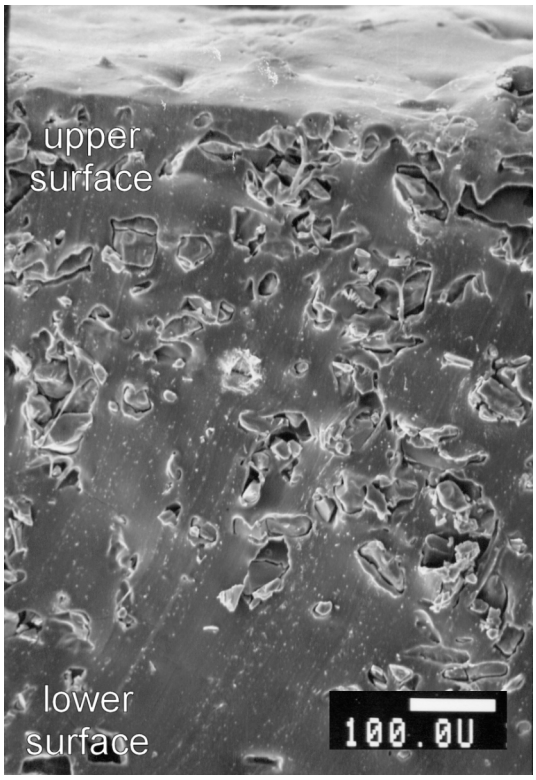

Figure 5-2. SEM of cross section of BioSpan -- echistatin / BSA matrix, post-release.
Bar = 100 μm.

The interconnected pore structure of this matrix at 50% w/w loading is readily apparent. The echistatin / BSA particulate material retains its structure even after the mixing, casting, and drying steps with the polymer solution. The diagonal streaks along the face of the cross-section are artifacts caused by a razor blade used for sectioning. Matrices appeared very similar to those described in previous publications [56], [57], even though the matrix systems in those publications were composed of a different polymer (ethylene vinyl acetate, EVAc) and polypeptide / excipient (BSA, myoglobin).

Figure 5-3 shows the upper surface (as cast) of the BioSpan – echistatin / BSA matrix, pre-release (that is, before introduction to release buffer, and after the end of the release experiment). The pre-release surface appears relatively continuous and non-porous, though a little uneven in places. (Plain, unloaded BioSpan cast as a film was smooth and uniform in appearance; photo not shown.)

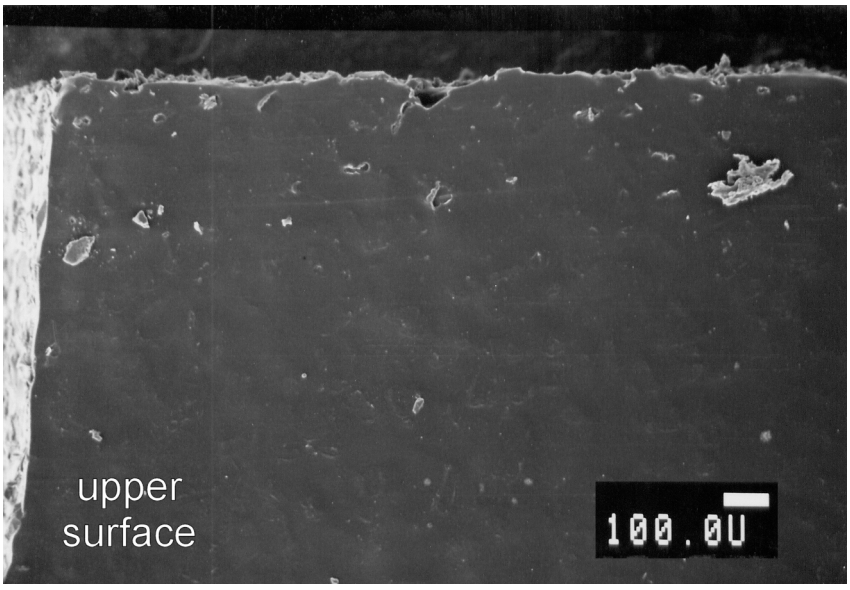

Figure 5-3. BioSpan – echistatin / BSA matrix, upper surface (as cast), pre-release.
Bar = 100 μm.

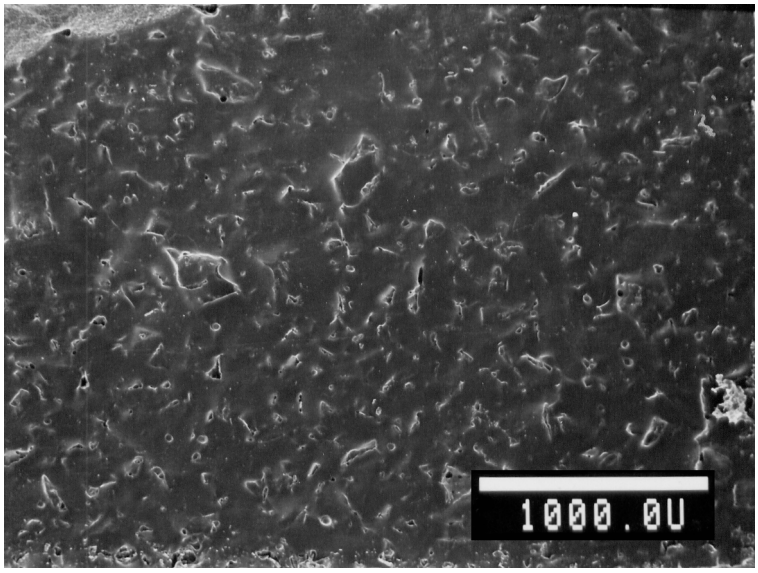

Figure 5-4. BioSpan – echistatin / BSA matrix, upper surface (as cast), post-release.
Bar = 1000 μm.

Figure 5-4 shows the upper surface after a 180 hour release in buffer. Pore structures are clearly visible where there were none pre-release. The matrix shows even distribution of particulate and

also even distribution of formed pores. Figure 5-5 shows the lower surface of the same matrix as in Figure 5-4 (after 180 hours release).

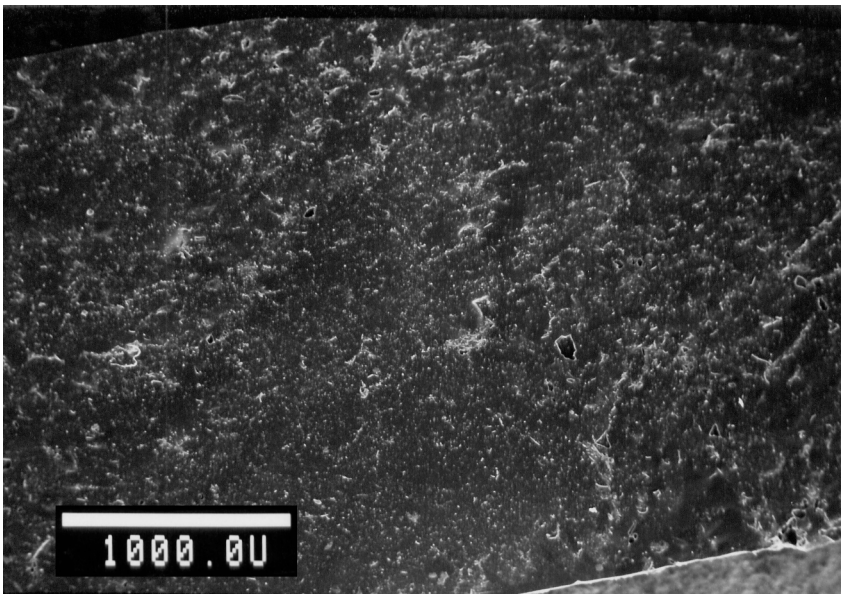

Figure 5-5. BioSpan – echistatin / BSA matrix, lower surface (as cast), post-release. Bar, 1000 μm.

The morphology of this surface is much different; it appears smoother, with fewer pores. This is most likely the result of this surface being the one formed in contact with the PFA casting tray, which had a very smooth machined surface. In addition, it appears that the echistatin / BSA particles did not settle to the bottom of the tray and form pores immediately at the surface of the matrix. This anisotropy can be seen in the cross-section (Figure 5-2), where the particles decrease in density toward the lower surface of the cast matrix. The reason for this anisotropy is not immediately clear, but one reason might be that the density of the particulate material is less than the curing polymer, and therefore the particles may have slight buoyancy and float toward the surface of the casting tray as the matrix cures. This may happen even though the polymeric solution is very viscous.

5.4 Controlled Release Results

Based on previous studies of plasma-treated porous membranes, it was hypothesized that increasing the argon pretreatment times would cause a decrease in the release rate. The postulated

mechanism for this effect was that longer argon treatment would produce more reactive sites on the matrix surface, and therefore more available sites for subsequent HEMA monomer attachment and polymerization. A thicker and/or more crosslinked HEMA membrane surface was thought to be the end result of this treatment, and therefore lead to a reduced release rate through this membrane.

The control set of matrices ("A", Figure 5-6) showed a quick initial release phase within about 24 hours to almost 95% complete fractional release. The shape of the release curve was as expected, following a classical model of diffusion [27] for this type of matrix system.

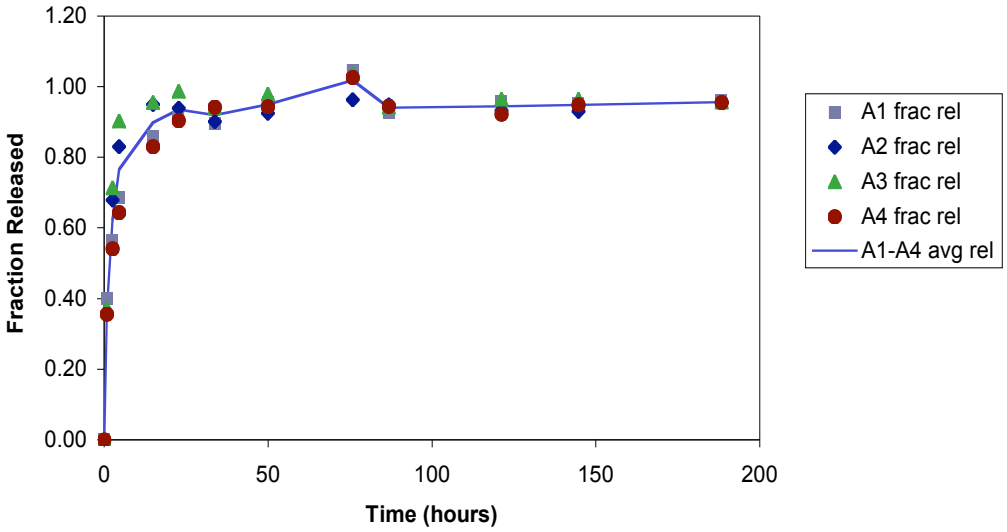

Figure 5-6. Echistatin release from untreated control matrices.
n = 4; line denotes the calculated average release.

Release curves for the HEMA plasma treated matrices (30 s Ar-plasma pretreatment, Figure 5-7; and 240 s Ar-plasma pretreatment, Figure 5-8) show trends similar to the control matrices. The rates of release of the plasma-treated matrices (slope of the graph) were not greatly affected in aggregate, when taken in an average sense; however, some individual matrices show a trend toward decreased release rate. Individual matrix release data are included here with average release data for this reason.

For example, in control sample set “A”, individual samples A2 and A3 (diamond and triangle symbols, Figure 5-6) show an early tendency to release quickly, even though the final fraction released by all samples is essentially the same at later timepoints. In another case, individual sample “B1” (diamond symbols, Figure 5-7) exhibited lower release at later timepoints (ca. 0.80 fraction released) than samples B2 or B3 (ca. 0.93 – 0.95 fraction released).

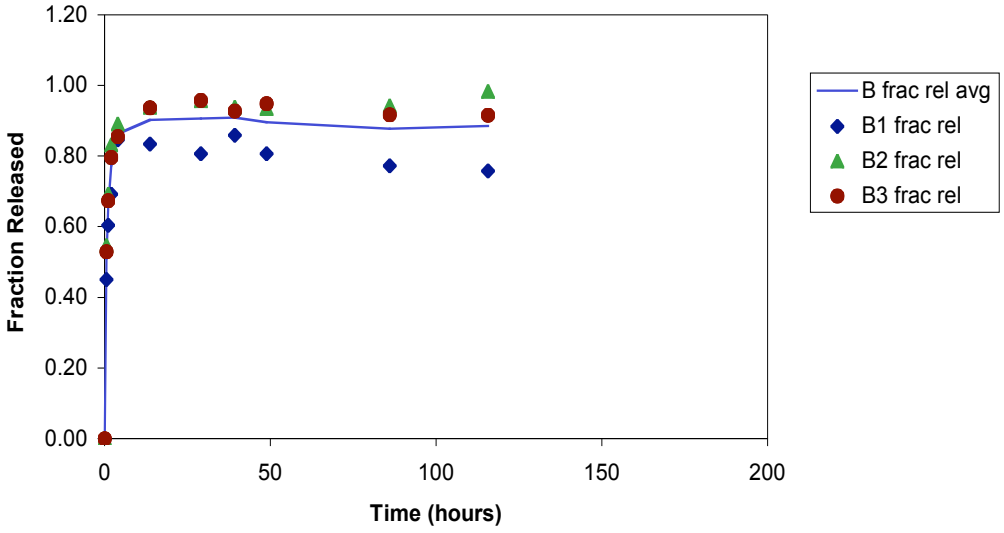

Figure 5-7. Echistatin release from ppHEMA-treated matrices 30 s Ar pretreatment. Time scale is adjusted to allow visual comparison with control data.

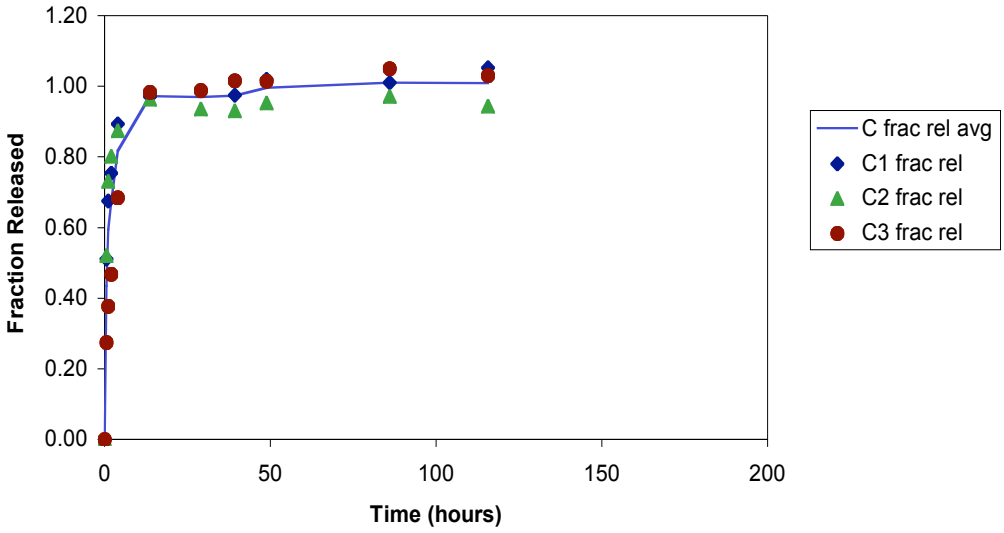

Figure 5-8. Echistatin release from ppHEMA-treated matrices, 240 s Ar pretreatment. Time scale is adjusted to allow visual comparison with control data.

Matrix set "C" (240 s Ar pretreatment) shows a final release level at approximately 0.97 fractional release. At early timepoints, sample C3 shows a initial release rate that is significantly lower than the average release for set C. This can be visually emphasized by plotting the release curves on a time$^{0.5}$ scale (Figure 5-9, sample C3 shown with square markers).

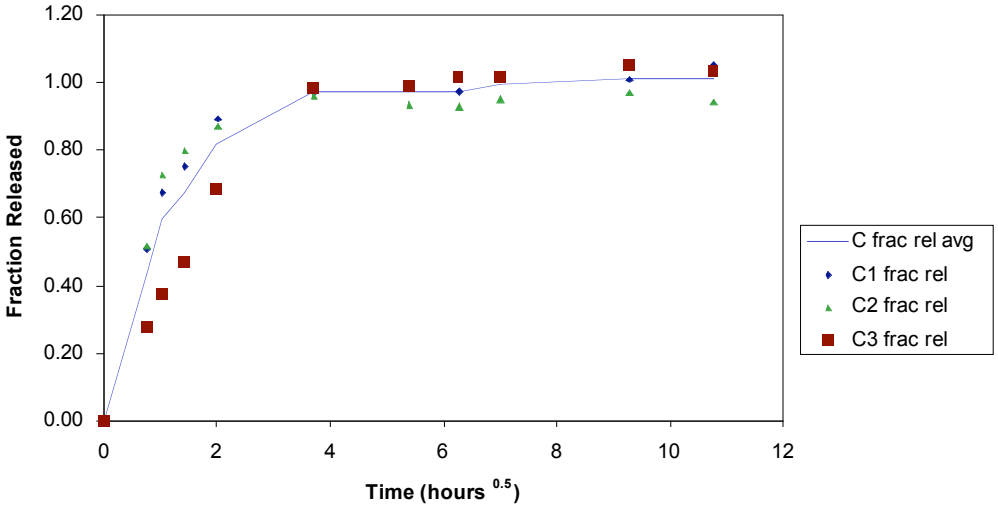

Figure 5-9. Echistatin from ppHEMA-treated matrices, 240 s Ar pretreatment, early timepoints. Note that time scale shows the square root of time.

Figure 5-10 shows the calculated average release rates for the two plasma-treated matrix sets plotted vs. control untreated matrices.

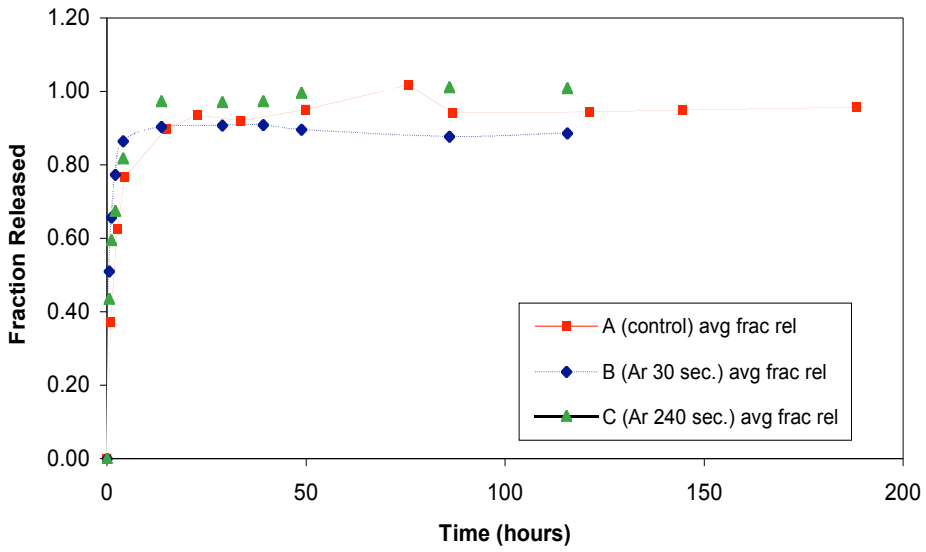

Figure 5-10. Average fractional release from echistatin-loaded matrices.

The overall impression of this set of data at this time scale is that there is little difference in the release characteristics of the control vs. treated matrices.

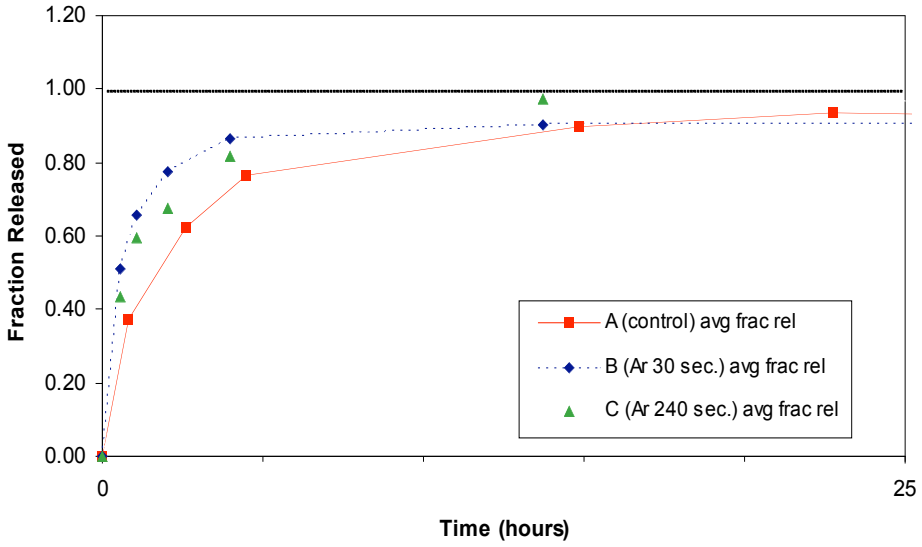

Figure 5-11. Average fractional release from echistatin-loaded matrices, early timepoints.

Comparison of individual matrices at early timepoints (Figure 5-11) shows some observable differences between plasma-treated vs. control matrices. Most notable, early timepoints seem to indicate that the release rate during the initial 24-hour period from the control matrix (square symbols, solid line) was lower than that of either plasma-treated membrane, which is contrary to the expected result. In addition, the variability within individual matrix sample sets would make direct comparison difficult.

Reasons for this discrepancy could be due to unexpected effects of the plasma treatment on the matrix, for example, damaging or opening the surface pores of the matrix. This might negate any reduction in diffusion properties away from the surface of the matrix due to plasma treatment. Differences in the spatial distribution of peptide throughout the thickness of the matrix could cause differences in the release characteristics between sets of matrices as well.

5.5 Biological Assay of Released Echistatin

Released echistatin was assayed in a stirred cuvette aggregometer as described in Section 3.13. The purpose of this was to determine if released echistatin retained its activity and potency after the matrix preparation, plasma treatment, and release protocols. Samples of release buffer from preparation B1, described in section 5.2, were taken at the final time point of 115 hours.

Platelets responded in a dose-dependent manner; that is, as the concentration of the released echistatin increased in the mixed platelet preparation, the inhibition of aggregation also increases, and therefore light transmittance does not increase as much as the control, untreated, non-inhibited platelets. This effect manifests itself on the aggregometry trace as a smaller curve (suspension still turbid) and a smoother curve (fewer clumping platelets and a more uniform solution).

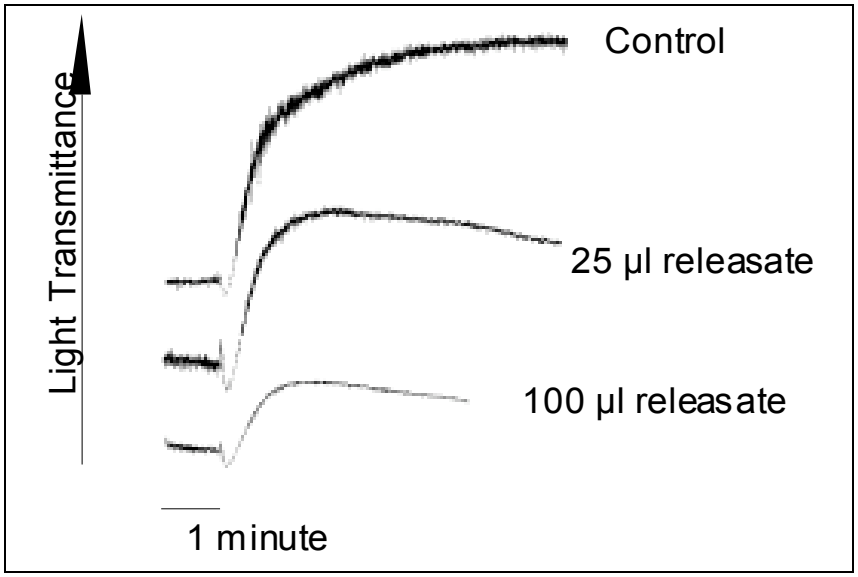

Figure 5-12. Effect of echistatin released from matrix B1 upon platelet aggregation.

Samples of release buffer were also taken from release preparation C2, described in Section 5.2, were diluted and mixed with platelets.

Platelets responded in a similar dose-dependent manner as with released echistatin from sample B1.

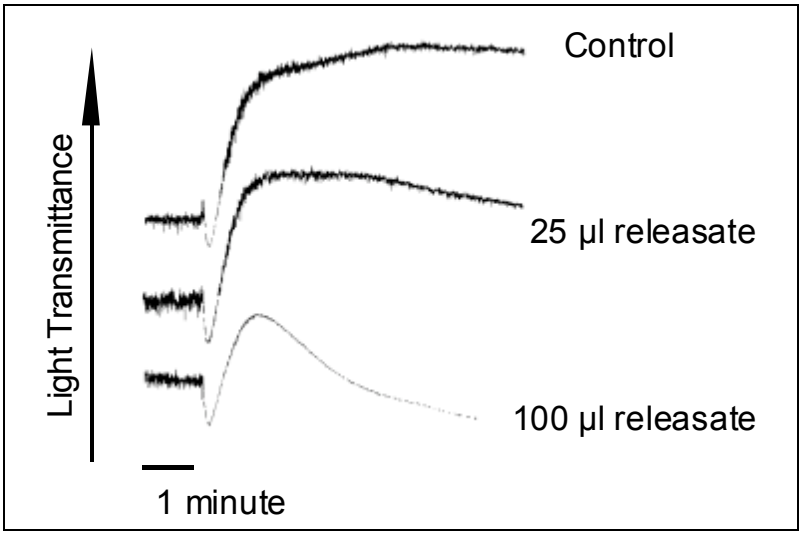

Figure 5-13. Effect of echistatin released from matrix C2 upon platelet aggregation.

A control experiment was performed on as-received echistatin, to demonstrate the potency and action of the source material. The results are shown in Figure 5-14. A known dilution series of echistatin was prepared in platelet suspension buffer (PSB) and the inhibitory effect of the echistatin on the aggregation response of platelets was measured.

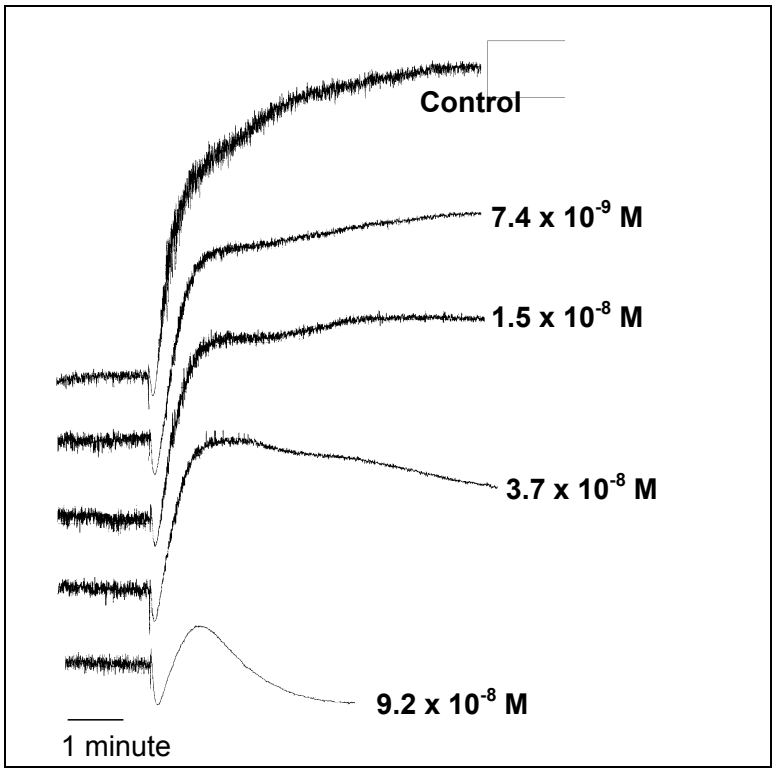

Figure 5-14. Aggregometry with as-received (control) echistatin.

Aggregometry traces were quantified by a semi-graphical method by measuring the final level and normalizing it to the control aggregation (no echistatin in buffer). By the trend shown in this graph, it could be estimated that the IC_{50} of this particular echistatin-platelet experiment was approximately 3 x 10^{-8} M, or about 30 nM. This is in excellent agreement with the published literature value (see Section 3.5.1).

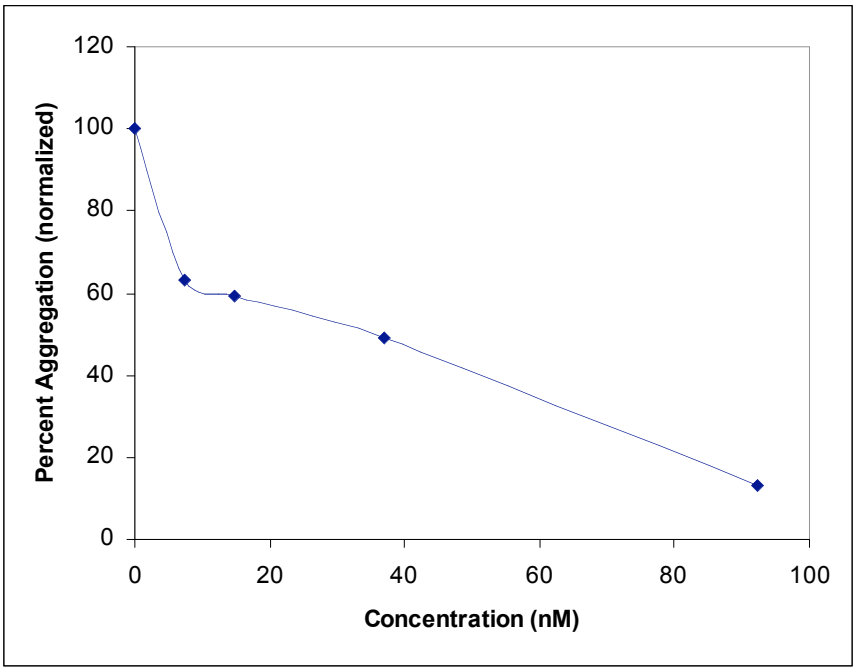

Figure 5-15. Aggregation with as-received (control) echistatin.

Exact quantification of released echistatin was difficult at best because a separate mass determination was not done. That is, the measured amount of echistatin used to calculate release values was calculated based on measured released labeled echistatin; a determination independent of iodine label concentration, was not done. Also, quantification of aggregometry data with this experimental setup can be highly subjective; for instance, drawing a slope to express the initial aggregation rate based on visual estimation of the aggregometry trace can be error-prone. In addition, some researchers use the kinetics of aggregation (rate) rather than the final extent of aggregation to compare inhibition of aggregation. Bearing this in mind, a preliminary calculation based on the control aggregometry experiment can yield a rough estimate of the echistatin present in the sample.

Assuming that the released echistatin was fully labeled, at the end of release of disk B1, the final fraction released was 0.76 times the initial loading, measured by radioactivity, which was estimated to be 9.6 μg per disk. The released amount of 7.3 μg was in a volume of 3 mL of releasate, yielding a final release concentration of 2.4 μg/mL, or 4.4 x 10^{-7} M (formula weight of echistatin =

5417 g/mole). This concentration of the released aliquot volume was diluted into the final aggregometer volume, which was 500 μL. By visual interpolation of the final aggregation extent and using the graph of control aggregometry (Figure 5-15), an estimate of the concentration can be determined. This was compared with the calculated echistatin concentration from amounts contained in the matrix, and it was assumed that all measured radioactivity was directly attributed to labeled echistatin (no free ^{125}I), which was a good assumption based on gel chromatography results (not shown).

Table 5-2. Echistatin concentration estimation.

B1 release volume added to aggregometry (μL)	Final aggregation (percent of control)	Estimated concentration by aggregation (nM)	Estimated concentration by calculation (nM)
100	20	80	89
50	34	60	44
25	43	40	22

Comparing the last two columns, visual estimation by aggregometry agreed with calculated echistatin amount, at least in trend and magnitude. Upon inspection of Figure 5-15, it is apparent that the most reliable portion of the constructed calibration curve is the 'linear' region from approximately 10 nM to 95 nM concentration. Clearly there is a steep nonlinear relationship at very low echistatin concentrations, the region less than 10 nM to zero (control). The likely presence of aggregating and dis-aggregating clusters of platelets in this low concentration region would complicate visual inspection analysis of aggregation data. At high echistatin concentration, greater than 90 nM for example, measuring the volumetric effects of light shining through a turbid platelet solution might complicate graphical analysis in this region. These factors would probably limit effective calibration and interpretation of aggregation with echistatin inhibition results to a region from approx. 10 to 90 nM concentration in our experimental setup.

In conclusion, matrices were formulated that contained stable echistatin, and that echistatin was released in a fashion that conformed to previous models of drug elution and release from a matrix-

type device. These matrices delivered active echistatin with potency that was very similar to control echistatin. Moreover, the general experimental method of matrix fabrication, testing, handling, and radioactive labeling and measurement as a tracer system was validated.

The coating method using RFGD plasma-polymerization, however, showed little difference among the matrices tested. This concern led to refinement of the matrix casting protocol, and attempted improvements of the plasma polymerization coating procedure. Some of these refinements will be discussed in conjunction with the controlled release of other agents, namely hirudin and RGDS-6, in the following chapters.

6 CONTROLLED RELEASE OF HIRUDIN

Hirudin was chosen for a model release system because it was thought that, like echistatin, surface release of an antithrombotic agent would be desirable in the design of an actively antithrombotic material. Hirudin was chosen because it is potent, is a so-called "direct" antithrombin (does not require cofactors for its activity), and is readily available for purchase from several commercial sources. In addition, it is currently available in recombinant form, which has decreased its cost and increased its availability over naturally isolated sources (e.g. leech preparations). Hirudin is also comparable in size and molecular weight to echistatin.

Because of these factors, hirudin-containing matrices were fabricated to test another possible route of antithrombotic agent release. These experiments were performed in collaboration with Dr. Dae-Duk Kim.

6.1 Hirudin-containing Matrix Fabrication

Hirudin was incorporated into polyurethane matrices in a similar fashion to echistatin-containing matrices. Two different substances were used as pore-forming agents: bovine serum albumin (BSA) and mannitol, and the release characteristics of matrices formed by these two different pore-formers were compared.

Specific fabrication conditions are as follows: 1800 units of hirudin (518 U/mg, lyophilized) were reconstituted in deionized H_2O. The hirudin solution was added to a 1 g / 10 ml H_2O (100 mg/ml) solution of pore former (BSA or mannitol), lyophilized to dryness, and ground to a powder. This powdered hirudin/pore-former mixture was then sieved to three particle size fractions (< 63, 63-90, 90-125 μm). Size-fractionated powder was then mixed with BioSpan at approximately 15% solids concentration in order to yield a final weight fraction of hirudin/pore-former of 40% wt/wt. Films were cast in PTFE trays, degassed, dried at 60 °C, ambient pressure, for 24 hours, then at room temperature and vacuum for 48 hours. Matrices were then cut into 9.5 mm diameter disks, and then stored at 4 °C until used in release experiments.

This procedure produced hirudin-containing films that were reasonably smooth, uniform, and suitable for plasma treatment. Matrices made with BSA had a slightly more mottled appearance than those made with mannitol as the pore-former.

6.2 HEMA RFGD Plasma Treatment

A procedure similar to that used to treat echistatin-containing matrices was used to treat hirudin-containing matrices. Hirudin matrices were pre-treated with argon plasma (40 W, 175 mtorr, 5 minutes), then coated with HEMA plasma, conditions of 40 W, 150 mtorr, and 10 minutes deposition time.

The suitability of the plasma treatment was verified using ESCA analysis and microscopic analysis. Matrices were found to have expected chemical composition and physical appearance.

6.3 Microscopy of Hirudin-Containing Matrices

Scanning electron microscopy of BioSpan – BSA – Hirudin matrices showed a marked change in matrix morphology due to the dissolution and release of entrapped protein – peptide mixture (Figure 6-1). The orientation of the matrix in the micrograph is a vertical cross section; that is, the top of the photograph represents the upper surface of the matrix, as cast in the PFA mold. The matrix shows some anisotropy in the distribution of particles (and therefore, voids, after dissolution and release) from top to bottom. At the bottom surface of the matrix, near the mold, it appears that the matrix contains fewer connecting inclusions. This type of anisotropic distribution was also seen in other mixtures of BioSpan, with the other proteins / peptides (echistatin and RGDS-6), and excipients (such as PEG). Therefore, it was most likely due to the casting protocol, rather than specific interactions and characteristics of the materials used in any particular matrix formulation.

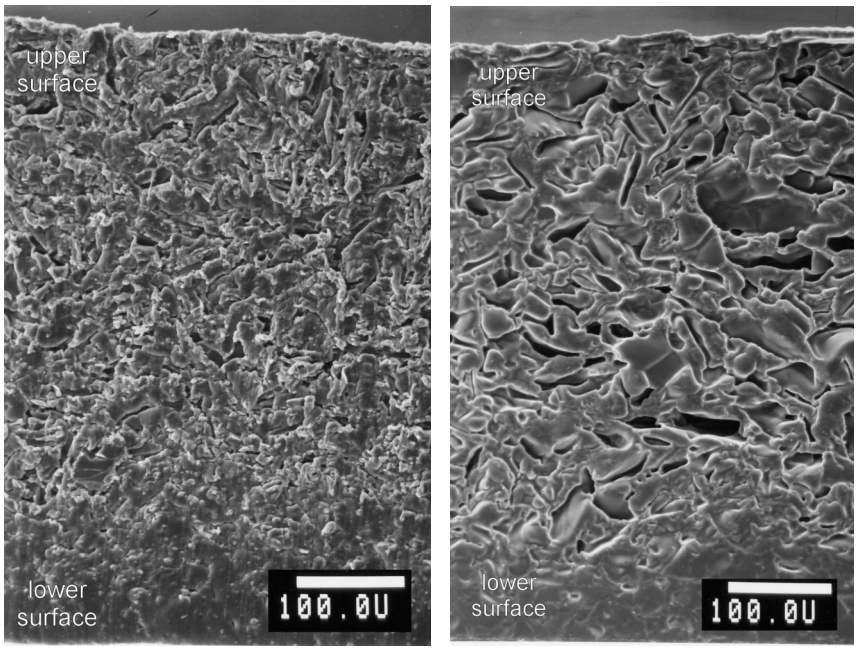

Figure 6-1. SEM of BioSpan - BSA - Hirudin matrix (40% loading).
Left panel, matrix pre-release; right panel, post-release. Bar = 100 μm.

6.4 Controlled Release Results

Release of hirudin was measured using a thrombin inhibition assay (Section 3.14). The assay was a functional, calibrated quantitative measurement for hirudin and its activity. Specifics of the assay are discussed further in Section 6.5.

Figure 6-2 shows the controlled release data from matrices fabricated with hirudin and mannitol as the excipient. Particles were sieved to less than 90 μm before incorporation with the polymer casting solution. As the amount of "pore-former", or excipient, was increased as a weight fraction of matrix, the rate of release, and total amount of hirudin released, also increased.

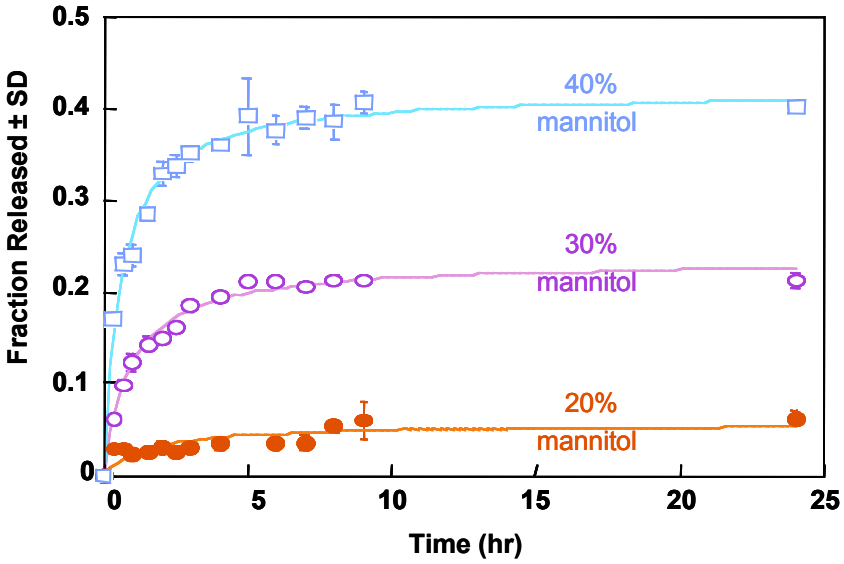

Figure 6-2. Loading of mannitol-hirudin matrices.

For both BSA and mannitol as pore formers, increasing particle size increased the total amount of released hirudin (Figure 6-3).

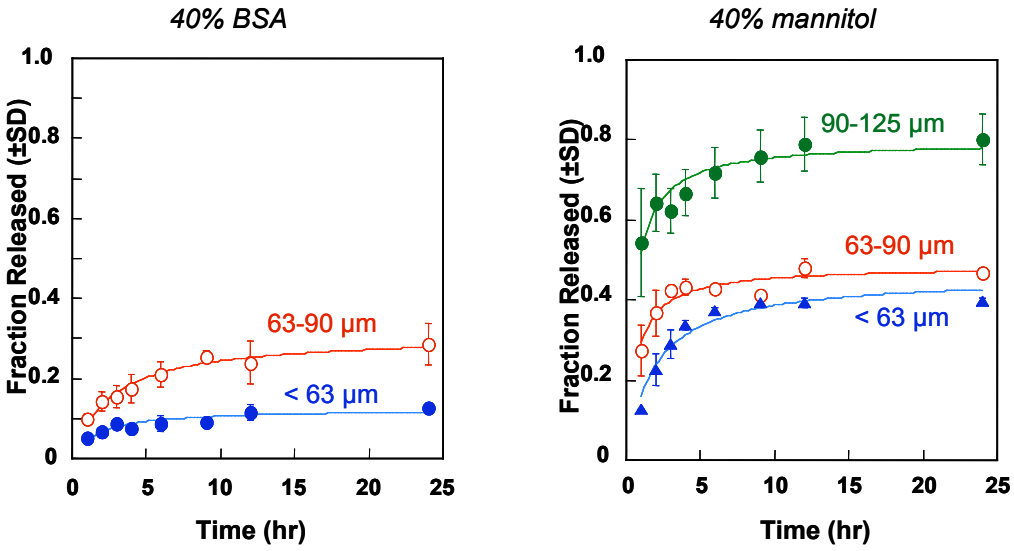

Figure 6-3. Hirudin release as a function of particle size.

HEMA-coated matrices showed a decreased release rate and amount as compared to control.

Figure 6-4 shows the release from a matrix containing hirudin with mannitol as a pore-forming agent, and Figure 6-5 shows release from a matrix with BSA as a pore-forming agent. HEMA coating has a proportionally greater effect of reducing release from BSA-hirudin matrices than mannitol-hirudin matrices. The reason for this difference in release rates, despite identical coating protocols, is unclear.

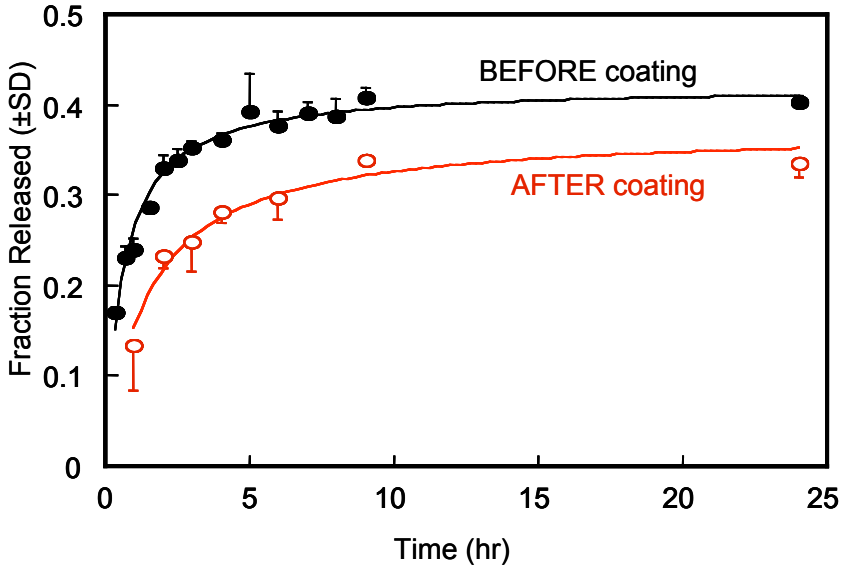

Figure 6-4. HEMA plasma treatment reduced release from mannitol-hirudin matrices.

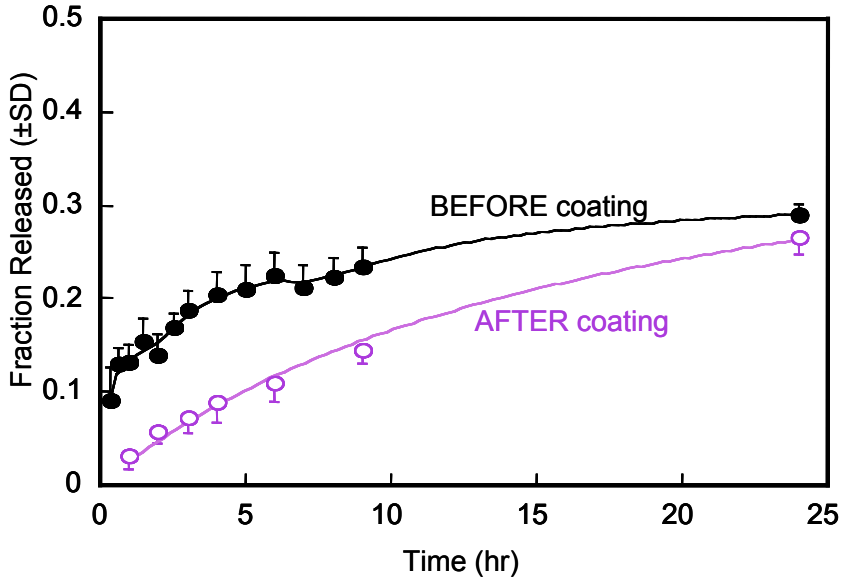

Figure 6-5. HEMA plasma treatment reduced release from BSA-hirudin matrices.

Although the release rate was not decreased to a completely zero-order regime, the coating protocol was shown to be effective in reducing the rate of release. Additionally, the formulation and coating protocol was shown to preserve a significant fraction of the hirudin activity.

6.5 *Biological Assay of Released Hirudin*

Hirudin was assayed by a thrombin inhibition method, as described in Section 3.14 and the mechanism of action of which is shown in Figure 6-6.

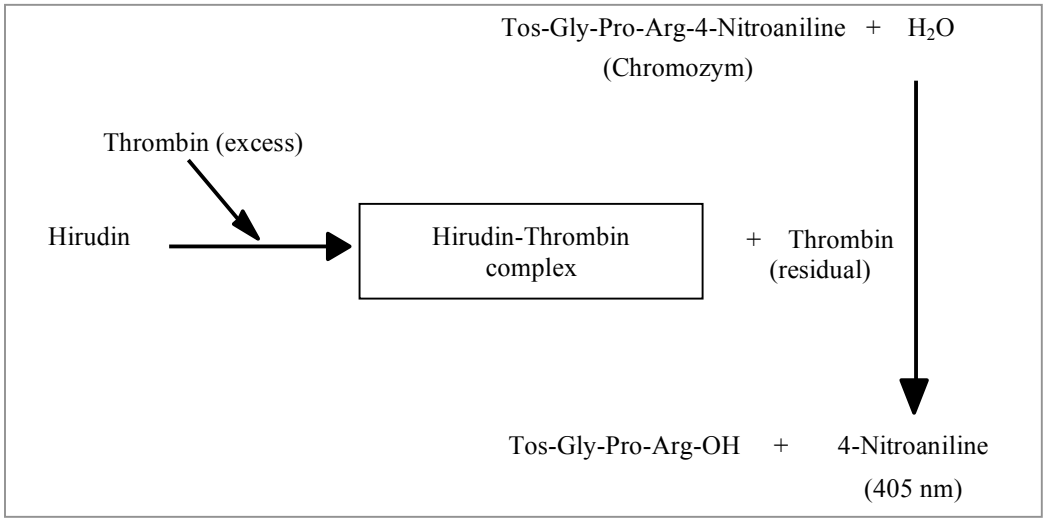

Figure 6-6. Reaction scheme for hirudin assay.

The release medium was sampled at various timepoints and assayed for activity, and this assay was assumed to be quantitative. The hirudin assay showed a very linear response in the concentration range expected from the release experiments (Figure 6-7). A hirudin dilution series was made in Tris-HCl, pH 7.4; thrombin was added to 0.83 U/ml final concentration and incubated for 1 minute. Chromozym substrate was added to 0.32 mM final concentration, and kinetic analysis was performed at 2 minutes reaction time at 405 nm. In addition, the hirudin preparation demonstrated expected normal thrombin inhibitory activity.

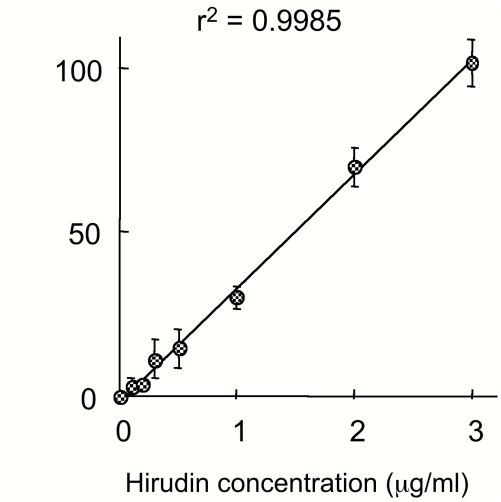

Figure 6-7. Hirudin calibration assay with as-received hirudin.

Studies were also conducted in order to determine the stability of hirudin in a BioSpan – mannitol – hirudin (BMH) matrix. Samples cut from the same original matrix were stored at 4 °C for 42 days. It was found that released hirudin had essentially the same release profile and activity in the stored samples as the original samples (Figure 6-8).

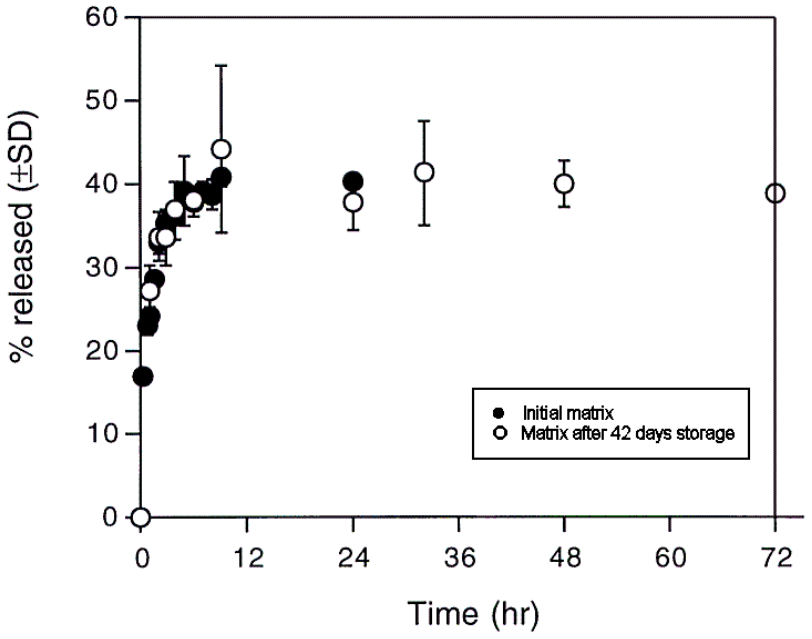

Figure 6-8. Stability of hirudin in BioSpan – Mannitol matrices.
Hirudin matrix was kept refrigerated (at 4 °C), then released into Tris-HCl (pH 7.4) buffer after storage time. n=3

7 CONTROLLED RELEASE OF RGDS-6

7.1 RGDS-6-containing Matrix Fabrication

RGDS-6 (also referred to as RGDSGY) peptide-containing matrices were fabricated in a similar fashion to echistatin and hirudin matrices. Several formulations of RGDS-6, with a range of PEG excipient molecular weights, were made to determine if PEG molecular weight (MW) had an effect on:

- the ease of overall handling and formulation;
- the morphology of the resulting matrices, and in particular, to determine the MW (or range of MW) that produced the smoothest, most uniform films;
- the release characteristics of the RGDS-6; and
- the plasma deposition characteristics of the various monomers.

The number average molecular weights for the PEG excipients used were, in Daltons: 3,400 (3.4k); 10,000 (10k); 20,000 (20k); 100,000 (100k); 200,000 (200k); 400,000 (400k); and 1,000,000 (1M). 2,000,000 MW PEG was used in preliminary formulations but did not produce a suitable film when cast.

PEG was initially intended to serve as a discrete pore-forming agent in this formulation. However, under certain formulation conditions, PEG formed what appeared to be a polymer blend with BioSpan and appeared to form domains, and possibly phase-separate after mixing and drying. The morphology of this blend is discussed later in this chapter.

In addition, four different plasma treatments were applied to the various PEG MW matrices: argon, HEMA, n-BMA, and NIPAAm.

The loading level, or amount of PEG used, was held constant at 28% wt. /wt. for the different PEG molecular weights. This was done in order to reduce the possible confounding variables in the experimental design.

The initial RGDS-6 peptide was labeled to a specific activity of 283 mCi/mmol, or 432 μCi/mg. The final activity of each individual film casting was adjusted to be 1 x 10^7 cpm, to yield suitable counts per punched sample and per aliquot solution. As an example, an individual 9.5 mm matrix punched from a film casting emitted ~15,000 cpm at the start of a release experiment. This was equivalent to 8.5 x 10^{-6} mCi per sample.

Formulations and treatment options are summarized in the following table, although not all possible combinations were fabricated. The full selection of prepared samples is presented in Table 3-1.

Table 7-1. RGDS-6 formulation options.

PEG Molecular Weight, (Daltons)	Gas / Monomer	Plasma Variables
3,400	Argon	Time
10,000	HEMA	Power
20,000	nBMA	Pressure
100,000	NIPAAm	Continuous Wave (CW) or Pulsed
200,000		
400,000		
1,000,000		

7.2 Ar Plasma Treatment

Plasma treatment of matrices was performed as described in Section 3.9.3. In place of the monomeric deposition step, an argon plasma etch was conducted that was considerably longer than the initial short cleaning etch. This was done to compare argon treatment alone with the control matrices, which did not receive any plasma treatment at all. Also, formulations with three different PEG

molecular weights were used to determine if argon plasma treatment produced detectable differences in release characteristics.

Samples with this treatment are coded G72A (PEG-3.4k), G72B (PEG-10k), and G72C (PEG-20k).

7.3 HEMA RFGD Plasma Treatment

RGDS-6 matrices were treated with plasma polymerized HEMA to produce a coating on the cast matrices. Matrices were subjected to two different plasma polymerization treatments: 1) HEMA for 10 minutes, 40 W power, 150 mtorr pressure (sample code F190B, PEG-4k); and 2) 20 minutes, 40 W power, 250 mtorr pressure (sample codes G61A (PEG-3.4k), G65A (PEG-10k), G65B (PEG-20k), G65C (PEG-100k), G65D (PEG-200k)).

7.4 n-BMA RFGD Plasma Treatment

Matrices were treated in a similar fashion to the HEMA-treated matrices, with plasma polymerized n-BMA. Matrices were subjected to two different plasma polymerization treatments: 1) 10 minutes, 40 W power, 150 mtorr pressure (sample code F190C, PEG-4k); and 2) 20 minutes, 40 W power, 250 mtorr pressure (sample codes G68D (PEG-3.4k), G68E (PEG-10k), G68F (PEG-20k), G68G (PEG-100k), G68H (PEG-200k)).

7.5 NIPAAm RFGD Plasma Treatment

RGDS-6 containing matrices were treated with NIPAAm plasma in similar fashion as HEMA and n-BMA monomers, with continuous wave deposition of similar parameters (10 and 20 minutes, 40 W, 250 mtorr). An additional plasma deposition method was employed with NIPAAm which used a pulsed RF field (Section 3.9.4). This was done to investigate another possible route for control of plasma film characteristics.

Depositions with NIPAAm included an initial short duration, high power step (1 minute, 80 W power) that was thought to enhance adhesion of the NIPAAm layer to the substrate (Y. Vickie Pan, personal communication).

Samples were deposited with the following conditions: 1) 1 minute at 80 W / 10 minutes at 40 W, continuous wave conditions, 250 mtorr (sample codes G159 (PEG-400k), G165 (PEG-1M)); 2) 1 minute at 80 W / 20 minutes at 40 W, continuous wave conditions, 250 mtorr (sample codes G161 (PEG-400k), G167 (PEG-1M)); 3) 1 minute at 80 W / 20 minutes pulsed plasma, cycling between 40 W and 0 W, 100 ms duration, 50% duty cycle, 290 mtorr (sample codes G163 (PEG-400k), G169 (PEG-1M)). Control samples, with no plasma treatment, are coded G172A (PEG-400k) and G172B (PEG-1M).

7.6 Microscopy of RGDS-6-Containing Matrices

Figure 7-1 shows a cross-section of a matrix with PEG-4k as an excipient. The matrix was not plasma treated and was sectioned in its pre-release state. Small domains formed throughout the thickness of the matrix and were distributed fairly evenly. There was a small zone of fewer inclusions toward the lower surface of the matrix.

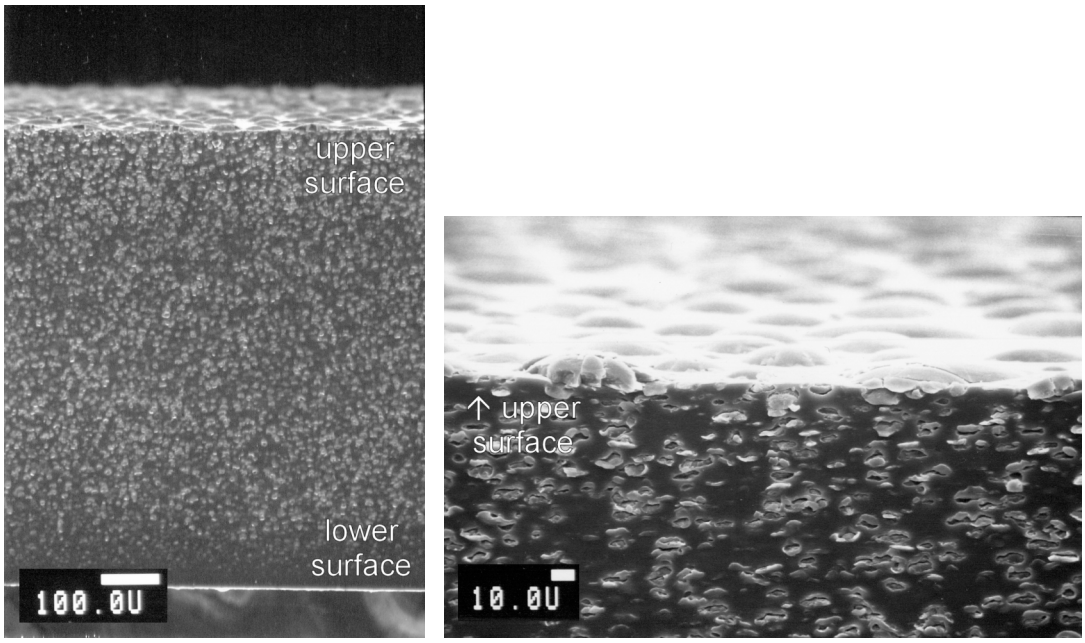

Figure 7-1. SEM of a matrix with PEG-4k excipient.
Cross sections; higher magnification on right. Control matrix – no plasma treatment, pre-release.
Bars = 100 μm and 10 μm, respectively.

Figure 7-2 shows the lower and upper surfaces of the matrix with PEG-4k as an excipient. The lower surface appears relatively smooth as it is the surface in contact with the PFA casting tray, which had a smooth machined surface. The upper surface has a "blistered" appearance and is due to some incorporated domains migrating to the surface and possibly coalescing together (surface features are larger than the incorporated particles in the cross-section view).

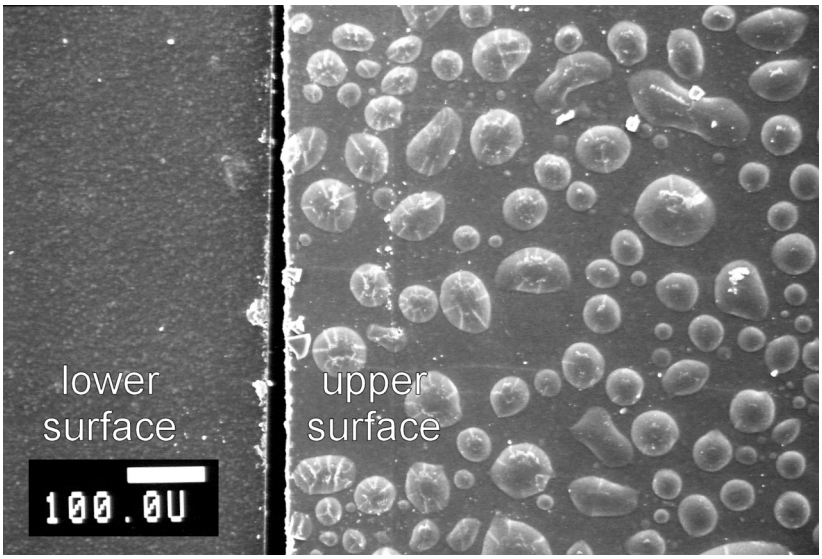

Figure 7-2. SEM of matrices with PEG-4k excipient, pre-release.
Control matrix – no plasma treatment. Bar = 100 μm.

Post-release, the matrices have nearly the same appearance in cross section, but a smoother appearance on the surface; and the larger upper surface "bump" features seem to have dissolved away, leaving a surface covered with small depressions (Figure 7-3).

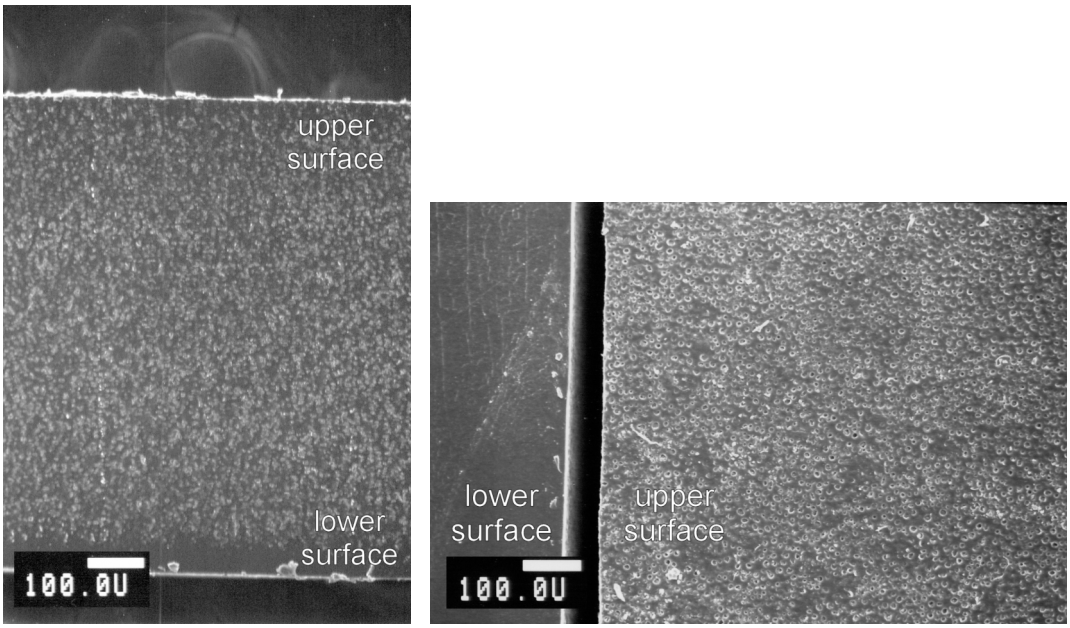

Figure 7-3. SEM of matrices with PEG-4k excipient, post-release.
Left, cross section; right, surface views. Control matrix – no plasma treatment. Bars = 100 μm.

Increasing the molecular weight of the incorporated PEG had a dramatic effect on the morphology of the matrix. Figure 7-4 shows the appearance of a matrix with PEG-10k as an excipient. Large (~400 x 200 µm) domains formed in the matrix and the surface had a pockmarked appearance with various sizes of pores. Note that although the appearance of the matrix suggests air bubble formation, all matrices were thoroughly degassed after casting and prior to drying steps, in order to avoid trapped air bubbles.

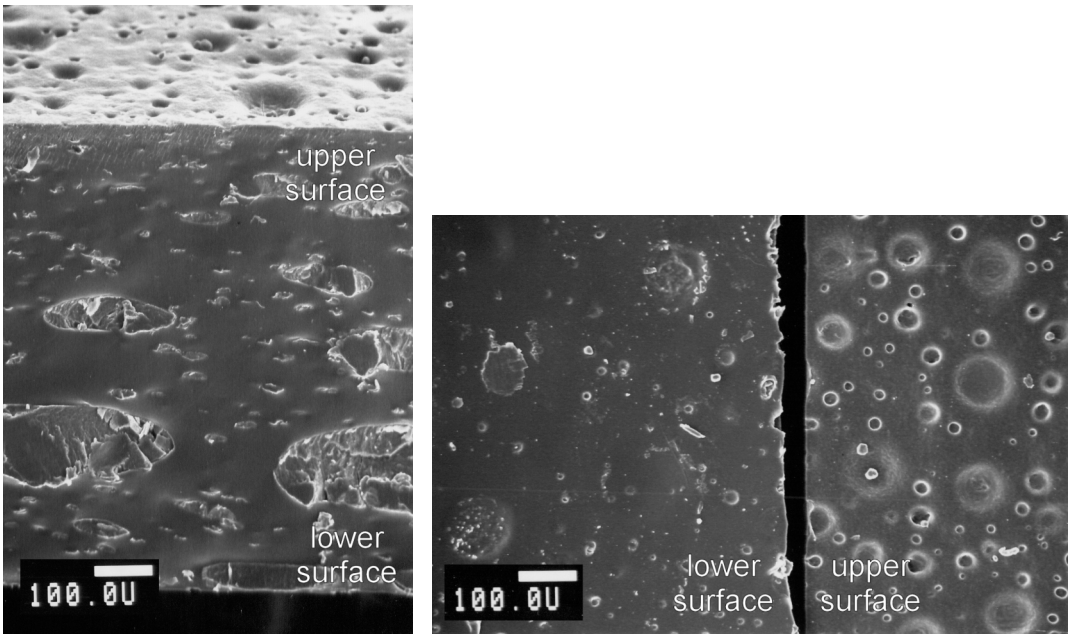

Figure 7-4. SEM of matrices with PEG-10k excipient, pre-release.
Left, cross section; right, surface views. Control matrix- no plasma treatment. Bars = 100 µm.

Post-release, the matrix with PEG-10k excipient had voids mostly at the upper surface of the matrix (as cast; Figure 7-5, left), and the surfaces of the matrix (both upper and lower; Figure 7-5, right) had flat, crater-like depressions where excipient and active agent were released into the medium. A fibrous internal structure appears in some voids in cross section.

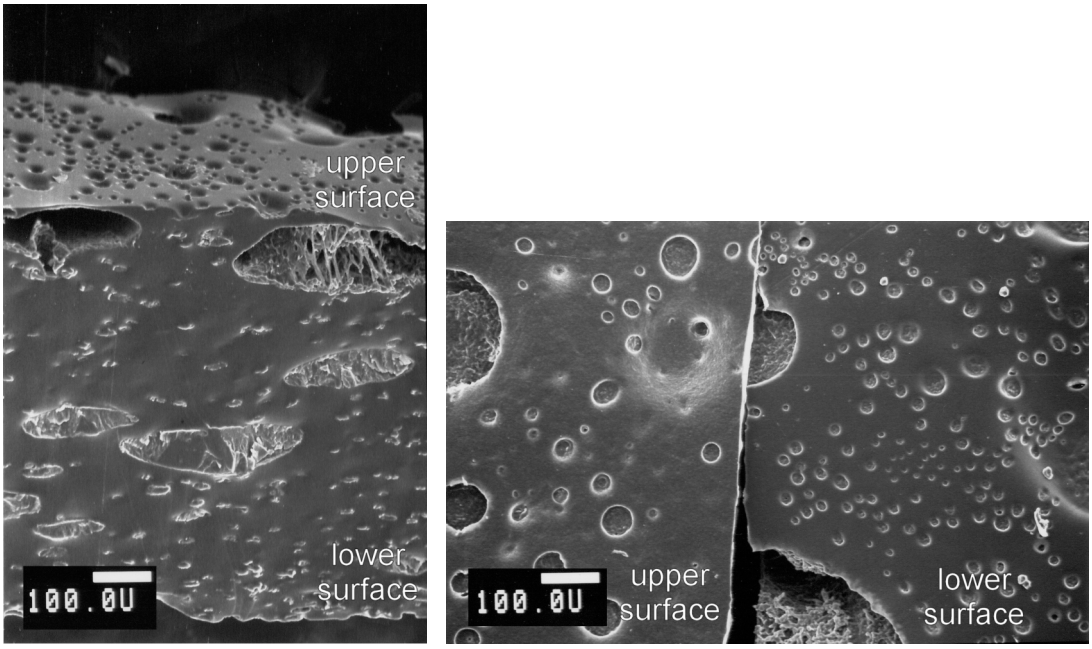

Figure 7-5. SEM of matrices with PEG-10k excipient, post-release.
Left, cross section; right, surface views. Control matrix- no plasma treatment. Bars = 100 μm.

In comparison, matrices with PEG-20k excipient (Figure 7-6) had a slightly more homogeneous composition, with fewer large lenticular domains in cross section and fewer large crater-like features at the surface.

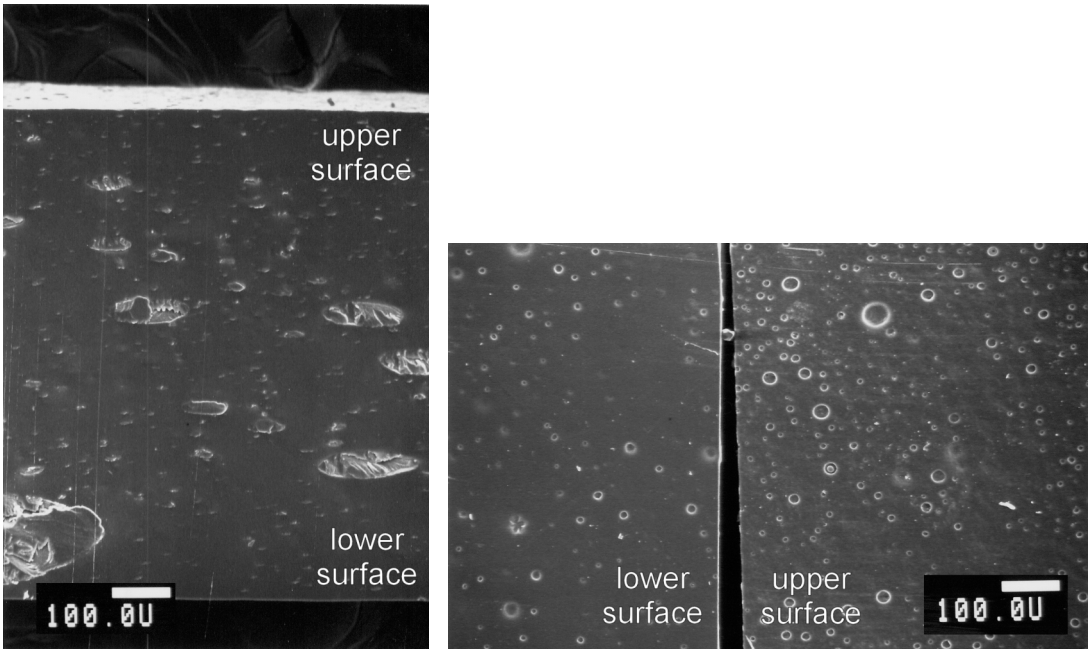

Figure 7-6. SEM of matrices with PEG-20k excipient, pre-release.
Left, cross-section; right, surface views. Control matrix- no plasma treatment. Bars = 100 μm.

Post-release, the PEG-20k matrices appeared similar to the PEG-10k matrices. Some large lenticular cavities were formed after release, and some of these were at the surface of the matrix where they apparently either burst or dissolved (Figure 7-7).

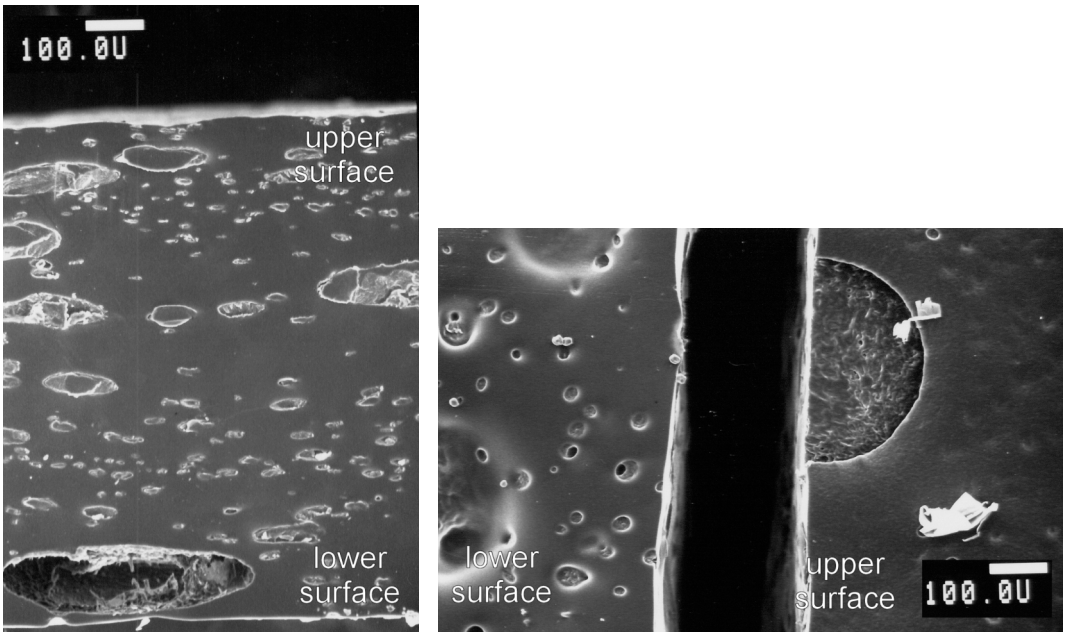

Figure 7-7. SEM of matrices with PEG-20k excipient, post-release.
Left, cross-section; right, surface views. Control matrix- no plasma treatment. Bars = 100 μm.

Matrices with PEG-100k excipient (Figure 7-8) had domains distributed throughout the matrix that were smaller than those in PEG-10k and PEG-20k excipient matrices, but larger than those of PEG-4k excipient matrices (the largest dimension on the order of 100 - 150 μm). Surface morphology was similar to that of matrices with PEG-4k excipient (Figure 7-3). Post release, the PEG-100k excipient matrix (Figure 7-9) showed some release from the lower surface as small pockmarks became visible, and the upper surface showed release from ~50 μm pores that appear somewhat interconnected beyond the surface-residing pores (smaller structures appear to be visible in the larger pores). In cross section, this pattern of release seems to be supported by the fact that there are some larger interconnected pores toward the upper matrix surface, while the lower surface shows a fairly even distribution of smaller, not well connected pores.

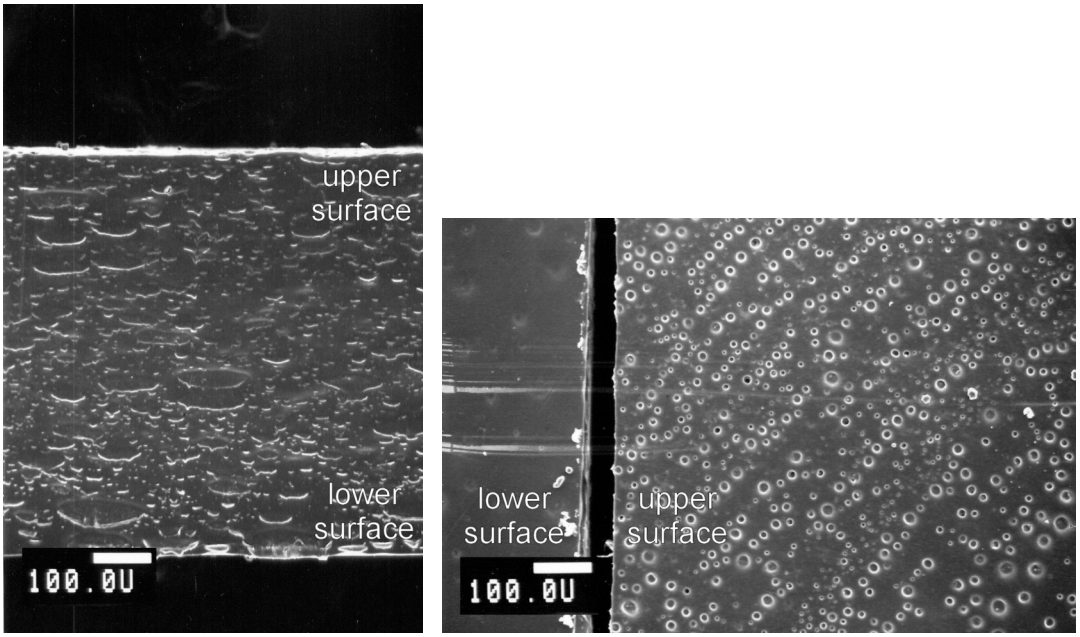

Figure 7-8. SEM of matrices with PEG-100k excipient, pre-release.
Left, cross-section; right, surface views (horizontal streaks are artifacts of photo processing). Control matrix- no plasma treatment. Bars = 100 μm.

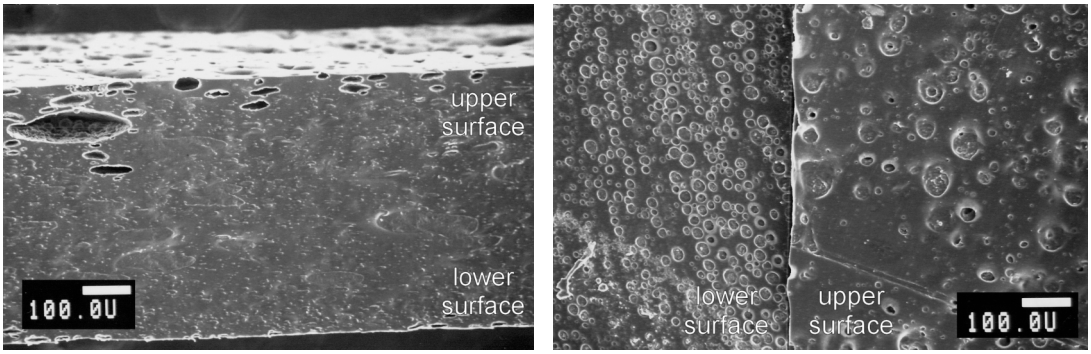

Figure 7-9. SEM of matrices with PEG-100k excipient, post-release.
Left, cross-section; right, surface views. Control matrix- no plasma treatment. Bars = 100 μm.

Plasma treatment of matrices reveals little visible structural changes from control matrices. For example, Figure 7-10 compares the surfaces of a PEG-4k matrix control matrix (no treatment) and after argon pretreatment. There is negligible difference in the appearance of the matrices at this magnification.

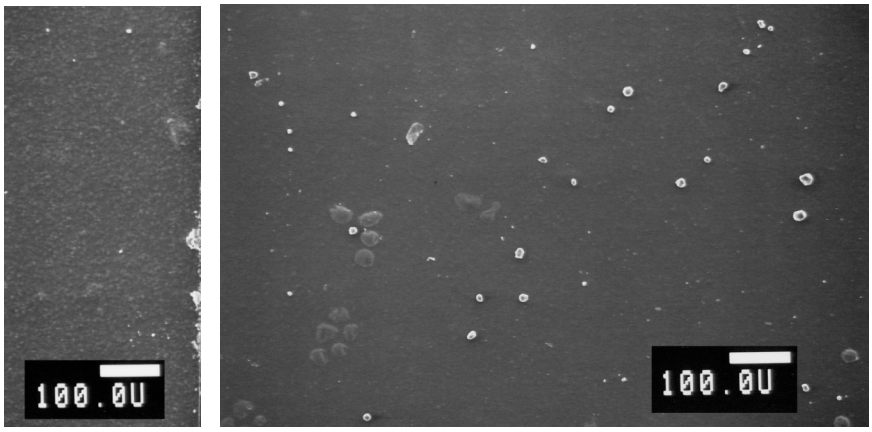

Figure 7-10. Comparison of PEU-4k matrices.
Control (left) and after Ar pretreatment (right). Bars = 100 µm.

Similarly, PEG-100k matrices show little difference between control and argon pretreatment (Figure 7-11).

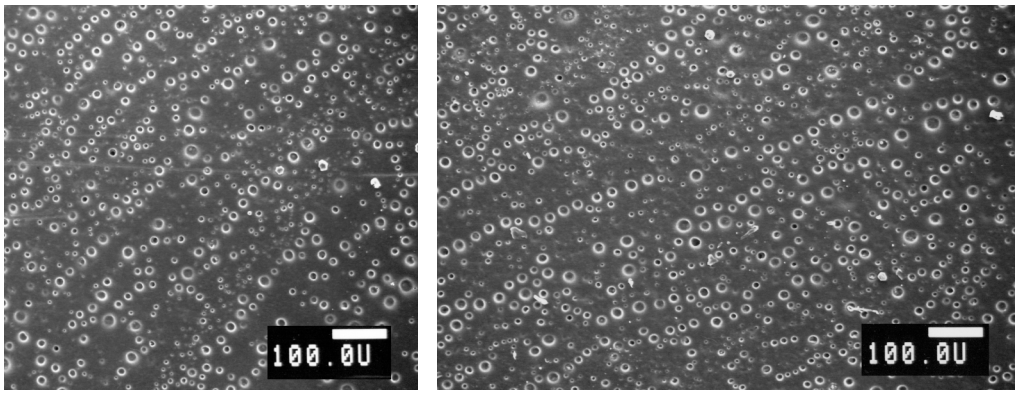

Figure 7-11. Comparison of PEU-100k matrices.
Control (left) and after Ar pretreatment (right). Bars = 100 µm.

Plasma polymer treatment of PEG-4k matrices produced a surface with a very different appearance from the control (Figure 7-12), the end product was a surface similar to that obtained by immersing the matrix in solution (e.g. post-release; see Figure 7-3). This could have been caused by plasma ablation or other processes.

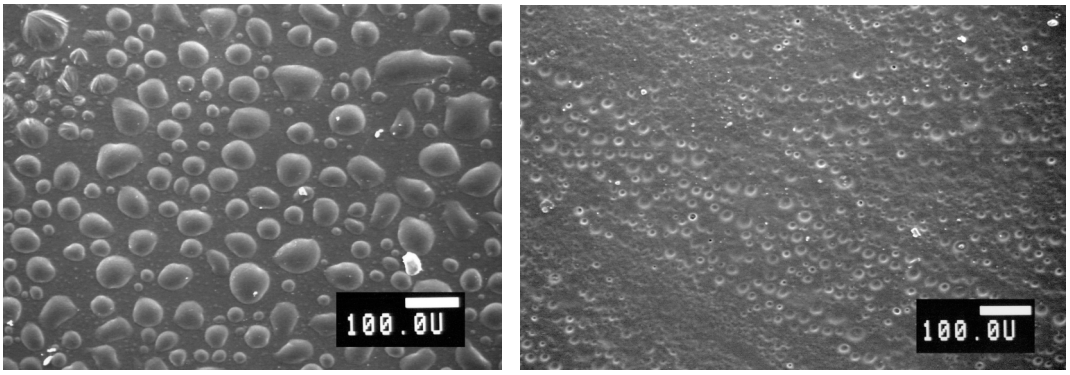

Figure 7-12. Comparison of PEG-4k matrix: BMA treatment.
Control (left) and post-plasma polymerized BMA treatment (right). Bars = 100 µm.

7.7 Controlled Release Results

7.7.1 Release from Ar RFGD Plasma-Treated Matrices

Compiled data for the Ar-plasma treated series of matrices is presented in Figure 7-13. Individual samples are plotted as symbols and designated “G72A-n”; averaged data (n = 2) is plotted with a line trend graph (designated “G72A avg”).

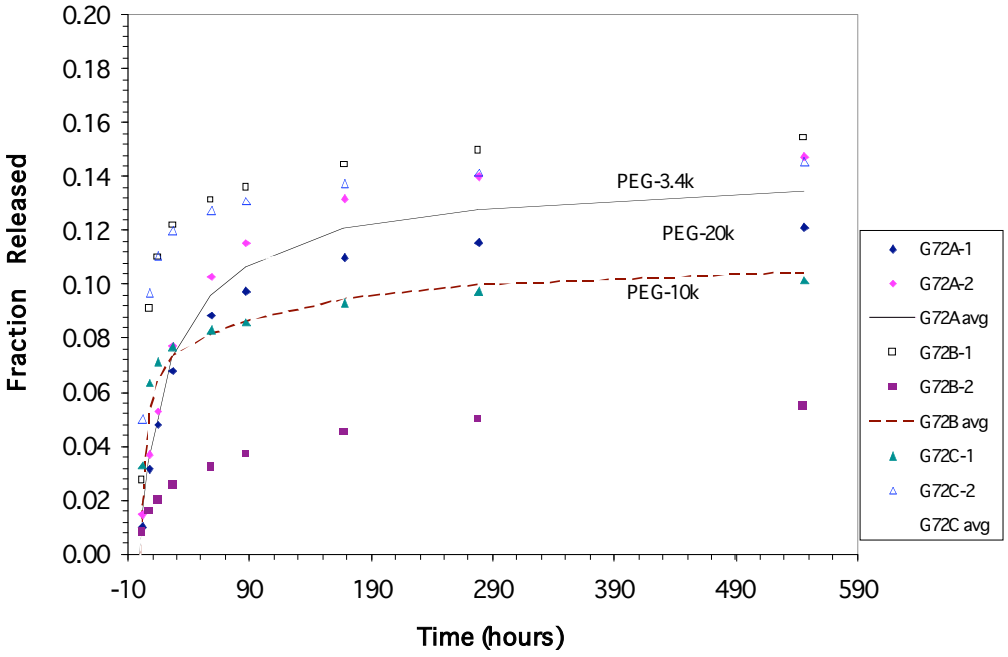

Figure 7-13. Release from Ar-treated RGDS-6 matrices.
G72A: PEG-3.4k; G72B: PEG-10k; G72C: PEG-20k

Sample set "G72A", containing PEG-3.4k as an excipient/pore-former, seemed to have the best agreement of its individual samples (diamond symbols). The other two formulations "G72B" and "G72C" have much greater variability in their release profiles (square and triangle symbols, respectively). This sample-sample variability could be due to several factors, including incomplete mixing; spatial variability after casting, in the plane of the surface or vertically in cross-section; spatial variability in the plasma treatment and its effects on the surface.

The overall shape of the release curve is similar to that observed with other systems, and the final released amount appears to plateau at a fractional release of approximately 0.10 – 0.15. If one focuses on the lines in the graph, representing the average release trends, there is a difference in the initial release rate of the three preparations; the PEG-10k and -20k preparations (dashed and dotted lines, respectively) appear to release at a faster initial rate than the PEG-3.4k preparation (solid line). This general trend, for the PEG-10k and PEG-20k preparations to show lower total release, is echoed in subsequent studies as shown below. However, since there is such sample-sample variability in this

control study, it would be difficult to draw more than general conclusions from this data. Other preparations present trends from samples that behave in a more cohesive fashion.

7.7.2 Release from HEMA RFGD Plasma-Treated Matrices

Compiled data for one set of HEMA-plasma treated series (F190B) of matrices is presented in Figure 7-14. Individual samples are plotted with symbols; averaged data (n = 3) is plotted with a line trend graph. This series of matrices was treated with HEMA plasma for 10 minutes, 40 Watts power, at 150 mtorr pressure. Matrices contained PEG-4k as an excipient.

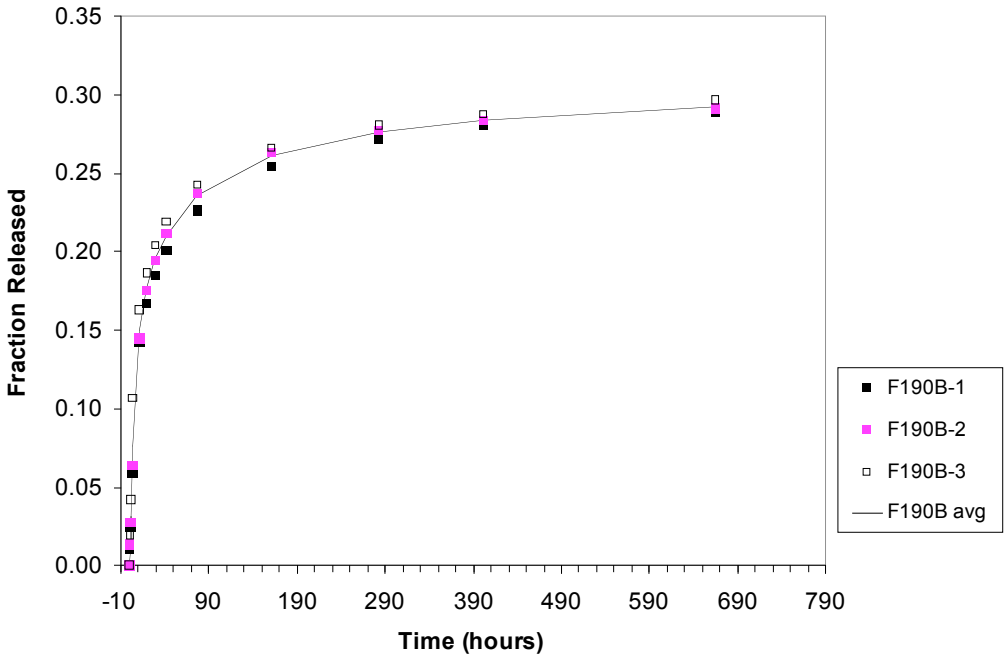

Figure 7-14. Release from ppHEMA-treated RGDS-6 matrices, PEG-4k excipient.
ppHEMA treatment parameters: 10 min / 40 W / 150 mtorr

In this case, matrices exhibit very good intra-sample agreement and the final release amounts appear to plateau near a fractional release of 0.30.

Figure 7-15 shows release from another set of ppHEMA matrices, with a longer deposition time and higher HEMA monomer deposition pressure. The G61 series of matrices was treated with

HEMA plasma for 20 minutes, 40 Watts power, at 250 mtorr pressure. Matrices contained PEG-3.4k as an excipient.

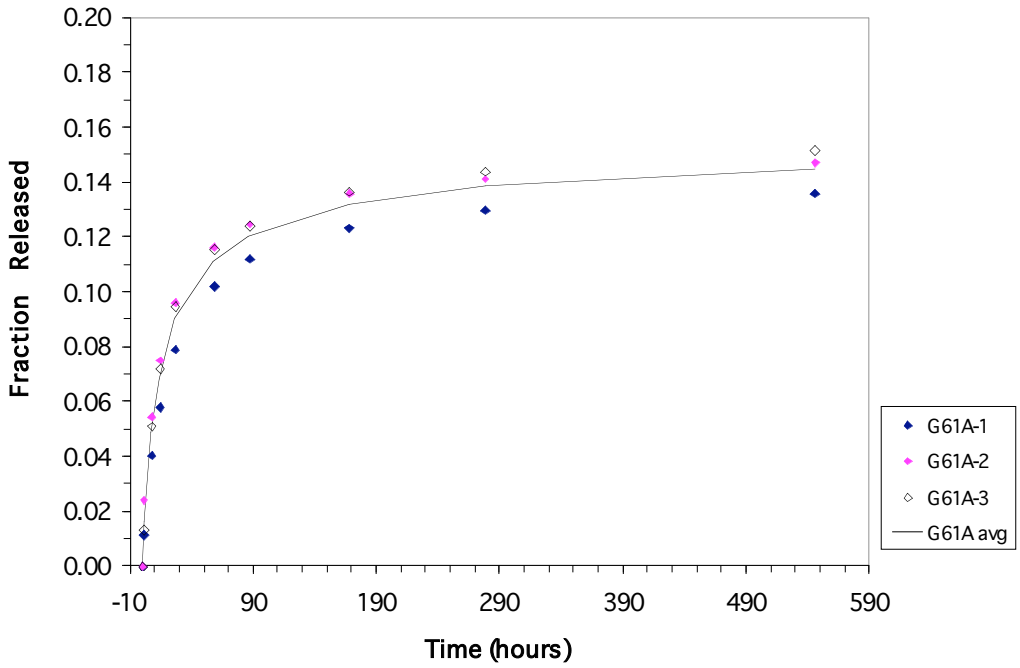

Figure 7-15. Release from ppHEMA-treated RGDS-6 matrices, PEG-3.4k excipient. ppHEMA treatment parameters: 20 min / 40 W / 250 mtorr

This set of matrices shows close agreement between individual samples, as does the F190B samples above. The final fraction released, however, is approximately 0.14 or half the fraction released from the F190B series. This may be due to the longer ppHEMA deposition time or higher deposition pressure than F190B, both conditions which lead to thicker polymeric film deposition.

A series of matrices, with increasing PEG molecular weights as excipients, was treated with ppHEMA at the same reaction conditions, in order to observe the effects of PEG molecular weight on release characteristics (Figure 7-16). Results are plotted on the same scale as Figure 7-15, PEG-3.4k / ppHEMA, for comparison.

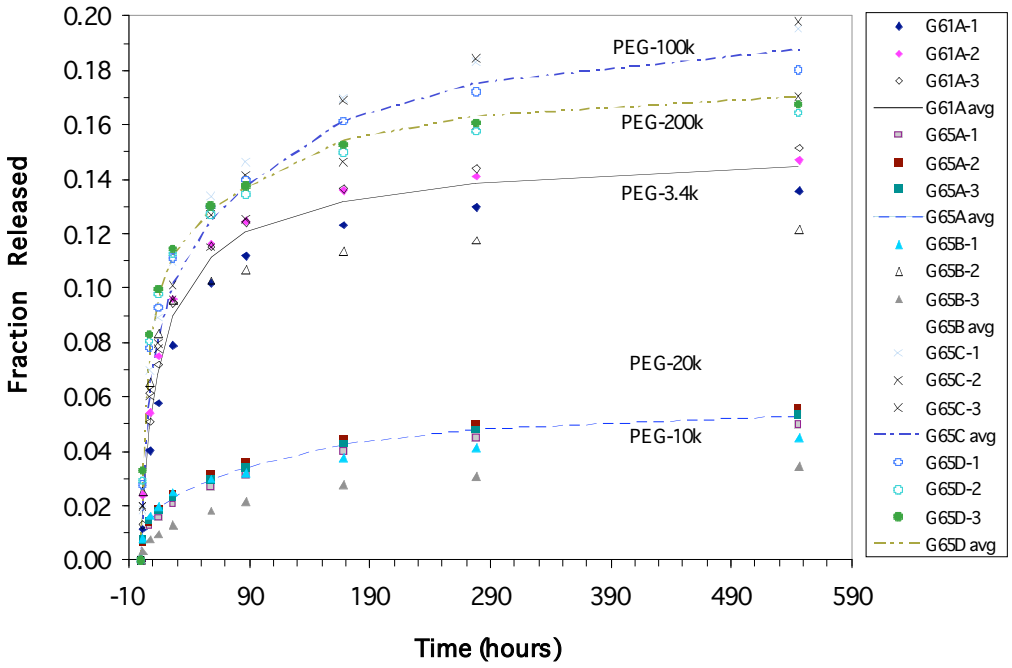

Figure 7-16. Release from ppHEMA-treated RGDS-6 matrices: PEG MW series.
G61A: PEG-3.4k; G65A: PEG-10k; G65B: PEG-20k; G65C: PEG-100k; G65D: PEG-200k

The matrices appear to divide into two groups: a relatively higher rate of release and final fraction released (G61A (PEG-3.4k), G65C (PEG-100k), G65D (PEG-200k)), and relatively lower release rates and final fraction released in two matrix preparations: G65A (PEG-10k, square symbols) and G65B (PEG-20k, triangle symbols). This might indicate that the morphology of the matrix might be different for the PEG-10k and -20k matrices, and that PEG of these molecular weights might lead to more uniform film with a more uniform distribution of peptide throughout. This would lead to a matrix that exhibited a reduced "burst response" (high initial release rate). A difference in ppHEMA reactivity to matrices with PEG-10k and -20k as excipients, versus other molecular weights, would lead to either a thicker ppHEMA film, more tightly crosslinked or stronger film, all of which would lead to a lower release rate as a result.

A pseudo-instantaneous release rate can be calculated at each timepoint, by taking the amount released and dividing it by the time interval for that release. The results of that analysis, performed for

the averages of two sample sets in the ppHEMA group (G61A, PEG-3.4k; and G65A, PEG-10k) are presented in Figure 7-17.

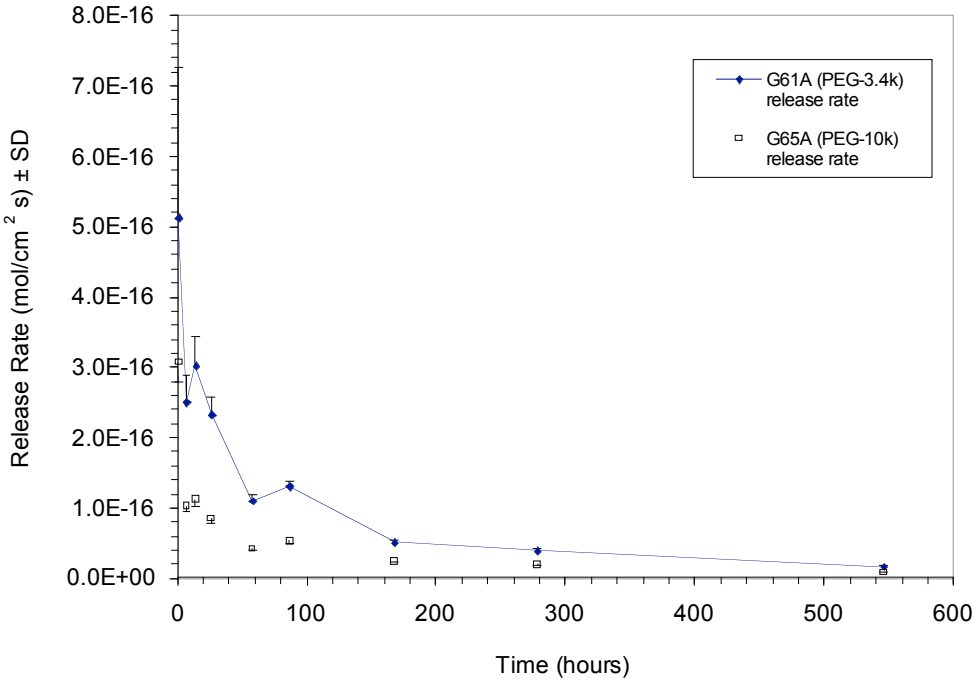

Figure 7-17. Calculated release rates for ppHEMA-treated RGDS-6 matrices.
G61A, matrix with PEG-3.4k excipient; G65A, matrix with PEG-10k excipient. n=3 ± std. dev.

Calculated release rates start in the range of approximately 3 - 5 x 10^{-16} mol/cm^2 s in the initial release period and decrease to 1.7 x 10^{-17} mol/cm^2 s (PEG-3.4k) and 9 x 10^{-18} mol/cm^2 s (PEG-10k) at the end of the experiment (546 hours). These rates were calculated based upon the starting counts of each matrix and a 2-sided release area from each disk of 1.42 cm^2. Release rates for ppBMA matrices would be comparable to those obtained for ppHEMA treated matrices, simply because the release curves are very similar (Figure 7-19).

By comparison, a theoretically required release rate to inhibit platelet aggregation by the small peptide RGDS in a flowing tube can be calculated with the following parameters (cf. Equation 2.2, Section 2.2):

Cs = IC_{50} for ADP-stimulated platelets in platelet-rich plasma = 9.5 x 10^{-5} M (reference [58])

r_0 = 0.3 cm (tube diameter of 6 mm)

D = 1 x10^{-6} cm^2/s, an estimate based on a peptide of ~ 450 MW

A = 1.22, which is a constant for tube geometry

x/ r_0 = 10

Re = 200

Sc = ν/D = kinematic viscosity / diffusivity ≈ 5.8 x 10^4 (dimensionless)

The required release rate at the wall for a small diameter tube with these flow parameters, $N_{required}$ = 2.6 x 10^{-11} mol/cm^2 s. This is a much larger (ca. 5 orders of magnitude) required release rate than is observed with this experimental system (on the order of 1 x 10^{-16} mol/cm^2 s). It should be noted that the calculation of this rate takes place in a flowing regime, and with a required surface concentration that is fairly high compared to echistatin. This is because RGDS is a much weaker antiaggregatory agent than echistatin. As can be seen from Equation 2.2, the required release rate N is directly proportional to the surface concentration required. In a static or implanted system, however, RGDS might be released at a high enough flux to be effective in the near-surface regime, so this experimental system might still show promise for studying RGDS delivery from a matrix in such a static system.

7.7.3 Release from n-BMA RFGD Plasma-Treated Matrices

Compiled data for one set of n-BMA plasma treated series (F190C) of matrices is presented in Figure 7-18. Individual samples are plotted with symbols; averaged data (n = 3) is plotted with a line trend graph. This series of matrices was treated with n-BMA plasma for 10 minutes, 40 Watts power, at 150 mtorr pressure. Matrices contained PEG-4k as an excipient.

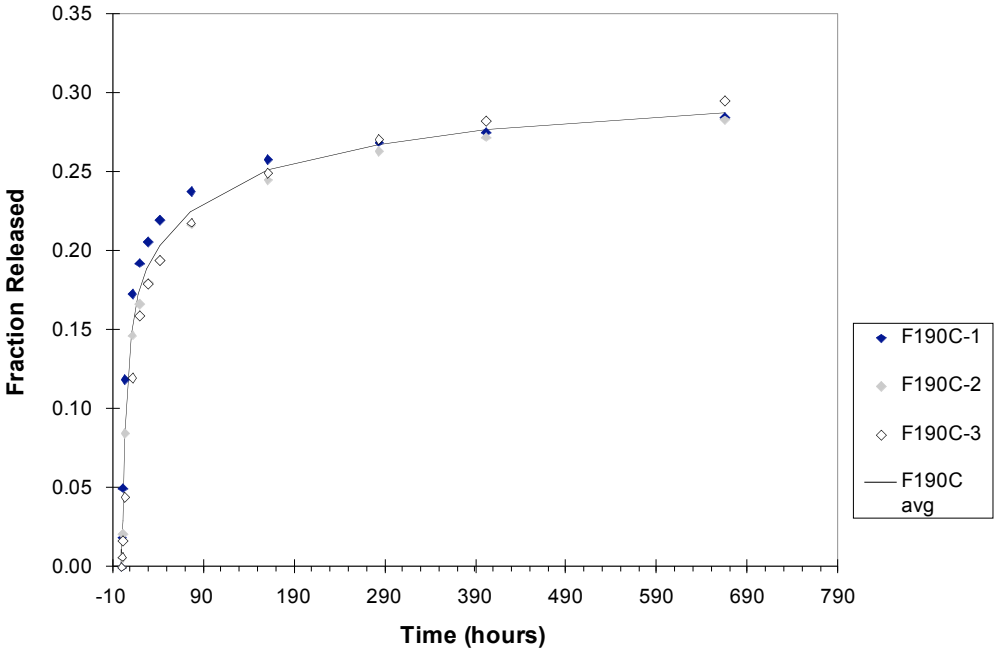

Figure 7-18. Release from ppBMA-treated RGDS-6 matrices.
ppBMA treatment parameters: 10 min / 40 W / 150 mtorr

As with the ppHEMA treated matrices, the samples showed good intra-sample agreement. The final fraction released approached 0.30.

Figure 7-19 shows a PEG molecular weight series of matrix preparations for ppBMA-treated matrices.

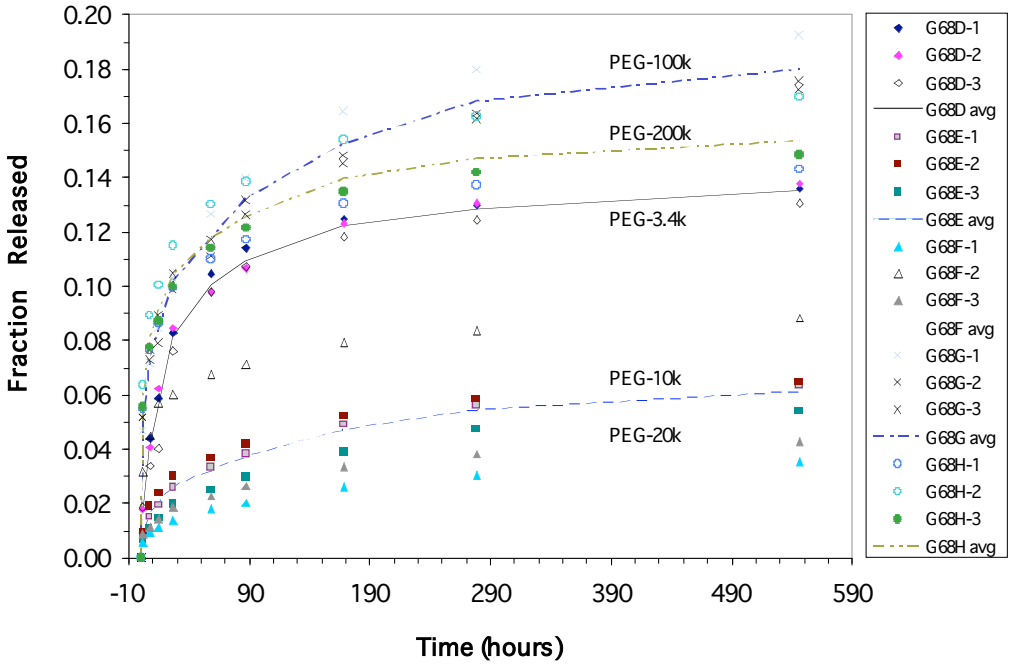

Figure 7-19. Release from ppBMA-treated RGDS-6 matrices: PEG MW series.
G68D: PEG-3.4k; G68E: PEG-10k; G68F: PEG-20k; G68G: PEG-100k; G68H: PEG-200k

As with ppHEMA, the ppBMA matrices exhibit two general groups of release: high and low. The higher group consists of those matrices fabricated with PEG-3.4k, PEG-100k, and PEG-200k. Sample groups G68E (PEG-10k, square symbols, long dashed line) and G68F (PEG-20k, triangle symbols, thicker dotted line) again show the possible trends of lower release due to enhanced film formation with ppBMA.

7.7.4 Release from NIPAAm RFGD Plasma-Treated Matrices

During RGDS-6 release experiments, the NIPAAm-plasma-polymer-treated samples were subjected to a temperature change after the 46 hour time point. This temperature reduction (from ~ 60 °C to ~ 18 °C) was intended to cause the putative poly(N-isopropylacrylamide) at the material surface to undergo a phase transition through its lower critical solution temperature (LCST). It was

thought that this transition, in turn, would affect the release rate of peptide from the surface of the matrix.

Figure 7-20 shows the release from control matrices with PEG-400k excipient.

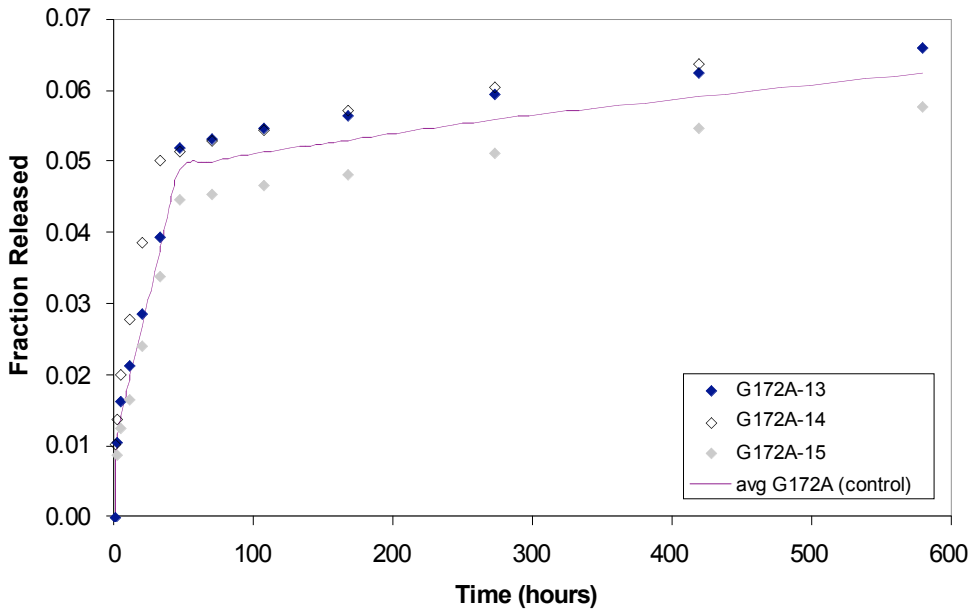

Figure 7-20. Release from RGDS-6 matrices, PEG-400k excipient.
G172A13-15: control matrices

Individual symbols designate individual matrices, and the line denotes the average release profile. The most prominent feature in this graph is the break in slope after timepoint number 6, which corresponds to the temperature change after hour 46. The samples exhibit fair sample-sample reproducibility, with standard error in the 7 – 10% range.

Figure 7-21 plots the averages for various treatments of the PEG-400k excipient matrices.

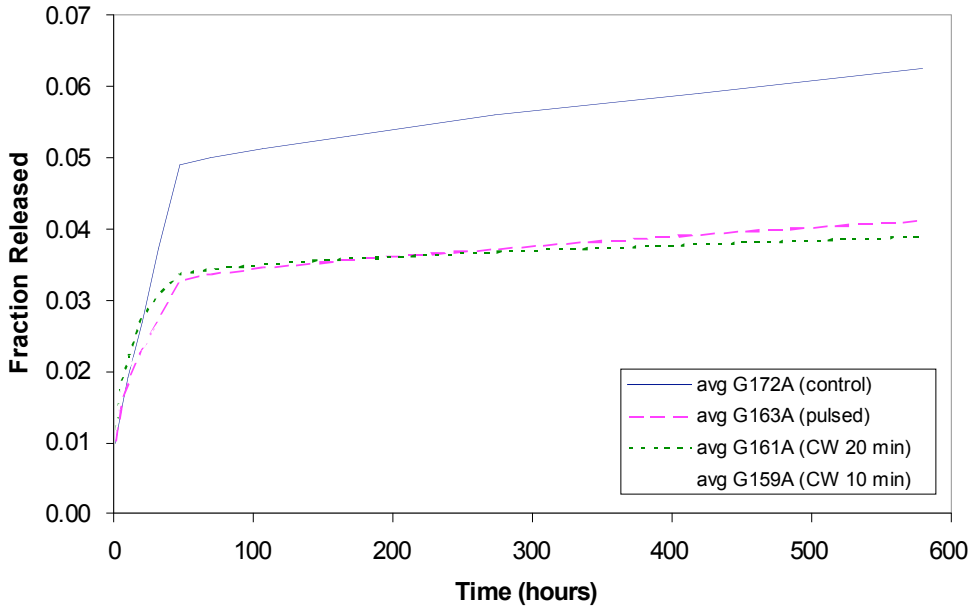

Figure 7-21. Release from ppNIPAAm-treated RGDS-6 matrices, PEG-400k excipient.

The solid line ("avg G172A") denotes the control set of matrices (as graphed in Figure 7-20); the long dashed line ("avg G163A"), denotes the set treated with pulsed plasma; short dashed line ("avg G161A"), the continuous wave treatment for 20 minutes, and dotted line ("avg G159A"), continuous wave treatment for 10 minutes. In early timepoints, the treated matrices appear to release at a faster rate than the control matrices. However after approximately 30 hours, the release rate from the treated matrices tapers off and at the end of the experiment, the final mean fractional release for the treated matrices does not exceed 0.04, whereas the control matrix released greater than a mean fractional release of 0.06. Additionally, the rate of release from the plasma treated matrices after the temperature change appears slower than the control matrices.

Figure 7-22 shows the release from control matrices with PEG-1M as an excipient.

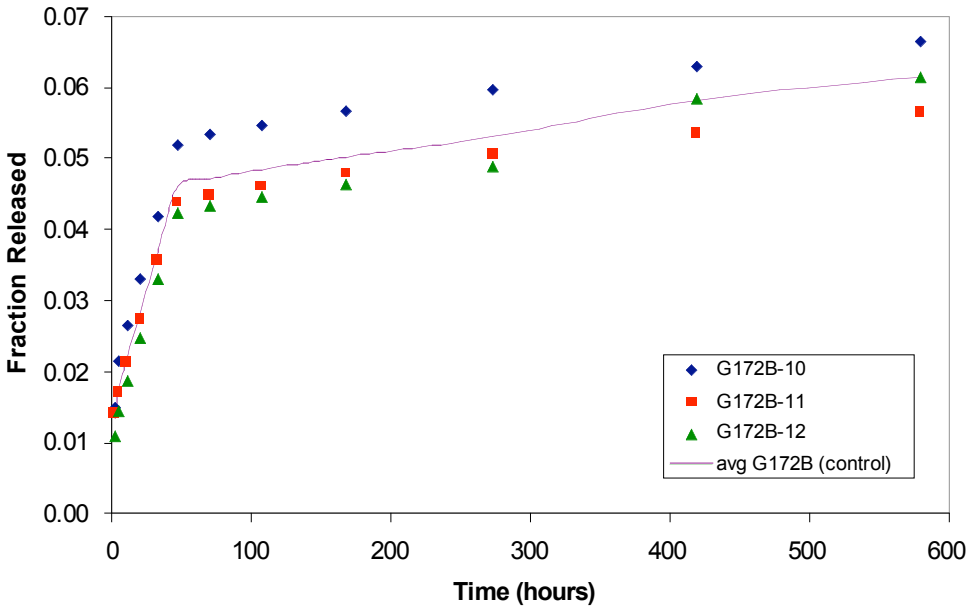

Figure 7-22. Release from RGDS-6 matrices, PEG-1M excipient.

The overall form is similar to the data from the control PEG-400k matrices graphed in Figure 7-20. Sample-sample variability was fair in this case, with errors of the mean from 8 – 20%.

Figure 7-23 shows the fractional release from PEG-1M matrices treated with pulsed NIPAAm plasma. This treatment yielded samples with low variability.

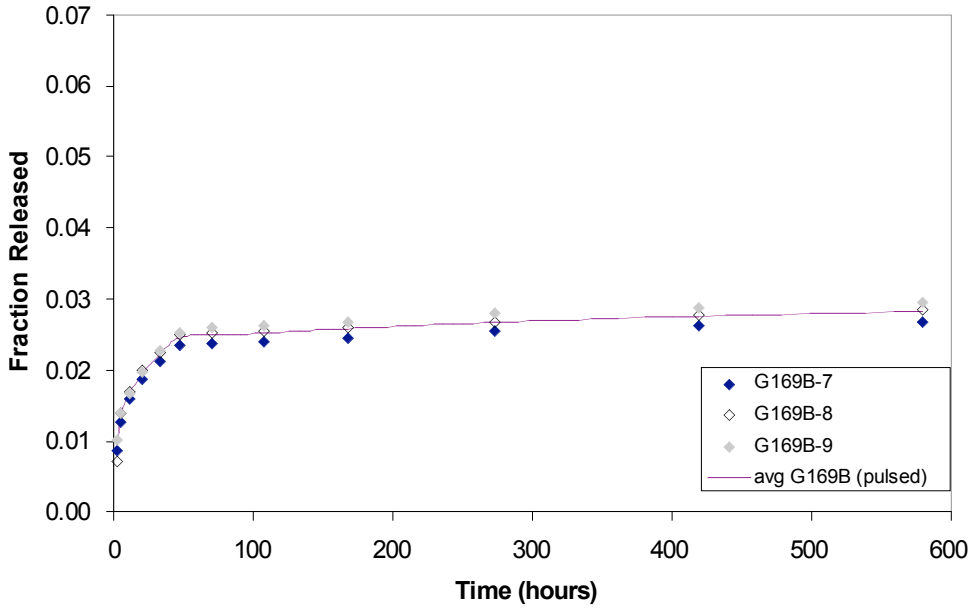

Figure 7-23. Release from ppNIPAAm-treated RGDS-6 matrices, PEG-1M excipient.

In addition, the overall release rate appears to be reduced compared to control and the total fractional release is reduced as well.

Averages for the plasma-treated matrices are plotted along with the average of the control matrices in Figure 7-24.

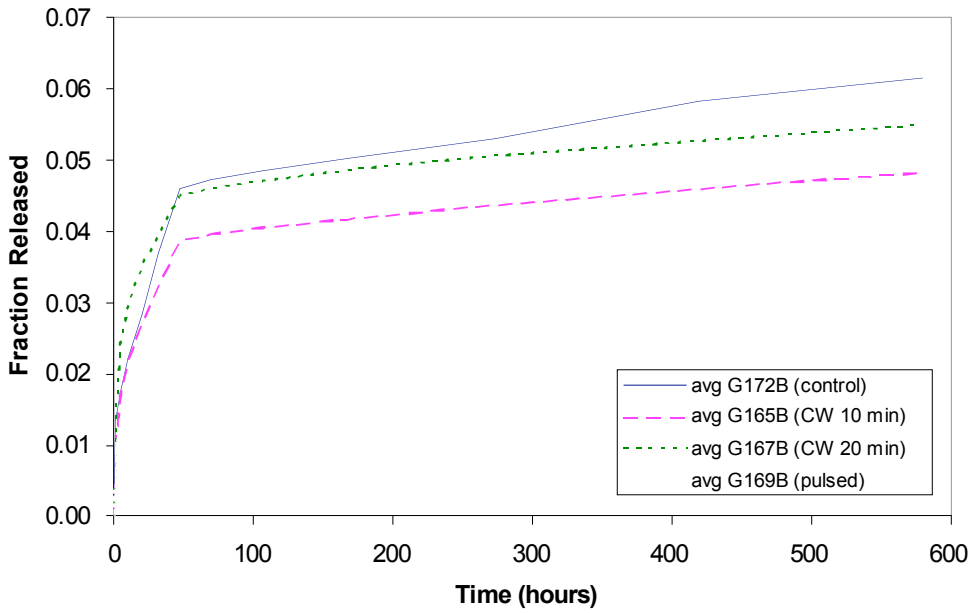

Figure 7-24. Release from ppNIPAAm-treated matrices, PEG-1M excipient.

Plasma treatments for the PEG-1M formulations of matrices affected the release rate to different extents; the greatest reduction in release rate occurred with the pulsed plasma protocol (G169B). Continuous wave (CW) treatments of 10 and 20 minutes (G165B, G167B) reduced the mean fractional release slightly but within error of the control matrix set (G172B).

In conclusion, RGDS-6 was successfully incorporated into the poly(ether urethane urea) solid matrix system with PEG as an excipient. Release of the RGDS-6 was reduced by plasma treatment protocols with HEMA, BMA, and NIPAAm as monomeric precursors. Formulations with various PEG molecular weights produced somewhat unexpected results, with the PEG-10k and PEG-20k formulations yielding the greatest reduction in release rate in combination with ppHEMA and ppBMA treatment. It was initially expected that the release rate trend would follow a molecular weight trend, either directly or inversely. However, the lower release rate and amount may be a result of

thermodynamic conditions that favor more complete mixing and partitioning of the PEG excipient with PTMO soft segments in the BioSpan matrix.

Inhomogeneities in the matrix formulation and spatial variability in plasma treatment may account for some variability seen between samples in the same treatment group.

8 CONCLUSIONS

A solid, polymeric, controlled release matrix system was fabricated from a polyurethane elastomer. Three biologically active peptides: echistatin, hirudin, and RGDSGY, were incorporated into the elastomeric matrix using several excipients (BSA, mannitol, and PEG) as pore-forming agents. These studies were, at the time and to the best of the author's knowledge, one of the first to examine the release of an antithrombotic peptide from a solid polyurethane matrix fabricated by solvent casting.

These matrices were then coated via radio frequency glow discharge (RFGD) plasma polymerization. In addition to being one of the first studies of antithrombotic peptide release from polyurethane matrices, these studies were also one of the first applications of RFGD plasma polymerization to control the release of peptides from said matrices.

Release of incorporated peptide into a buffered saline solution showed that the peptide retained considerable activity, even after being subjected to conditions known to inactivate or denature many proteins, i.e. exposure to organic solvents and physical entrapment in a polymeric matrix.

Results with echistatin, an inhibitor of platelet integrin binding (so-called "disintegrin") showed almost 80% of the initial peptide loading was released, and of that released peptide, 55 - 73% was active as measured by platelet aggregometry. Plasma coating of echistatin matrices showed little change in the release characteristics with plasma-polymerized HEMA.

Results with hirudin, a thrombin inhibitor, showed a final release amount of 40% of the initial loading. This released hirudin was also biologically active as measured by a thrombin inhibition assay, for both BSA and mannitol as excipients. Plasma coating of hirudin matrices showed reduction in the initial rate of release ("burst effect") but the reduction in the total amount of peptide released was smaller than expected. Other experiments with hirudin also showed that increasing initial loading level of peptide/excipient mixture yielded a higher final release amount, but no appreciable difference in the time to maximum release; and that increasing the size of the peptide/excipient particle also increased the total amount released.

These results from the plasma coating experiments gave initial indications that the release rate could be reduced, but not to the extent desired. This suggested further studies of reformulation of the matrices and further plasma deposition investigations.

RGDS-6, a small peptide oligomer, was formulated with PEG of a range of molecular weights (number averages 3,400; 10,000; 20,000; 100,000; 200,000; 400,000; and 1,000,000). Matrices were treated with four different plasma treatments: argon, HEMA, BMA, and NIPAAm.

Matrices with PEG molecular weights of 10,000 (10k) and 20,000 (20k) showed the best response to plasma treatment. RGDSGY-PEG-10k matrices treated with HEMA plasma and BMA plasma showed an overall reduction of 50% in total mass of peptide released. RGDSGY-PEG-20k matrices showed a reduction of 45% of total mass released. There was no clear correlation between PEG molecular weight and release amount; however, it is thought that the PEG-10k and PEG-20k excipients may have formed a polymeric blend that causes a reduction in release. The mechanism of this blending and/or mixing is not known; however, it may be related to thermodynamic conditions and end group concentration to form a matrix with lower release characteristics.

NIPAAm plasma treatment was performed to see if differences in matrix release environment could affect release rate; conventionally polymerized NIPAAm shows dramatic changes in the water swelling ratio with changes in temperature and pH. It was hypothesized that plasma polymerized coatings of NIPAAm would show similar changes with temperature of the release buffer. Best results were obtained with matrices formulated with PEG-400,000 MW (400k). NIPAAm plasma treatment reduced release in these matrices by approximately 44%.

Sectioned matrices were observed to exhibit swelling and bursting under hydration. Comparison with other systems indicated that an osmotic swelling mechanism was the likely mechanism responsible for this behavior. One approach to minimize this osmotic water uptake by entrapped excipient/agent domains is to use a larger molecular weight excipient. This would have the effect of reducing the relative concentration of excipient, and therefore the relative osmotic driving force for rupture.

In conclusion, active biological agents were successfully delivered from polyurethane matrices. These matrices were coated with a RFGD plasma polymerization process and still yielded substantial active agent, even after several potentially damaging formulation steps. Formulation with different excipients indicated certain combinations of excipient and active agent, and processing conditions, that indicate lower release; however, trends and relationships between formulation material properties and the end result of release rate are often more complex than expected. Plasma polymerization did reduce total amounts and rates of release, but not as much as expected. This relative difficulty in coating matrices with thin plasma polymer prompted further investigation, and observation of osmotic bursting phenomena was a likely explanation. The need for stronger coating materials and future directions in formulation is a result of these observations of osmotic effects.

9 FUTURE DIRECTIONS

This matrix delivery system has the potential to be a flexible, powerful, and unique solution to many biomaterials and drug delivery problems. However, as is often the case in drug delivery, general principles serve only as guidelines to matrix fabrication. There are many variables in matrix fabrication and post-processing that can be manipulated, and some of these variables are independent and some may be correlated.

Specific combinations of therapeutic agent, matrix material, and excipient system must be evaluated for their chemical and processing compatibility. RFGD plasma deposition is usually substrate-independent, but specific plasma coating protocols should always be verified for compatibility with a particular matrix system. Potential areas of concern, such as the lack of damage to possible labile compounds in a formulation; surface adhesion to a matrix; and suitability of the coating protocol to control the diffusion out of a matrix in a solution or implant situation, should be evaluated.

9.1 Improvements to Matrix Homogeneity

A concern with the fabrication system to date has been the heterogeneity of the resulting cast matrix. This can be addressed by employing better mixing methods, that is, more thorough and more repeatable; and by employing better materials. This includes preparations of the primary components of the matrix: BioSpan, solvent, excipient, and active agent (peptide or protein). In addition to the primary materials studied so far, another material could be incorporated to make these components more compatible. It is hypothesized that a neutral, large molecule composed of "compatibilizing domains" between the active peptide agent and soft segment of polyurethane can serve to co-compatibilize the PEUU and peptide and create a more homogenous blend.

A "compatibilizer" is often used in commercial polymer blends to thermodynamically stabilize the two mixed phases of polymer [B. Ratner, personal communication]. In the system described here, it was initially thought that the release mechanism of discrete, but interconnected peptide-containing domains was essential to the successful delivery of peptide. It was found, however, that these discrete

domains contributed to osmotic bursting, and a suitable coating protocol was not possible with plasma coating technology alone, due to the tremendous pressures resulting from osmotic forces.

However, if a method is used to disperse the peptide in smaller particles or in a more intimately mixed blend, it may be possible to reduce osmotic bursting by reducing the chance of a highly concentrated solution of peptide or any active agent to build up and induce an osmotic pressure gradient. Therefore, in conjunction with the use of smaller-molecular weight peptides, a compatibilizer of PEG or PTMO coupled to a polypeptide (e.g. poly-glycine or alanine) could be synthesized and evaluated. In addition, the neutrality of the excipient molecule may help to reduce the water uptake by the excipient-drug blend, as opposed to a charged molecule that might encourage additional water uptake due to ionic hydration effects.

One possible synthesis strategy for this compatibilizer could use a succinimidyl carbonate-derivatized PEG (SC-PEG) to react with the terminal amino group of a peptide (or protein) [59]. The resulting PEG-peptide is expected to partially partition into the PEUU polymer soft segment phase and also with the peptide phase. If the PEG is not compatible with BioSpan, poly(tetramethylene oxide), PTMO, may be more conducive to blending.

Other possible synthetic pathways to derivatized PEG and conjugated PEG-polypeptide are outlined in the following diagram.

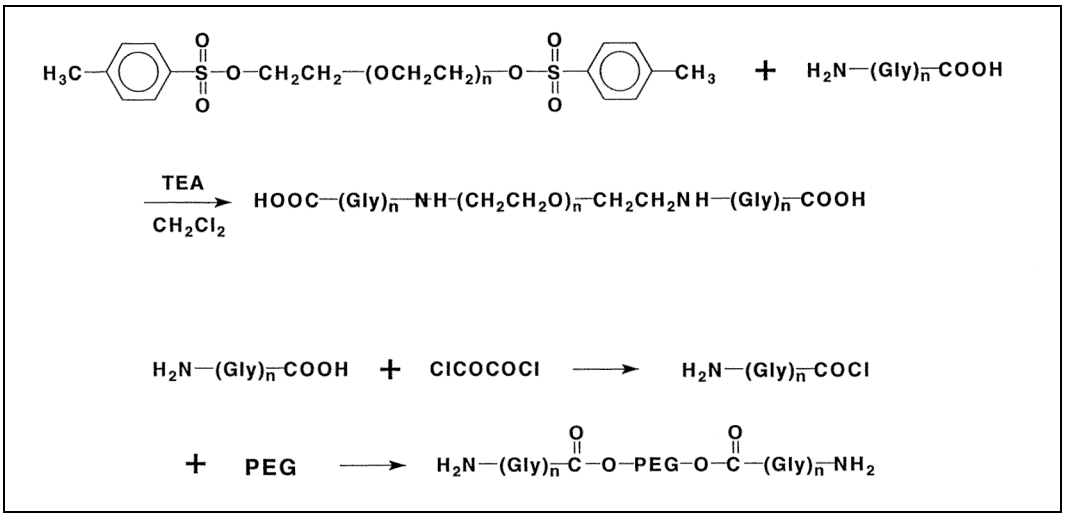

Figure 9-1. Sample synthetic routes to PEG-poly(glycine) compatibilizer.
Top, using PEG-tosylate; bottom, using oxalyl chloride.

It is expected that only small amounts of this compatibilizer would be necessary for better blending of the matrix and incorporated protein. If the compatibilizer behaves in a similar fashion to a surfactant, by migrating to the interfacial surfaces of domains in the material, the ratio of compatibilizer to bulk material could be low.

Similar to the use of RFGD-plasma to coat protein-containing polymers, this use of a compatibilizer would be a novel approach to develop better matrix properties.

A possible drawback to this compatibilizer method might be the denaturation of certain peptides that may be sensitive to such compounds.

9.2 Other Plasma Deposition Precursor Monomers and Methods

In order to improve the mechanical and permeability properties of the plasma coatings, other plasma precursors and treatment protocols can be investigated. Studies from the coatings and plasma treatment literature - which can be extremely diverse, and from disparate fields - can provide insight into potentially fruitful avenues of investigation.

9.2.1 Cyclohexyl Methacrylate (CHMA)

The extension of methacrylate monomers to include cyclohexyl methacrylate might yield a deposited plasma film that is more flexible and with lower water permeability [60]. Analysis of films from CHMA would be similar to that performed for HEMA and n-BMA, and therefore comparison of ESCA spectra and other characteristics would be straightforward. In addition, a useful comparison library could be created with a series of methacrylate monomers.

9.2.2 Hexamethyldisiloxane (HMDSO)

Hexamethyldisiloxane (HMDSO) has been used in other applications [32] to produce more mechanically stable films (for instance, in gas separation membranes, and in tribology). In addition, films resulting from such plasma polymerization may be more hydrophobic and therefore better barriers to the diffusion of water into the matrix. This could slow the resultant swelling and dissolution of the active agent out of the matrix.

In addition, there are other similar monomers in the silane family that might be useful, for example: hexamethyldisilane, tetramethyldisiloxane, and divinyltetramethyldisiloxane.

9.2.3 Tetrafluoroethylene (TFE)

Another possible plasma polymer might be tetrafluoroethylene (C_2F_4, TFE), for similar reasons as HMDSO. TFE (or other fluorocarbon precursors) may yield more a more hydrophobic plasma polymerized film, and ppTFE may act as a barrier to water diffusion into a matrix [61] thereby slowing the resultant swelling and bursting.

9.3 Other Analysis Methods

In order to more fully characterize the chemical interactions of matrix, excipient, and active agent, and other morphological changes in matrices, it would be useful to complement ESCA and microscopic studies with a microchemical imaging analysis method. Preliminary studies with static ToF-SIMS in imaging mode were performed by the author, but were not expanded due to time and material constraints. Other micro-imaging modalities with high spatial resolution and chemical contrast

imaging capability, such as imaging ESCA (e.g. Kratos AXIS Ultra), SIMS, and FTIR would provide insight into the distribution and chemical state of diverse components in a controlled-release matrix [62].

9.4 Other Applications of Matrix Delivery

Because echistatin is a "disintegrin," it can be useful in studies of cell adhesion and cell signaling. In a more specific vein, echistatin has been shown to have anti-osteoclastic activity [8, 63-65]. Matrices that release a controlled amount of echistatin could prove useful in studies of bone resorption and remodeling. In addition to delivering active agents, the matrices could serve as scaffolding or structural template for regrowth [66].

This same system of peptide / protein delivery could be used to study many other systems of interest in the biomaterials, tissue engineering, and cell biology fields, such as the mechanism of action of growth factors, cell signaling, cell colonization and extracellular matrix scaffolding and remodeling. Polyurethanes have been processed in many different ways in cell and biomaterial studies, including microcellular foams, and spun and woven textures. The techniques of protein and peptide incorporation and plasma coating technology could be adapted to such polyurethane systems for further study. Multiple proteins and peptides could be incorporated together in order to study the synergistic effect of simultaneous delivery of such compounds [67].

Echistatin and a related process to RFGD, chemical vapor deposition (CVD), was used to study cell adhesion in a microfluidic analysis device, and it was mentioned that such devices could be useful in clinical fields such as angiogenesis research [68]. Similarly, this type of matrix system could be used in a microfluidic device since solvent-cast polyurethanes can form finely detailed structures.

In addition, polyurethane matrices could be cast thin enough to be optically transparent, yet thick enough to release a significant amount of active agent over the course of an experiment; this would be useful in microscope thin-channel flow cell devices. For example, one surface of the flow cell could be coated or replaced with a polyurethane matrix releasing an active agent; the adhesion (or lack thereof) of cells could be observed in real-time under flow conditions.

As mentioned in the introduction, controlled release technology can be important in a commercial research setting, as new formulation strategies can afford certain benefits such as product differentiation, market expansion, and patent extension for existing drugs.

LIST OF REFERENCES

1. Chinn, J.A., *Fibrinogen adsorption and platelet adhesion to polymeric materials*, in *Department of Chemical Engineering*. 1990, University of Washington: Seattle, WA. p. xvi, 254 leaves.

2. Edmunds, L.H., Jr., *Hastings lecture. Breaking the blood-biomaterial barrier.* Asaio-J, 1995. **41**(4): p. P 824-30.

3. Ratner, B.D., *Blood compatibility-a perspective.* J. Biomater. Sci. Polymer. Edn., 2000. **11**(11): p. 1107–1119.

4. Berson, A., *NHLBI/FDA conference on thrombosis and infections with cardiovascular devices.* J Biomed Mater Res, 1998. **42**(3): p. 341-6.

5. Topol, E.J., et al., *Randomised trial of coronary intervention with antibody against platelet IIb/IIIa integrin for reduction of clinical restenosis: results at six months. The EPIC Investigators [see comments].* Lancet, 1994. **343**(8902): p. 881-6.

6. Hall, J.D., S.E. Rittgers, and S.P. Schmidt, *Effect of controlled local acetylsalicylic acid release on in vitro platelet adhesion to vascular grafts.* J Biomater Appl, 1994. **8**(4): p. 361-84.

7. Marois, Y. and R. Guidoin, *Biocompatibility of Polyurethanes*, in *Biomedical Applications of Polyurethanes*, P. Vermette, et al., Editors. 2001, Landes Bioscience: Georgetown, TX.

8. Gan, Z.R., et al., *Echistatin. A potent platelet aggregation inhibitor from the venom of the viper, Echis carinatus.* J Biol Chem, 1988. **263**(36): p. 19827-32.

9. Verstraete, M., *New developments in antiplatelet and antithrombotic therapy.* Eur Heart J, 1995. **16 Suppl L**: p. 16-23.

10. Lefkovits, J. and E.J. Topol, *Platelet glycoprotein IIb/IIIa receptor antagonists in coronary artery disease.* Eur Heart J, 1996. **17**(1): p. 9-18.

11. Lincoff, A.M., E.J. Topol, and S.G. Ellis, *Local drug delivery for the prevention of restenosis. Fact, fancy, and future.* Circulation, 1994. **90**(4): p. 2070-84.

12. Slack, S.M. and V.T. Turitto, *Fluid Dynamic and Hemorheologic Considerations.* Cardiovascular Pathology, 1993. **2**(3): p. S11-S21.

13. Basmadjian, D., *The effect of flow and mass transport in thrombogenesis.* Ann Biomed Eng, 1990. **18**(6): p. 685-709.

14. Basmadjian, D. and M.V. Sefton, *Relationship between release rate and surface concentration for heparinized materials.* J Biomed Mater Res, 1983. **17**(3): p. 509-18.

15. Siegel, R., E.M. Sparrow, and T.M. Hallman, *Steady laminar heat transfer in a circular tube with prescribed wall heat flux.* Appl. Sci. Res. A, 1958. **7**: p. 386-392.

16. Langer, R. and J. Folkman, *Polymers for the sustained release of proteins and other macromolecules.* Nature, 1976. **263**(5580): p. 797-800.

17. Brown, L.R., et al., *Characterization of glucose-mediated insulin release from implantable polymers.* J Pharm Sci, 1996. **85**(12): p. 1341-5.

18. Edelman, E.R., D.H. Adams, and M.J. Karnovsky, *Effect of controlled adventitial heparin delivery on smooth muscle cell proliferation following endothelial injury.* Proc Natl Acad Sci U S A, 1990. **87**(10): p. 3773-7.

19. Edelman, E.R., et al., *c-myc in vasculoproliferative disease.* Circ Res, 1995. **76**(2): p. 176-82.

20. Soldani, G., et al., *Development of small-diameter vascular prostheses which release bioactive agents.* Clin Mater., 1991. **8**: p. 81-88.

21. Muller, D.W., et al., *Sustained-release local hirulog therapy decreases early thrombosis but not neointimal thickening after arterial stenting.* Am Heart J, 1996. **131**(2): p. 211-8.

22. Levy, R.J., et al., *Inhibition of calcification of bioprosthetic heart valves by local controlled-release diphosphonate.* Science, 1985. **228**(4696): p. 190-2.

23. Sintov, A., et al., *Cardiac Controlled Release For Arrhythmia Therapy - Lidocaine- Polyurethane Matrix Studies*. Journal of Controlled Release, 1988. **8**(2): p. 157-165.

24. Greisler, H.P., *Growth factor release from vascular grafts.* J Control Release, 1996a. **39**(2-3): p. 267-280.

25. Parkhurst, M.R. and W.M. Saltzman, *Controlled delivery of antibodies against leukocyte adhesion molecules from polymer matrices.* Journal Of Controlled Release, 1996. **42**(3): p. 273-288.

26. Aggarwal, R.K., et al., *Antithrombotic potential of polymer-coated stents eluting platelet glycoprotein IIb/IIIa receptor antibody.* Circulation, 1996. **94**(12): p. 3311-7.

27. Higuchi, T., *Rate of release of medicaments from ointment bases containing drugs in suspension.* J Pharm Sci, 1961. **50**: p. 874-5.

28. Keely, S., et al., *In vitro and ex vivo intestinal tissue models to measure mucoadhesion of poly (methaerylate) and N-trimethylated chitosan polymers.* Pharmaceutical Research, 2005. **22**(1): p. 38-49.

29. Oh, J.M., C.S. Cho, and H.K. Choi, *A mucoadhesive polymer prepared by template polymerization of acrylic acid in the presence of poly(vinyl alcohol) for mucosal drug delivery.* Journal of Applied Polymer Science, 2004. **94**(1): p. 327-331.

30. Bernkop-Schnurch, A., et al., *Preparation and in vitro characterization of poly(acrylic acid)-cysteine microparticles.* Journal of Controlled Release, 2003. **93**(1): p. 29-38.

31. Davies, M.C., et al., *The surface characterisation and modification of biodegradable polyesters and their sterilization by oxygen glow discharge plasma treatment.* ACS Polym. Mater. Sci. Eng., 1988. **59**: p. 739–743.

32. d'Agostino, R., *Plasma deposition, treatment, and etching of polymers*. 1990, Boston :: Academic Press,. 528 p.

33. Yasuda, H., *Plasma polymerization*. 1985, Orlando, Florida: Academic Press, Inc. 432p.

34. Denes, F., *Synthesis and surface modification by macromolecular plasma chemistry.* Trends in Polymer Science, 1997. **5**(1).

35. Susut, C. and R.B. Timmons, *Plasma enhanced chemical vapor depositions to encapsulate crystals in thin polymeric films: a new approach to controlling drug release rates.* International Journal of Pharmaceutics, 2005. **288**(2): p. 253-261.

36. Lee, Y.M. and J.K. Shim, *Preparation of pH/temperature responsive polymer membrane by plasma polymerization and its riboflavin permeation.* Polymer, 1997. **38**(5): p. 1227-1232.

37. Lee, Y.M., et al., *Preparation of Surface-Modified Stimuli-Responsive Polymeric Membranes by Plasma and Ultraviolet Grafting Methods and Their Riboflavin Permeation.* Polymer, 1995. **36**(1): p. 81-85.

38. Lee, Y.M. and I.K. Shim, *Plasma surface graft of acrylic acid onto a porous poly(vinylidene fluoride) membrane and its riboflavin permeation.* Journal of Applied Polymer Science, 1996. **61**(8): p. 1245-1250.

39. Cartier, S., T.A. Horbett, and B.D. Ratner, *Glucose-sensitive membrane coated porous filters for control of hydraulic permeability and insulin delivery from a pressurized reservior.* J. Membr. Sci., 1995. **106**: p. 17–24.

40. Kwok, C.S., T.A. Horbett, and B.D. Ratner, *Design of infection-resistant antibiotic-releasing polymers: II. Controlled release of antibiotics through a plasma-deposited thin film barrier.* Journal of Controlled Release, 1999b. **62**(3): p. 301-311.

41. Ward, R.S. and K.A. White. *Development of a new family of polyurethaneurea biomaterials*. in *The Eigth CIMTEC Forum on New Materials*. 1994. Florence, Italy.

42. Carpenter, J.F., et al., *Interactions of stabilizers with proteins during freezing and drying*, in *Formulation and Delivery of Proteins and Peptides*, J.L. Cleland and R. Langer, Editors. 1994, American Chemical Society: Washington, D.C. p. 134-147.

43. Hsu, T.T. and R. Langer, *Polymers for the controlled release of macromolecules: effect of molecular weight of ethylene-vinyl acetate copolymer.* J Biomed Mater Res, 1985. **19**(4): p. 445-60.

44. Knapp, A., T. Degenhardt, and J. Dodt, *Hirudisins. Hirudin-derived thrombin inhibitors with disintegrin activity.* J Biol Chem, 1992. **267**(34): p. 24230-4.

45. Challapalli, R., J. Lefkovits, and E.J. Topol, *Clinical trials of recombinant hirudin in acute coronary syndromes*. Coron Artery Dis, 1996. **7**(6): p. 429-37.

46. Weast, R.C., ed. *Handbook of Chemistry and Physics*. 57th ed. ed. 1976, CRC Press, Inc.: Cleveland, OH.

47. Castner, D.G. and B.D. Ratner, *Surface characterization of butyl methacrylate polymers with XPS and static SIMS.* Surf. Interface Anal., 1990. **15**: p. 479–486.

48. McFarlane, A.S., *Efficient trace-labelling of proteins with iodine.* Nature, Lond., 1958. **182**(4627): p. 53.

49. Contreras, M.A., W.F. Bale, and I.L. Spar, *Iodine monochloride (IC1) iodination techniques.* Methods Enzymol, 1983. **92**: p. 277-92.

50. Bale, W.F., et al., *High specific activity labeling of protein with I-131 by the iodine monochloride method.* Proc Soc Exp Biol Med, 1966. **122**(2): p. 407-14.

51. Tsomides, T.J. and H.N. Eisen, *Stoichiometric labeling of peptides by iodination on tyrosyl or histidyl residues.* Anal Biochem, 1993. **210**(1): p. 129-35.

52. Lopez, G.P., et al., *Plasma Deposition of Ultrathin Films of Poly(2-Hydroxyethyl Methacrylate) - Surface-Analysis and Protein Adsorption Measurements.* Macromolecules, 1993. **26**(13): p. 3247-3253.

53. Rinsch, C.L., et al., *Pulsed radio frequency plasma polymerization of allyl alcohol: Controlled deposition of surface hydroxyl groups.* Langmuir, 1996. **12**(12): p. 2995-3002.

54. Kim, D.D., et al., *Glow discharge plasma deposition (GDPD) technique for the local controlled delivery of hirudin from biomaterials*. Pharm Res, 1998. **15**(5): p. 783-6.

55. Ratner, B. and B. McElroy, *Electron spectroscopy for chemical analysis: applications in the biomedical sciences.*, in *Spectroscopy in the Biomedical Sciences*, R. Gendreau, Editor. 1986, CRC Press: Boca Raton, FL. p. 107-140.

56. Rhine, W.D., D.S.T. Hsieh, and R. Langer, *Polymers for sustained macromolecule release: procedures to fabricate reproducible delivery systems and control release kinetics*. J. Pharm. Sci., 1980. **69**: p. 265–270.

57. Siegel, R.A. and R. Langer, *Controlled release of polypeptides and other macromolecules*. Pharmaceutical Research, 1984. **1**: p. 2–10.

58. Nicholson, N.S., et al., *Antiplatelet and antithrombotic effects of platelet glycoprotein IIb/IIIa (GPIIb/IIIa) inhibition by arginine-glycine-aspartic acid-serine (RGDS) and arginine-glycine-aspartic acid (RGD) (O-me)Y (SC-46749).* J Pharmacol Exp Ther, 1991. **256**(3): p. 876-82.

59. Miron, T. and M. Wilchek, *A simplified method for the preparation of succinimidyl carbonate polyethylene glycol for coupling to proteins.* Bioconjug Chem, 1993. **4**(6): p. 568-9.

60. Hill, D.J.T., et al., *Copolymer hydrogels of 2-hydroxyethyl methacrylate with n-butyl methacrylate and cyclohexyl methacrylate: synthesis, characterization and uptake of water.* Polymer, 2000. **41**(4): p. 1287-1296.

61. d'Agostino, R., et al., *Plasma polymerization of fluorocarbons*, in *Plasma Deposition, Treatment and Etching of Polymers*, R. d'Agostino, Editor. 1990, Academic Press: Boston. p. 95–162.

62. John, C.M., et al., *XPS and TOF-SIMS microanalysis of a peptide/polymer drug delivery device.* Anal. Chem., 1995. **67**(21): p. 3871–3878.

63. Dolce, C., et al., *Effects of echistatin and an RGD peptide on orthodontic tooth movement.* J Dent Res, 2003. **82**(9): p. 682-6.

64. Dresner-Pollak, R. and M. Rosenblatt, *Blockade of osteoclast-mediated bone resorption through occupancy of the integrin receptor: a potential approach to the therapy of osteoporosis.* J Cell Biochem, 1994. **56**(3): p. 323-30.

65. Sato, M., et al., *Echistatin is a potent inhibitor of bone resorption in culture.* J Cell Biol, 1990. **111**(4): p. 1713-23.

66. Martin, I., D. Schaefer, and B. Dozin, *The Repair of Osteochondral Lesions*, in *Engineered Bone*, H. Petite, Editor. 2004, Landes Bioscience: Georgetown, TX.

67. Edelman, E.R., L. Brown, and R. Langer, *Quantification of insulin release from implantable polymer-based delivery systems and augmentation of therapeutic effect with simultaneous release of somatostatin.* J Pharm Sci, 1996. **85**(12): p. 1271-5.

68. Lahann, J., et al., *Reactive polymer coatings: a first step toward surface engineering of microfluidic devices.* Anal Chem, 2003. **75**(9): p. 2117-22.

VITA

Marc Takeno was born in Honolulu, Hawaii and attended Iolani School for his primary education. He attended The Johns Hopkins University where, in 1991, he earned a Bachelor of Science degree in Biomedical Engineering. In 2005 he earned a Doctor of Philosophy at the University of Washington, Seattle, in Bioengineering. He currently resides in Seattle.